The role of NAT8L (N-acetyltransferase 8-like) in lipid metabolism of murine adipocytes

Diploma Thesis
at the
Graz University of Technology

Submitted by

Lorenz Sonnberger

Institute for Genomics and Bioinformatics
Graz University of Technology
A-8010 Graz

28. March 2012

Supervised by

Assoc.Prof.Mag.rer.nat.Dr.rer.nat. Juliane Bogner-Strauß

TU Graz
Graz University of Technology

Acknowledgements

Abstract

In the last several years statistical observations detected a severe increase related to overweight and obesity in the world's population. This rise of the nowadays as a disease stated phenotype with almost epidemic proportions strongly promoted the research related to intra- and inter-functional aspects on fat tissue and the development of adipocytes. Especially, the circumstance that obesity is correlated with numerous health-threatening diseases which are also known to shorten lifespan brought this topic into focus of scientific investigations. Some of these studies exhibited a crucial relevance of genetic impacts on the appearance and expansion of obesity. This work deals with the functional analysis and the endogenous localisation of one of those genes which is denoted as Nat8l. Previous investigations revealed that Nat8l is mainly expressed in brain followed by brown (BAT) and white adipose tissue (WAT). Furthermore, it was demonstrated by microarray analysis that Nat8l was significantly down-regulated in WAT of ob/ob (genetically obese mice) and adipose triglyceride lipase (ATGL)-knockout mice and up-regulated in JunB-knockout mice, indicating a possible role of Nat8L on the energy homeostasis of adipocytes. The Nat8l gene encodes the amino acid sequence for the synthesis of the protein N-acetyltransferase 8-like (Nat8L). In this diploma thesis the influence of this enzyme which catalyses the acetylation of aspartate to N-acetylaspartate using acetyl-CoA was studied in the 3T3-L1 cell line, which represents one of the most widespread cellular models for the examination of the terminal differentiation and the maintenance of mature adipocytes. Due to the fact that until now nothing is published about the function of Nat8L in adipose tissue, a common way for the functional analysis represents the detection of the consequences of expression changes through knock-down and overexpression of the gene of interest. The knock-down attempt by antisense RNA constructs revealed a decreased triglyceride accumulation, which might be explained by the endogenous localisation of Nat8L in mitochondria. The stable overexpression of Nat8L, for investigating the influence during the differentiation of preadipocytes to lipid-filled adipocytes, could demonstrate a significant and drastic reduction of triglycerides. Additionally, lipid synthesis and genes responsible for lipid synthesis as Acsl1 and Dgat1 were decreased. This might be controversial in the light of the knock-down result but could be explained by favouring the endoplasmic reticulum (ER) as main locus for overexpressed Nat8L. The transient overexpression of Nat8L, which was tended to identify interactions of Nat8L in mature

adipocytes, exhibited a reduction of triglycerides by a rather high expression of Nat8L but this reduction was not as tremendous as during the stable overexpression. Using fluorescence microscopy, the localisation of Nat8L was investigated by an overexpressed protein complex, consisting of a fluorescent co-protein and Nat8L which detected Nat8L in the ER. Additionally, it was attempted to localise the endogenously expressed Nat8L protein by immunofluorescence staining. However, this experiment did not work as the endogenous expression seems not to be strong enough for the polyclonal antibody we have. In summary, the obtained findings could be incorporated in a possible metabolic pathway model suggesting a bimodal localisation of Nat8L and a direct influence of Nat8L on the cytosolic and mitochondrial acetyl-CoA levels and thus on the TG content of adipocytes.

Kurzfassung

Laut statistischen Aufzeichnungen kam es in den letzten Jahren zu einer drastischen Zunahme von Personen mit Übergewicht und Fettleibigkeit rund um die Welt. Dieser Anstieg mit nahezu epidemieartigen Ausmaßen von einem heutzutage als Krankheit bezeichneten Phenotyp, förderte die Forschung von intra- und inter-funktionalen Aspekten des Fettgewebes und der Entwicklung von Adipozyten. Speziell die Tatsache, dass Fettleibigkeit begünstigend auf eine große Anzahl gesundheitsschädlicher Krankheiten wirkt, die bekanntermaßen auch die Lebenserwartung verkürzen, rückte dieses Forschungsgebiet in den Fokus der Wissenschaft. Einige dieser Arbeiten konnten einen erheblichen Zusammenhang zwischen genetischen Faktoren und der Ausprägung von Fettleibigkeit feststellen. Die vorliegende Arbeit beschäftigt sich mit der funktionalen Analyse und der endogenen Lokalisation eines Gens mit der Bezeichnung Nat8l. Vorangegangene Untersuchungen konnten zeigen, dass Nat8l hauptsächlich im Gehirn, gefolgt von braunem und weißem Fettgewebe, exprimiert wird. Darüberhinaus detektierten Microarray-Analysen eine signifikante Reduktion von Nat8l im weißen Fettgewebe von ob/ob und ATGL-Knockout Mäusen, wohingegen eine stärkere Expression in JunB-Knockout Mäusen feststellbar war. Diese Indizien deuten darauf hin, dass Nat8l eine mögliche Rolle bei der Regulation der Energiehomeostase von Adipozyten spielt. Das Nat8l Gen kodiert die Aminosäuresequenz für die Synthese des Proteins N-acetyltransferase 8-like (Nat8L). Der Einfluss diese Enzyms, das die Acetylierung von Aspartat unter Verwendung von Acetyl-CoA zu N-Acetylaspartat katalisiert, wurde mit Hilfe von 3T3-L1 Zellen analysiert. Diese Zellen repräsentieren eines der weitverbreitetsten Zellmodelle für die Erforschung der terminalen Differenzierung und der Aufrechterhaltung von gereiften Adipozyten. Da bis jetzt noch keine Daten über die Funktion von Nat8L in Fettgewebe publiziert worden sind, ist die Untersuchung der metabolischen Konsequenzen durch den Knock-down und die Überexpression des zu untersuchenden Gens in den entsprechenden Zellen eine weit verbreitete Methode. Der Knock-down mittels eines antisense-RNA Konstruktes führte zu einer Reduktion der Triglyzeridakkumulation im Zytosol, was möglicherweise mit der endogenen Lokalisation von Nat8L in den Mitochondrien zusammenhängt. Die stabile Überexpression von Nat8L, für die Erforschung des Einflusses während der Differenzierung von Präadipozyten zu gereiften Fettzellen, zeigte eine signifikante und drastische Verringerung der Triglyzeride

gefolgt von einer Abnahme der Lipidsynthese. Dieses Resultat erscheint zwar etwas kontrovers unter Einbeziehung der Ergebnisse des Knock-down Versuches ist aber durch eine Lokalisation von überexprimierter Nat8L im Endoplasmatischen Retikulum erklärbar. Die transiente Überexpression von Nat8L war darauf abgezielt Interaktionen des Enzyms in gereiften Adipozyten zu identifizieren. Es konnte dabei eine Verminderung der Triglyzeride bei höheren Expressionswerten von Nat8L festgestellt werden. Die endogene Lokalisation von Nat8L wurde mittels Fluoreszenzmikroskopie durch Detektion eines, aus Nat8L und einem fluoreszierenden Co-proteins bestehenden, Proteinkomplexes analysiert. Nat8L wurde dabei vorrangig in Regionen in der Nähe des Nucleus detektiert, die auf das ER schließen lassen. Weiters wurde versucht die Lokalisation des endogen exprimierten Proteins mittels Immunofluoreszenz-Analyse zu eruieren, was aber aufgrund der zu geringen Expression nicht möglich war. Die Forschungsergebnisse dieser Arbeit konnten mit einem hypothetischen Stoffwechselmodell, das eine bimodale Lokalisation von Nat8L vorsieht, in Einklang gebracht werden. Nat8L scheint einen direkten Einfluss auf den zytosolischen und mitochondrialen Acetyl-CoA Gehalt und damit auf den TG von Adipozyten zu haben und könnte damit ein weiterer Kandidat sein, der in der Entstehung der Fettleibigkeit eine tragende Rolle spielt.

Statutory Declaration

I declare that I have authored this thesis independently, that I have not used other than the declared sources/ resources, and that I have explicitly marked all material which has been quoted either literally or by content from the used sources.

Place	Date	Signature

Eidesstattliche Erklärung

Ich erkläre an Eides statt, dass ich die vorliegende Arbeit selbständig verfasst, andere als die angegebenen Quellen/Hilfsmittel nicht benutzt, und die den benutzten Quellen wörtlich und inhaltlich entnommene Stellen als solche kenntlich gemacht habe.

Ort	Datum	Unterschrift

Contents

Figure Legends

Table Legends

1 Abbreviations

1 Abbreviations

Acetyl-CoA	acetyl coenzyme A
Acsl1	acyl-CoA synthetase long-chain family member 1
Acss1	acyl-CoA synthetase short-chain family member 1
Acss2	acyl-CoA synthetase short-chain family member 2
ADP	adenosine diphosphate
AP-1	activating protein 1
as	antisense
Aspa1	aspartoacylase 1
Atf3	activating transcription factor 3
Atgl	adipose triglyceride lipase gene
BAT	brown adipose tissue
BiP	binding immunoglobulin protein
BMI	body-mass-index
BS1	blocking solution 1
BS2	blocking solution 2
BSA	bovine serum albumin
cAMP	cyclic adenosine monophosphate
cDNA	complementary DNA
CDS	coding sequence
C/EBP ($\alpha,\beta,\gamma,\delta$)	CCAAT-enhancer-binding protein ($\alpha,\beta,\gamma,\delta$)
CFP	cyan fluorescent protein
CHO	Chinese hamster ovary
CHOP	transcript factor homologous to CCAAT-enhancer-binding proteins
CHOP10	C/EBP-homologous protein 10
CREB	cAMP regulatory element-binding protein
DAPI	4′,6-Diamidino-2-phenylindol
DC	direct current
Dgat1	diacylglycerol O-acyltransferase 1
Dgat2	diacylglycerol O-acyltransferase 2
dH_2O	distilled H_2O
ddH_2O	double distilled H_2O
DEPC	diethylpyrocarbonate
DEX	dexamethasone
DIC	dicarboxylic acid translocase

1 Abbreviations

DM1	differentiation medium 1
DM2	differentiation medium 2
DMEM	Dulbecco's modified eagle medium
DMSO	dimethyl sulfoxide
DNA	deoxyribonucleic acid
dNTP	deoxyribonucleotide triphosphate
dsDNA	double stranded DNA
DTE	dithioerythritol
DTT	dithiothreitol
EDTA	ethylenediaminetetraacetate
ER	endoplasmic reticulum
EtBr	ethidium bromide
FA	fatty acid
FBS	foetal bovine serum
fw	forward
GA	glutaraldehyde
GATA2/3	GATA-transcription factor 2/3
GOI	gene of interest
His-Tag	codon for six histidines in a row
HLH	helix-loop-helix
HSL	hormone-sensitive lipase
IBMX	3-Isobutyl-1-methylxanthine
IGF1	insulin-like growth factor-1
Ins	insulin
KLF	kruppel-like factor
KROX20	early growth response 2
L-Asp	L-aspartate
L-Glu	L-glutamine
MAS	malate-aspartate-shuttle
MCS	multiple cloning site
mRNA	messenger RNA
NAA	N-acetylaspartate
Nat8l	N-acetyltransferase 8-like gene
Nat8L	N-acetyltransferase 8-like protein

1 Abbreviations

OL	oligodendrocyte
ORO	Oil red O staining
PBS	phosphate buffered saline
PBST	Tween including phosphate buffered saline
PCR	polymerase chain reaction
pECFP-N1	plasmid enhanced cyan fluorescent protein N clonal of MCS
pEYFP-C1	plasmid enhanced yellow fluorescent protein C clonal of MCS
PIC	protease inhibitor cocktail
PFA	paraformaldehyde
pMSCV	plasmid murine stem cell virus
PMSF	phenylmethanesulfonyl fluoride
POI	protein of interest
PPARγ	peroxisome proliferator-activated receptor γ gene
P/S	penicillin/streptomycin
qPCR	quantitative polymerase chain reaction
Retn	resistin
RNA	ribonucleic acid
dsRNA	double stranded RNA
mRNA	messenger RNA
rv	reverse
RXR	retinoid X receptor
SOC	super optimal broth with catabolite repression
StdM	standard medium
SREBP1c	sterol regulatory element binding protein 1c
TAC	tricarboxylic anion carrier
TAE-buffer	tris-acetate-EDTA-Buffer
TCA	tricarboxylic acid cycle
TF	transcription factor
TG	triglyceride
TNF-α	tumor necrosis factor-α
WAT	white adipose tissue
WB	western blot
YFP	yellow fluorescent protein

2 Introduction

The roots of obesity as an influencing factor of life and mankind reach back over 30,000 years when the efficiency of energy storage was a crucial and by evolution promoted aspect which assured the survival of individuals during periods of fast and famine[1]. Nowadays, the knowledge about the negative and health-threatening effects of excess body fat has led to the designation of obesity as a disease[2]. Furthermore, it can already be defined as an epidemic, regarding to the worldwide phenomenon of rapid expansion of overweight and obese people (see Table 1 for definitions) across all ages during the last 2 decades (doubled since 1980[3])[4]. According to the WHO in 2008, 1.5 billion adults, over the age of 20, were overweight. In this group about 500 million individuals already crossed the threshold to obesity with a distribution between men and women of about 2 to 3. Additionally, a study from 2010 revealed that a terrifying quantity of over 43 million children under the age of five is overweight. This early onset of overweight results in a higher risk of obesity during adulthood and an increased prevalence for all its related disorders.[5,6] Even though, overweight and obesity are sometimes described as the "New World Syndrome", affecting only western society, the trend during the last years exhibited an increase of this problem in low and middle income countries, with a focus on urban settings. Especially, among children of developing countries (35 million), obesity reaches drastic proportions. As a result, nowadays, 65 % of the world's population lives in countries where overweight and obesity are responsible for more deaths than undernutrition.[7] To define overweight and obesity it is necessary to determine the body fat of an individual. One of the most common and simple ways of diagnosis in medicine and epidemiological studies is the body-mass index (BMI). The BMI is a calculation method which combines weight and height. The hypothesis behind this algorithm is the consumption that most variations of body weight are caused through changes of fat mass.[8] The formula is described as division of weight (in kilograms) by square of height (in meters). The classification of overweight and obesity depending on the BMI is shown in Table 1.

---

[1] Haslam, "Obesity: a Medical History."
[2] Kopelman, "Obesity as a Medical Problem."
[3] "Fact Sheet N°311."
[4] Bray and Bellanger, "Epidemiology, Trends, and Morbidities of Obesity and the Metabolic Syndrome."
[5] Kotani et al., "Two Decades of Annual Medical Examinations in Japanese Obese Children."
[6] Dietz, "Critical Periods in Childhood for the Development of Obesity."
[7] "Fact Sheet N°311."
[8] Kopelman, "Obesity as a Medical Problem."

	BMI (kg/m^2)	Obesity class
Underweight	<18.5	
Normal	18.5 to 24.9	
Overweight	25.0 to 29.9	
Obesity	30.0 to 34.9	I
	35.0 to 39.9	II
Extreme obesity	≥40	III

Table 1: Classification of overweight and obesity depending on the BMI[9]

The BMI classification criteria for Asia and Oceania are slightly different then the one presented in Table 1: overweight is a BMI equal to or greater than 23 kg/m^2 and obesity is a BMI equal to or greater than 25 kg/m^2 [10]. Additionally, there are also differences in the evaluation of childhood obesity. The classification is performed with the help of a BMI scale which depends on age and sex in which the 97th percentile represents the boarder to obesity and children with a BMI in between the 97th and 90th percentile are rated to be overweight[11]. At this point it should be stated that especially this valuation method with the help of the BMI contributes to this drastic numbers of increased obesity. Because alterations of body weights are continuous changes but BMI classifies overweight and obesity with a dichotomous trait. This calculation method results in a disproportional increase of people stated as obese when the mean value of body weight of a population becomes slightly higher. For example, in 1990 the increase of obesity in United States was reported with 33 % during a decade but the average weight gain was only 3-5 kilograms. So, the increment of obese people is not as severe as generally appreciated.[12] Furthermore, the BMI evaluation criterion, even though it represents the easiest way to classify obesity, cannot distinguish between weight gain caused from fat or muscle mass, and the usage of height squared as a demographic depending value is completely empirical. So, other methods for directly assessing body fat, such as air displacement to calculate density or the more sophisticated magnetic resonance imaging and Dual-Energy X-Ray Absorptiometry are better suited for the precise evaluation of obesity, especially for individuals.[13,14]

---

[9] Aronne, "Classification of Obesity and Assessment of Obesity-related Health Risks."
[10] Stommel and Schoenborn, "Variations in BMI and Prevalence of Health Risks in Diverse Racial and Ethnic Populations."
[11] Ogden et al., "Prevalence of Overweight and Obesity in the United States, 1999-2004."
[12] Friedman, "Obesity: Causes and Control of Excess Body Fat."
[13] Ibid.
[14] Gesta, Tseng, and Kahn, "Developmental Origin of Fat: Tracking Obesity to Its Source."

Nevertheless, the fact that today half of the U.S. and European population is classified as overweight or obese still remains.[15],[16]

For better understanding of obesity and its changes, it is necessary to take a closer look at the circumstances which influence the body weight. Genetic, environmental, and psychosocial factors contribute to variations in body weight by affecting physiological substances responsible for energy intake and expenditure.[17] So, the simple energy balance equation which was also described by Hippocrates thousands of years ahead of his time[18] and is derived from the first law of thermo dynamics can be expressed through:

$$\text{Energy intake} = \text{energy burned} + \text{energy stored} \ ^{[19]}$$

According to a huge amount of studies, related to the percental distribution of the above mentioned factors, about 30 % to 40 % of the BMI variation is caused from genetics and the rest is attributed to environmental influences.[20] Even though genetics has a significant influence on fat metabolism, the main reasons for the increase of obesity are that energy intake has gone up because of the abundance of cheap food in the developed world and the decline of physical activity due to a more sedentary life style.[21],[22]

The problem with obesity and the reason why it is nowadays so extensively studied is the fact that it is related with several serious diseases. The complexity of these widespread investigations is so enormous due to the fact that obesity is not a single disorder but a heterogeneous group of conditions with multiple causes expressing an obese phenotype.[23]

These diseases associated with obesity can be classified into one of two pathophysiologic categories[24]. "The first category includes diseases whose increased risks result from metabolic changes associated with the products secreted from the excess fat such as diabetes mellitus, gall bladder disease, hypertension, cardiovascular disease, and some forms of cancer associated with overweight. The second category of disabilities arises from the increased mass of fat itself. These include osteoarthritis, sleep apnoea, the stigma of

---

[15] Friedman, "A War on Obesity, Not the Obese."
[16] Hyde, "Europe Battles with Obesity."
[17] Kopelman, "Obesity as a Medical Problem."
[18] Haslam, "Obesity: a Medical History."
[19] Rosen and Spiegelman, "Adipocytes as Regulators of Energy Balance and Glucose Homeostasis."
[20] Pi-Sunyer, "The Obesity Epidemic: Pathophysiology and Consequences of Obesity."
[21] Kimm et al., "Decline in Physical Activity in Black Girls and White Girls During Adolescence."
[22] Prentice and Jebb, "Obesity in Britain."
[23] Nammi et al., "Obesity: An Overview on Its Current Perspectives and Treatment Options."
[24] Bray, "Medical Consequences of Obesity."

obesity, and the behavioural responses it produces."[25] A more detailed presentation of diseases correlated with obesity is shown in Table 2.

Cardiovascular diseases	Hypertension Coronary heart disease Cerebrovascular disease Varicose veins Deep venous thrombosis
Respiratory diseases	Breathless Sleep apnoea Hypoventilation syndrome
Metabolic disorders	Hyperlipidemia Diabetes mellitus Insulin resistance Menstrual irregularities
Gastrointestinal disorders	Fatty liver and cirrhosis Haemorrhoids Hernia Colorectal cancer Gallstones
Malignancies	Breast cancer Endometrial cancer Prostrate cancer Cervical cancer
Miscellaneous	Pregnancy complications Stress Arthritis and bone mass

Table 2: Obesity-associated diseases and risk factors[26]

The increased risk of obesity-related diseases is also dependent on the distribution of the accumulated fat mass[27]. Abdominal and visceral fat seem to promote the occurrence of negative health consequences more strongly than peripheral fat[28]. Furthermore, the risk of these diseases varies between the two different kinds of obesity (see: Figure 1). The lower risk form denoted as hypercellular obesity (or hyperplasia), also referred sometimes as 'adipogenesis', evokes from an excessive development of new adipocytes through proliferation and differentiation of preadipocytes in adipose tissue,[29] leading to an increase

---

[25] Bray and Bellanger, "Epidemiology, Trends, and Morbidities of Obesity and the Metabolic Syndrome."

[26] Nammi et al., "Obesity: An Overview on Its Current Perspectives and Treatment Options."

[27] Pi-Sunyer, "The Obesity Epidemic: Pathophysiology and Consequences of Obesity."

[28] National Institutes of Health (NIH), National Heart, Lung, and Blood Institute (NHLBI), "Clinical Guidelines on the Identification, Evaluation, and Treatment of Overweight and Obesity in Adults--The Evidence Report. Obes. Res."

[29] Hausman et al., "The Biology of White Adipocyte Proliferation."

of the total number of fat cells. Hypertrophic obesity is characterised by fat accumulation in existing fat cells, resulting in an enlargement of cell volume accompanied by a dysregulation of substrates involved in the pathophysiology of obesity and can normally be found in truncal fat depots.[30]
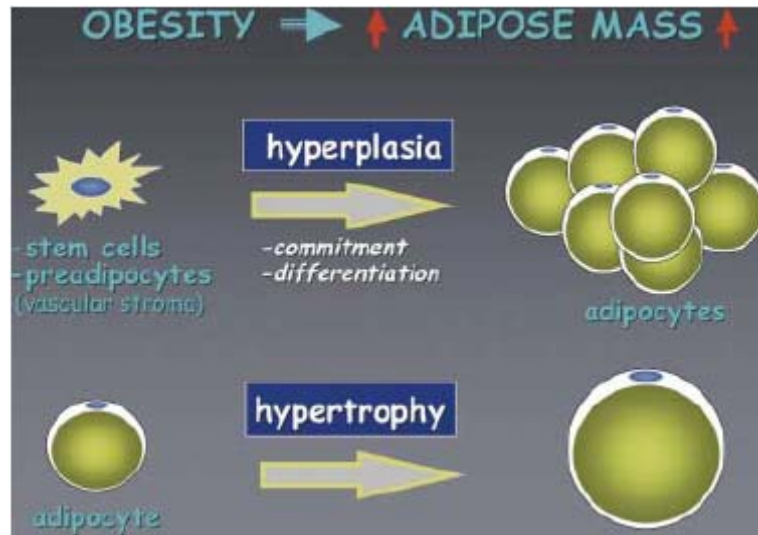
Figure 1: Adipocyte hyperplasia and hypertrophy are responsible for the increase of adipose tissue mass associated with obesity[31]

Adults of healthy weight have an adipose tissue mass about 10 % to 29 %, therefore it represents the largest organ inside the body.[32] The tissue itself has a very heterogeneous structure consisting of different cellular components. The predominant cells are mature, lipid-filled adipocytes, lipid-free preadipocytes, and endothelial cells but also other cell types like nerve fibers and monocytes/ macrophages are integrated.[33] Commonly, adipose tissue of mammals can be classified in two functionally different types. The majority is represented by WAT (white adipose tissue) which is capable to store and release energy in the form of triacylglycerols. The second class is represented by BAT (brown adipose tissue) which is involved in diet- or cold- induced thermogenesis, a process where energy is used for heat production in mitochondria.[34] Even though, both kinds of cells are thought to arise from the same precursors the morphology is different. Developed BAT cells possess small, multilocular lipid droplets and are rich in mitochondria, whereas mature

---

[30] Bray and Ryan, "Clinical Evaluation of the Overweight Patient."
[31] Otto and Lane, "Adipose Development."
[32] Kahn, "Medicine Can We Nip Obesity in Its Vascular Bud?".
[33] Hauner, "The New Concept of Adipose Tissue Function."
[34] Billon, Monteiro, and Dani, "Developmental Origin of Adipocytes: New Insights into a Pending Question."

WAT cells have one large, centred lipid filled vacuole which makes up almost the entire volume.[35] Humans have very distinctive BAT depots during infancy, in later life there remain only small quantities of it dispersed mainly throughout the different depots of WAT[36].[37,38] The major WAT localisations can be found in intra-abdominal depots around the omentum, intestine, and perirenal areas, as well as in subcutaneous depots in buttocks, thighs, and abdomen[39]. A pattern of the localisation of both tissue types is presented in Figure 2.
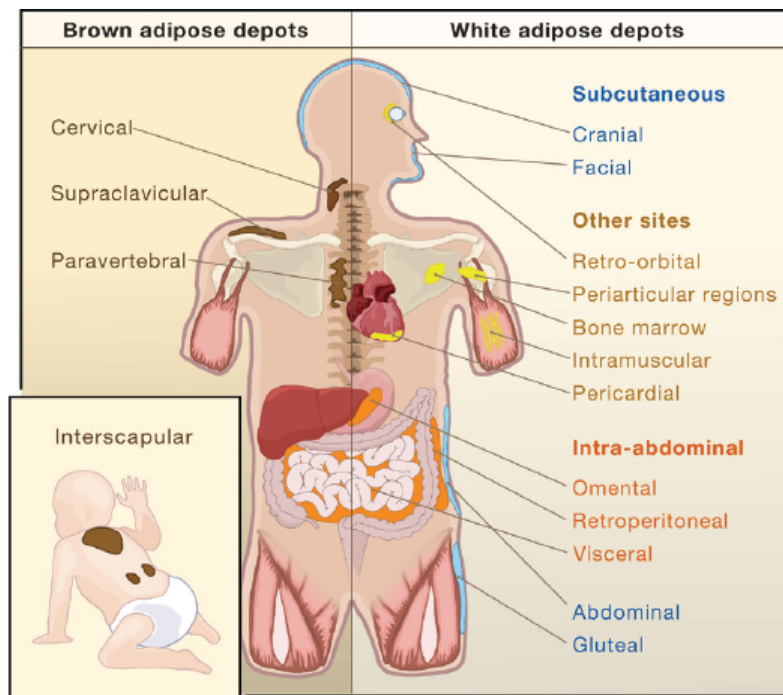
Figure 2: Localisation of BAT and WAT inside the human body[40]

After the identification of leptin, the obese gene product, the perception from adipose tissue as an organ of passive energy storage drastically changed. Leptin is a hormone secreted by fat cells which interacts with different organs throughout the body. [41,42] Mainly affecting the hypothalamus and thereby controlling the amount of food intake, promoting

---

[35] Rosen and Spiegelman, "Adipocytes as Regulators of Energy Balance and Glucose Homeostasis."
[36] Rosen and Macdougald, "Adipocyte Differentiation from the Inside Out."
[37] Cypess et al., "Identification and Importance of Brown Adipose Tissue in Adult Humans."
[38] Nedergaard, Bengtsson, and Cannon, "Unexpected Evidence for Active Brown Adipose Tissue in Adult Humans."
[39] Gesta, Tseng, and Kahn, "Developmental Origin of Fat: Tracking Obesity to Its Source."
[40] Ibid.
[41] Zhang et al., "Positional Cloning of the Mouse Obese Gene and Its Human Homologue."
[42] Friedman and Halaas, "Leptin and the Regulation of Body Weight in Mammals."

energy expenditure, and reducing body fat[43]. So, adipose tissue is an organ with a variety of different functions that creates and releases various metabolites that act either in an auto/ paracrine or an endocrine fashion[44], to regulate processes as diverse as haemostasis, blood pressure, immune function, angiogenesis, adipogenesis, and energy balance[45]. Even though, the understanding of all these aspects of adipose tissue is required for an effective treatment of health implications of obesity, especially the development and regulation of adipogenesis is from further interest for this work.[46] Adipogenesis is a multi-step process involving a cascade of transcription factors and cell-cycle proteins regulating gene expression and leading to adipocyte development[47]. An overview of the stages of adipogenesis is presented in <u>Figure 3</u> [48]. Generally, adipogenesis is divided into two phases. The first phase is known as determination, where a pluripotent stem cell precursor gives rise to a mesenchymal precursor cell which further converts to a preadipocyte. Their phenotype is undistinguishable from their precursors but they have lost the ability to transform into other cell types.[49,50] During the second step which is termed as terminal differentiation, preadipocytes convert to mature adipocytes. This step is accompanied by a change of the fibroblast like appearance of preadipocytes to a round lipid filled fat cell shape. Additionally, intracellular metabolic pathways which are essential for lipid transport and synthesis, insulin sensitivity, and the secretion of adipocyte-specific proteins are activated.[51,52] The development from preadipocytes to adipocytes can be further characterised in four phases: growth arrest (and not cell confluence or cell-cell contact per se appears to be required for differentiation[53]), clonal expansion, early differentiation, and terminal differentiation. During these stages, a transcriptional cascade is executed including the expression of the nuclear receptor PPARγ, which is the only essential factor for differentiation, and members of the C/EBPs family which are also very crucial for the regulation of the development of mature adipocytes.[54,55,56]

---

[43] Ahima, "Digging Deeper into Obesity."
[44] Hauner, "The New Concept of Adipose Tissue Function."
[45] Lau et al., "Adipokines."
[46] Otto and Lane, "Adipose Development."
[47] Lefterova and Lazar, "New Developments in Adipogenesis."
[48] Gregoire, Smas, and Sul, "Understanding Adipocyte Differentiation."
[49] Ibid.
[50] Rosen and Macdougald, "Adipocyte Differentiation from the Inside Out."
[51] Ibid.
[52] Butterwith, "Molecular Events in Adipocyte Development."
[53] Gregoire, Smas, and Sul, "Understanding Adipocyte Differentiation."
[54] Farmer, "Transcriptional Control of Adipocyte Formation."
[55] Gesta, Tseng, and Kahn, "Developmental Origin of Fat: Tracking Obesity to Its Source."
[56] Lefterova and Lazar, "New Developments in Adipogenesis."

Some of the important transcription factors of this cascade are presented in Figure 4 with a brief explanation of their possible function in the following text.
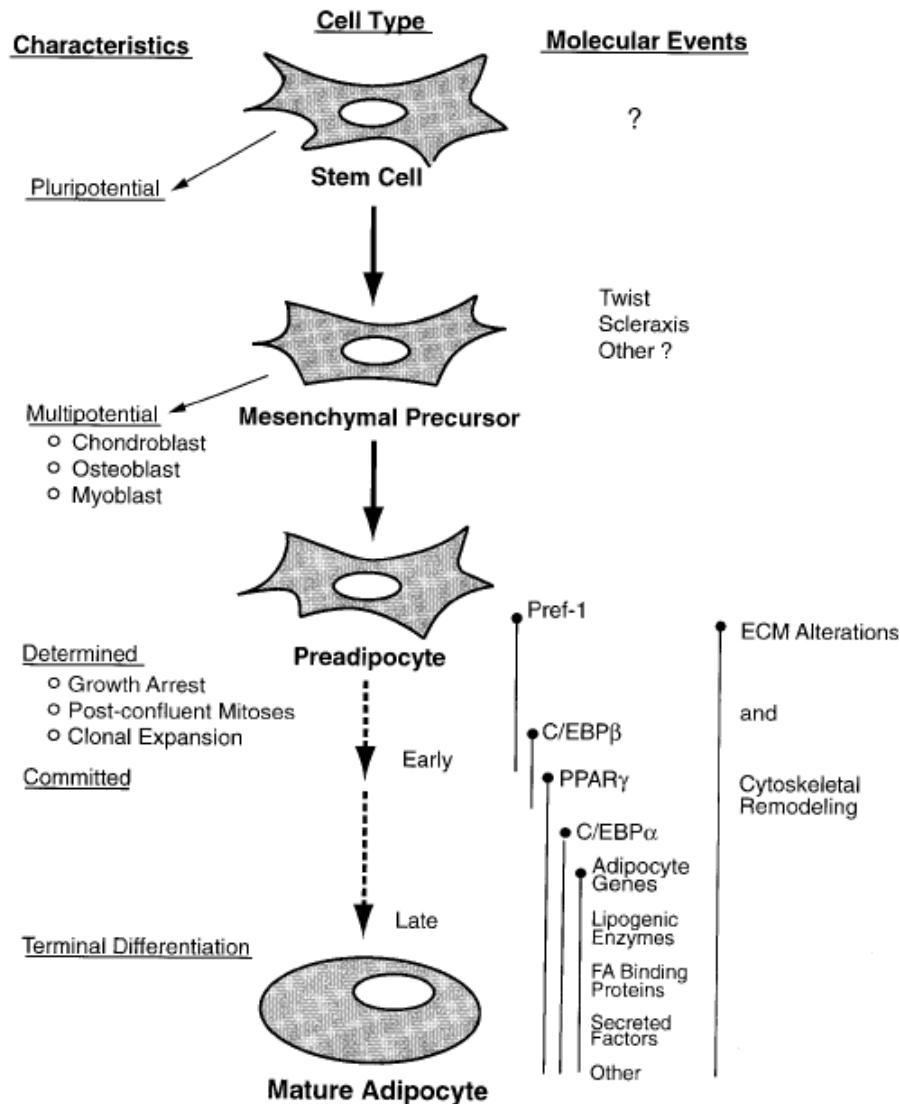
Figure 3: Overview of stages of adipogenesis[57]

As already mentioned and as can be seen in Figure 4, PPARγ has the role of a "master regulator" during differentiation which was proven by a tremendous amount of different *in vitro* and *in vivo* studies. Without PPARγ the transition of preadipocytes to mature adipocytes is completely prevented.[58,59] PPARγ belongs to the nuclear receptor superfamily and its activity is dependent on direct binding of steroid and thyroid hormones,

---

[57] Gregoire, Smas, and Sul, "Understanding Adipocyte Differentiation."
[58] Farmer, "Transcriptional Control of Adipocyte Formation."
[59] Rosen et al., "C/EBPalpha Induces Adipogenesis Through PPARgamma."

vitamins, lipid metabolites, and xenobiotics[60]. PPARγ can be divided in two isoforms, PPARγ1 and PPARγ2, which are expressed by the same gene through different promoter usage. PPARγ1 expression takes place in various tissues, whereas PPARγ2 is almost exclusively expressed in adipose organs.[61] The functionality of PPARγ as a transcription factor with binding to specific DNA sequences needs the building of a complex with the retinoic X receptor which pertains to the same receptor family as PPARγ[62]. Remarkable is the fact that even though PPARγ is so vital to adipogenesis, until now there have only a few number of genes been reported to be direct PPARγ targets[63]. The other already mentioned group of strongly influencing factors of differentiation are the CCAAT-enhancer binding proteins (C/EBP) -α, -β, and –δ[64]. Furthermore, C/EBPγ and CHOP (transcription factor homologous to C/EBP) which belong to the same family are also expressed in adipocytes, although their roles are not quite as important as for example C/EBPα. The expression of C/EBPβ and C/EBPδ occurs in the early phase of adipocyte differentiation and subsides later on. Both factors promote adipogenesis partially by inducing C/EBPα and PPARγ[65,66,67]. CHOP and C/EBPγ are anti-adipogenic factors, which are capable to bind to C/EBPβ and thereby inhibit its activity[68]. Conversely to CHOP and C/EBPγ, the cAMP regulatory element-binding protein (CREB) promotes an increase of C/EBPβ expression, explaining the need for inducers of cAMP (isobutylmethylxanthine) in differentiation induction cocktails[69]. In contrast, induction of C/EBPδ is facilitated by glucocorticoids (dexamethasone as a glucocorticoid agonist is therefore added to induction cocktails) and C/EBPβ.[70] The last ingredient which is normally added to common cocktails that induce the adipogenic program is insulin. It stimulates adipogenesis through the interaction with the insulin-like growth factor-1 (IGF-1) which may have a regulatory influence on fat cell formation[71]. The helix-loop-helix

---

[60] Chawla et al., "Nuclear Receptors and Lipid Physiology."
[61] Farmer, "Transcriptional Control of Adipocyte Formation."
[62] Lehrke and Lazar, "The Many Faces of PPARgamma."
[63] Lefterova and Lazar, "New Developments in Adipogenesis."
[64] Otto and Lane, "Adipose Development."
[65] Cao, Umek, and McKnight, "Regulated Expression of Three C/EBP Isoforms During Adipose Conversion of 3T3-L1 Cells."
[66] Yeh et al., "Cascade Regulation of Terminal Adipocyte Differentiation by Three Members of the C/EBP Family of Leucine Zipper Proteins."
[67] Rosen and Macdougald, "Adipocyte Differentiation from the Inside Out."
[68] Darlington, Ross, and MacDougald, "The Role of C/EBP Genes in Adipocyte Differentiation."
[69] Zhang et al., "Role of CREB in Transcriptional Regulation of CCAAT/enhancer-binding Protein Beta Gene During Adipogenesis."
[70] Cao, Umek, and McKnight, "Regulated Expression of Three C/EBP Isoforms During Adipose Conversion of 3T3-L1 Cells."
[71] Gregoire, Smas, and Sul, "Understanding Adipocyte Differentiation."

(HLH) transcription factor SREBP1c which can also be seen in <u>Figure 4</u> (sterol regulatory element binding protein-1c) effects PPARγ separately from C/EBPβ and C/EBPδ[72].
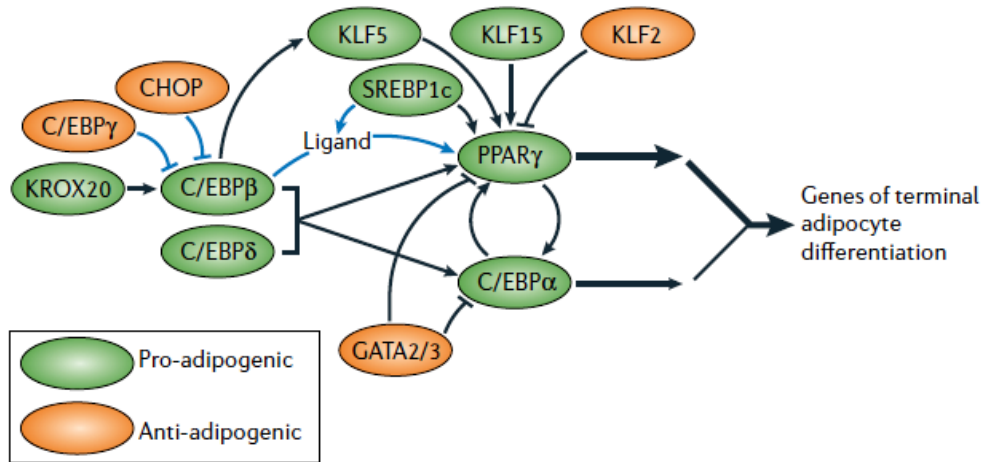
Figure 4: Overview of the transcriptional cascade which regulates adipogenesis[73]
Black lines indicate effects on gene expression, whereas blue lines represent effects on protein activity.

Another group of transcription factors which have an influence on adipogenesis are the krüppel like factors (KLFs) which belong to a large family of C2H2 zinc-finger proteins[74]. KLF4, for example, works in collaboration with KROX20 (another zinc-finger protein, also called early growth response protein-2), both are induced early in differentiation and promote C/EBPβ expression[75,76]. Other members of the KLF family like KLF15 and KLF5 are known to promote adipocyte differentiation and KLF2 and KLF7 are both anti-adipogenic factors.[77] GATA-binding protein-2 and -3 (GAT2/3), which are abundant in preadipocytes and progressively decrease during adipogenesis inhibit terminal differentiation, in part by repressing transcription of PPARγ[78]. All the above mentioned genes and the complexity of their interactions and the fact that over 100 other transcription factors are known to be influenced during differentiation, with largely un-described functionality, reveal the enormous dimension of the scientific field of adipogenesis. Even though, the main causes of adipocyte development and maintenance of the developed state seem to be known, especially *in vitro*, there is still a large part of unknown factors and

---

[72] Farmer, "Transcriptional Control of Adipocyte Formation."
[73] Rosen and Macdougald, "Adipocyte Differentiation from the Inside Out."
[74] Ibid.
[75] Birsoy, Chen, and Friedman, "Transcriptional Regulation of Adipogenesis by KLF4."
[76] Chen et al., "Krox20 Stimulates Adipogenesis via C/EBPbeta-dependent and -independent Mechanisms."
[77] Rosen and Macdougald, "Adipocyte Differentiation from the Inside Out."
[78] Ibid.

pathways which might interact or affect adipocyte development. As a consequence of increases in obesity all around the world, the investigation and understanding of fat tissue and therein incorporated cells become more and more important and should help to prevent and treat the health impairing effect which results from overweight.

A great amount of the scientific research on adipogenesis has been carried out with cell models. According to the part of differentiation which is investigated, two types of lineages are distinguishable. Multipotent stem cell lines are commonly used for evaluation of the determination process of adipocytes and preadipocyte cell lines for the terminal differentiation.[79] For the latter, 3T3-L1 cells which were derived from the established 3T3 line originating of 17 to 19 day old Swiss mouse embryos[80], represent one of the most widespread systems of exploration. Especially, the ability to accumulate a huge quantity of lipids consisting of triglycerides after reaching a growth resting state resembles significantly that of adipose cells[81]. This resting state can be achieved through confluence due to the fact that growth of 3T3 cells is ceased by contact inhibition or inoculation of cells in medium containing methyl cellulose.[82] During the differentiation process, there are markedly increased rates of triglyceride synthesis from palmitate, acetate, and glucose and these, especially from glucose, can be further elevated through addition of insulin to the medium. But, even though insulin promotes the accumulation of triglycerides in differentiated 3T3-L1 cells, the quantity of cells which underwent the conversion is not affected.[83] For that purpose, growth arrested cells can be treated with MeiBu-Xan (other name for IBMX) which is capable to increase intracellular levels of cAMP and advance the amount of 3T3-L1 cells which differentiate to mature adipocytes[84]. The morphology of 3T3-L1 cells appears fibroblast like when kept in a growing state and changes to brown adipose cell appearance with multiple fat droplets in the early phase of lipid accumulation. When the differentiation proceeds the phenotype resembles that of white adipocytes with a single large central lipid droplet.[85] All these factors together make the 3T3-L1 cell line

---

[79] Armani et al., "Cellular Models for Understanding Adipogenesis, Adipose Dysfunction, and Obesity."
[80] T OD and G RE, "Quantitative Studies of the Growth of Mouse Embryo Cells in Culture and Their Development into Established Lines."
[81] Green and Kehinde, "Sublines of Mouse 3T3 Cells That Accumulate Lipid."
[82] Green and Meuth, "An Established Pre-adipose Cell Line and Its Differentiation in Culture."
[83] Green and Kehinde, "An Established Preadipose Cell Line and Its Differentiation in Culture. II. Factors Affecting the Adipose Conversion."
[84] Russell and Ho, "Conversion of 3T3 Fibroblasts into Adipose Cells: Triggering of Differentiation by Prostaglandin F2alpha and 1-methyl-3-isobutyl Xanthine."
[85] Green and Kehinde, "An Established Preadipose Cell Line and Its Differentiation in Culture. II. Factors Affecting the Adipose Conversion."

well suited for investigations on the differentiation process from preadipocytes to adipocytes.

The fundamental principles of the current study of the N-acetyltransferase 8-like (Nat8l) gene in fat metabolism were provided by a research performed at the Institute of Genomics and Bioinformatics at the University of Technology Graz, which evaluated differentially expressed genes in HSL- (hormone sensitive lipase) and ATGL- (adipocyte triglyceride lipase) ko mice in comparison to wild-type animals. Especially, the influences of these lipases on TG metabolism were from further interest. The performed microarray analysis of white and brown adipose tissue revealed that Nat8l was severely down-regulated in both tissues from the ATGL-ko mice, but unaffected in HSL-ko mice.[86] According to the published data, ATGL seems to be essential in the initial step of TG hydrolysis. These finding and the coincidence that ATGL-deficient mice possess an obese phenotype, with increased fat depots in different tissues like WAT and BAT, made Nat8l to a promising candidate that might influence the fat metabolism in some kind of way. Furthermore, another study with JunB-ko mice could demonstrate an increase of Nat8l in WAT.[87] JunB is a known member of the AP-1 (activating protein-1) family of transcription factors which are correlated with the differentiation of adipocytes and expressed immediately after induction[88]. Until now, nothing of the published work related to Nat8l focuses on adipose tissue. The main locus of research lies in the functional analysis of Nat8l in neurons. The reason for the emphasis of neurons is the fact that Nat8l, as a member of the N-acetyltransferase superfamily, is able to catalyse the reaction of L-aspartate (L-Asp) and acetyl coenzyme A (acetyl-CoA) to N-acetylaspartate (NAA). The high specificity of this reaction for the acetylation of aspartate could be confirmed by molecular homology modelling studies.[89] In neurons, NAA represents the second most abundant metabolite which was demonstrated through previous work long before it turned out that Nat8l synthesises NAA[90]. Even though, the roles of NAA are not exactly resolved until today, existing evidences indicate that NAA is translocated after its production by an unknown transport mechanism along the axon to oligodendrocytes (OLs). There it is hydrolysed by the N-acetyl-L-aspartate amidohydrolase (aspartoacylase, ASPA) to acetate which serves

---

[86] Pinent et al., "Differential Transcriptional Modulation of Biological Processes in Adipocyte Triglyceride Lipase and Hormone-sensitive Lipase-deficient Mice."

[87] Pinent et al., "Adipose Triglyceride Lipase and Hormone-Sensitive Lipase Are Involved in Fat Loss in JunB-Deficient Mice."

[88] White and Stephens, "Transcriptional Factors That Promote Formation of White Adipose Tissue."

[89] Ariyannur et al., "Methamphetamine-induced Neuronal Protein NAT8L Is the NAA Biosynthetic Enzyme."

[90] TALLAN, MOORE, and STEIN, "N-Acetyl-L-aspartic Acid in Brain."

as a precursor for the synthesis of myelin lipids. This conclusion is supported by the fact that patients with Canavan disease, which is attributed to a lack of aspartoacylase, reveal an increase of NAA, exhibit a progressive loss of OLs and myelin.[91] Another related disorder which contributes to this assumption is hypoacetylaspartia. Even though, only one reported case is known it appears that a 19 bp deletion in the Nat8l gene prevents the synthesis of NAA leading to an aberrant myelination.[92] These results according to the probable influence of Nat8l on myelinogenesis constitute Nat8l as another factor that might be involved in adipogenesis as well. Another study demonstrated the correlation of methamphetamine induction with an increase of the Nat8l protein "shati"[93]. Other factors which are influenced as well by drug abuse are the already mentioned factor CREB, FosB (as JunB a member of the AP-1 family), and TNF-α[94] which have also been reported to have effects on adipogenesis. If this accordance is a result of a concerted cause, an interaction between these factors or just a coincidence should be a matter of research in further studies. Nevertheless, this aspect delivers another reason for the investigation of Nat8l in adipose tissue. And last but not least the substrate acetyl-CoA which is involved in the catalytic reaction of aspartate to NAA is also a very important metabolite of many pathways inside adipocytes. Previous to this work, an expression pattern analysis of different murine tissues (also performed at the Institute of Genomics and Bioinformatics) showed the highest expression of Nat8l mRNA in brain, followed by BAT and WAT. In ob/ob mice the same analysis revealed a decrease of Nat8l expression in WAT compared to wild type mice, whereas the expression levels in brain and BAT were not influenced. Furthermore, it could be demonstrated that Nat8l is expressed in 3T3-L1 fibroblasts and elevated about 2-fold during the differentiation process. The murine Nat8l protein itself consists of 299 amino acids with a predicted molecular weight of approximately 33 kDa and has a 94.6 % identity of the homology of human Nat8l. The amino acid structure exhibits a transmembrane segment suggesting an endogenous location in membranes. Even though, there is a large progress in findings related to Nat8l and its functionality, especially the localisation is highly controversial. Wiame and colleagues detected the overexpressed Myc-tagged Nat8l through confocal microscopy exclusively in the endoplasmic reticulum

---

[91] Chakraborty et al., "Intraneuronal N‑acetylaspartate Supplies Acetyl Groups for Myelin Lipid Synthesis."
[92] Wiame et al., "Molecular Identification of Aspartate N-acetyltransferase and Its Mutation in Hypoacetylaspartia."
[93] Niwa et al., "A Novel Molecule 'Shati' Is Involved in Methamphetamine-Induced Hyperlocomotion, Sensitization, and Conditioned Place Preference."
[94] Cawthorn and Sethi, "TNF-alpha and Adipocyte Biology."

(ER) of CHO cells[95,96]. At the time of publication this was an unexpected observation because all previous investigations on this topic rather suggested a mitochondrial and cytoplasmic localisation. For example Patel and Clark proposed a mitochondrial localisation derived from their studies on rat brain in 1979[97]. These finding was supported by the group around Namboodiri through different experiments on cell fractions, but they also conceded that Nat8l localises to a smaller extent in microsomes containing the ER[98,99,100]. Later on, they were able to confirm their results through detection of endogenously expressed Nat8l by immunostaining in SH-SY5Y neuroblastoma cells[101]. Another publication from Lu also established the bimodal expression pattern of Nat8l in microsomes and mitochondria of brain, but controversial to Namboodiri their observations revealed the major amount of Nat8l activity in microsomes[102]. In summary, it can be stated that this issue as well as all other findings related to Nat8l, especially in fat tissue, will need further investigations to detect the actual localisation of Nat8l, the metabolic pathway/s in which it is involved and the factors by which it is affected.

This work is concerned with these questions to contribute to the enlightenment of the properties of Nat8l.

---

[95] Wiame et al., "Molecular Identification of Aspartate N-acetyltransferase and Its Mutation in Hypoacetylaspartia."

[96] Tahay et al., "Determinants of the Enzymatic Activity and the Subcellular Localization of Aspartate N-acetyltransferase."

[97] Patel and Clark, "Synthesis of N-acetyl-l-aspartate by Rat Brain Mitochondria and Its Involvement in Mitochondrial/cytosolic Carbon Transport."

[98] Madhavarao et al., "Characterization of the N-acetylaspartate Biosynthetic Enzyme from Rat Brain."

[99] Ariyannur, Madhavarao, and Namboodiri, "N-acetylaspartate Synthesis in the Brain."

[100] Arun, Moffett, and Namboodiri, "Evidence for Mitochondrial and Cytoplasmic N-acetylaspartate Synthesis in SH-SY5Y Neuroblastoma Cells."

[101] Ariyannur et al., "Methamphetamine-induced Neuronal Protein NAT8L Is the NAA Biosynthetic Enzyme."

[102] Lu et al., "N-Acetylaspartate Synthase Is Bimodally Expressed in Microsomes and Mitochondria of Brain."

3   Materials and Methods

3.1 Materials

3.1.1 Cloning

Aqua bidestillatat sterilis „Fresenius", Fresenius

Taq DNA polymerase (recombinant) 5 u/µL, Fermentas Inc.

10x Taq buffer with potassium chloride (KCl), Fermentas Inc.

Magnesium chloride ($MgCl_2$) 25 mM, Fermentas Inc.

Phusion® High-Fidelity DNA polymerase, Finnzymes

5x Phusion® HF reaction buffer, Finnzymes

Dimethyl sulfoxide (DMSO) 100 %, Finnzymes

dNTP-Mix 10 mM, Fermentas Inc.

PCR device: PTC-225 Peltier Thermal Cycler, MJ Research

peqGOLD Universal Agarose, Peqlab. Biotechnology GmbH.

Ethidium bromide solution (EtBr) 1 %, Roth

Tris ((-hydroxymethyl)-aminomethane) Ultra Quality 99.9 %, Roth

Acetate 96 %, Roth

Ethylenediaminetetraacetic acid (EDTA) 99 %, Roth

Hydrochloric acid (HCl) 1 mol/L, Roth

Glycerol 98 % Ph.Eur., water free, Roth

Bromophenol blue, AppliChem GmbH.

1 kb DNA Ladder, Fermentas Inc.

Gel electrophoresis:	Multi Sub Midi, Cleaver Scientific Ltd.
	Multi Sub Choice, Cleaver Scientific Ltd.
	MP-300V omniPAC, Cleaver Scientific Ltd.
	ComPhor L Midi, Biozym Scientific GmbH.
	ComPhor L Mini, Biozym Scientific GmbH.
	E 132 Power Supply, Consort
Heating block:	Thermomixer compact, Eppendorf
Laboratory water bath:	Isotemp 202 S, Fisher Scientific GmbH.
	1002, Gesellschaft für Labortechnik mbH. (GFL)
Centrifuge:	Centrifuge 5415 D, Eppendorf
Vortex mixer:	MS 2 Minishaker, IKA®-Werke GmbH. & Co. KG.
Mini-Centrifuge:	Rotilabo-mini-centrifuge, Roth

Gel visualisation: UV-Transilluminator Universal Hood, BioRad

DNA extraction: peqGOLD Gel Extraction Kit, Peqlab. Biotechnology GmbH.

DNA purification: „Pure Link^{TM} PCR Purification Kit", Invitrogen corp.

DNA quantification: Nano Drop ND-1000 Spectrophotometer,

Peqlab. Biotechnologie GmbH.

Sodium hypochlorite solution 12 % Cl (NaClO), Roth

FastAP thermosensitive alkaline phosphatase, Fermentas Inc.

T4 DNA ligase 1 u/μL, Fermentas Inc.

10x T4 DNA ligase buffer, Fermentas Inc.

MF-Membrane Filters Type: 0,025 μm VSWP, Millipore

NEB 5-alpha chemically competent E. coli cells, New England BioLabs® Inc.

One Shot® TOP10 chemically competent E. coli cells, Invitrogen corp.

S.O.C. Medium, Invitrogen corp.

Peptone from casein, Roth

Select agar, Sigma-Aldrich H. GmbH.

Yeast Extract, Sigma-Aldrich H. GmbH.

Sodium chloride (NaCl) 99,5 %, p.a., ACS, ISO, Roth

Plasmid purification: „Pure Link^{TM} Quickplasmid Miniprep Kit", Invitrogen corp.

PCR-primers:

primer name: Nat8l_pMSCV_EcoRI_fw_as , Invitrogen corp.

sequence: GTT **GAATTC** ATGCATTGTGGGCCTCCCGACA

5' + EcoRI designed as antisense primer

primer name: Nat8l_pMSCV_BglII_rv_as , Invitrogen corp.

sequence: GAT **AGATCT** TCACTCCTCGCGCAGATGCAG

3' + BglII designed as antisense & antiparallel primer

primer name: Nat8l_pEYFP-C1_XhoI_fw_-ATG , Invitrogen corp.

sequence: GAT **CTCGAG** *CT* CATTGTGGGCCTCCCGACATG

5' + XhoI with frameshift correction, without start codon

primer name: Nat8l_pEYFP-C1_EcoRI_rv_+TGA, Invitrogen corp.

sequence: TTC **GAATTC** TCACTCCTCGCGCAGCTGCA

3' + EcoRI antiparallel with stop codon

primer name: Nat8l_pECFP-N1_XhoI_fw_+ATG , Invitrogen corp.

sequence: TCT **CTCGAG** ATGCATTGTGGGCCTCCCGACAT

5' + XhoI with start codon

primer name: Nat8l_pECFP-N1_EcoRI_rv_-TGA , Invitrogen corp.

sequence: CGT **GAATTC** *G* CTCCTCGCGCAGCTGCAGGC

3' + EcoRI antiparallel, with frameshift correction, without stop codon

Vectors: „pMSCVpuro", Clontech Laboratories Inc.

„pHisMaxC", Invitrogen corp.

„pECFP-N1", Clontech Laboratories Inc.

„pEYFP-C1", Clontech Laboratories Inc.

Restriction enzymes & buffers: BglII, Fermentas Inc.

EcoRI, Fermentas Inc.

XhoI, Fermentas Inc.

ApaI, Fermentas Inc.

KpnI, Fermentas Inc.

10x Buffer O with BSA, Fermentas Inc.

10x Buffer B with BSA, Fermentas Inc.

10x Buffer R with BSA, Fermentas Inc.

10x Buffer KpnI with BSA, Fermentas Inc.

10x Buffer Tango with BSA, Fermentas Inc.

TAE Buffer (50x): 242 g Tris Ultra Quality

57,1 g Acetate

16,8 g EDTA

1 L dH_2O

LB-Medium (liquid, solid): 10 g Peptone

10 g NaCl

5 g Yeast

1 L dH_2O

15 g Select agar (just added to solid medium)

3.1.2 Cell culture

Cell lines:

3T3-L1 (mouse embryonic fibroblasts, adipose like)

Cos7 (fibroblasts, recovered from kidney of green vervet monkey)

Phoenix (human embryonic kidney cell line, retroviral expression system)

3 Materials and Methods

Chemicals:

       Dimethyl sulfoxide (DMSO), Sigma-Aldrich H. GmbH.

Additives & Buffers:

       Dexamethasone (DEX), Sigma-Aldrich H. GmbH.

       Foetal Bovine Serum (FBS), Invitrogen corp., Lot.Nr.:07F0483K

       Hexa-dimethrine-bromide (Polybrene 8 mg/mL), Sigma-Aldrich H. GmbH.

       3-Isobutyl-1-methylxanthine (IBMX), VWR International

       Insulin (Ins), Sigma-Aldrich H. GmbH.

       L-Glutamine (L-Glu) 200 mM, Invitrogen corp.

       Metafectene, Biontex Laboratories GmbH.

       Normocin, Eubio

       PBS pH 7.4, Invitrogen corp.

       Penicillin/Streptomycin (P/S) Soln. 10,000 U/mL / 10,000 µg/mL, Invitrogen corp.

       Trypsin/EDTA (10x) 0.5 % Trypsin 5.4 mM EDTA*4NA, Invitrogen corp.

       Puromycin dihydrochloride CELL CULTURE, Sigma-Aldrich H. GmbH.

Culture media:

       Standard medium (StdM):   Dulbecco's Modified Eagle Medium

                              (DMEM) +4.5 g/L Glucose++, Invitrogen corp.)

                       FBS 10 %

                       Normocin 1:500

                       L-Glu 2 mM

                       P/S 100 U/mL / 100 µg/mL

       Differentiation medium 1 (DM1):   StdM

                       DEX 1 µM

                       IBMX 0.5 mM

                       Ins 2 µg/mL

       Differentiation medium 2 (DM2):   StdM

                       Ins 2 µg/mL

3.1.3 RNA isolation

Cell culture cells:

„Gen Elute^{TM} Mammalian Total RNA Miniprep Kit", Sigma-Aldrich H. GmbH.

ß-Mercaptoethanol, Sigma-Aldrich H. GmbH.

RNA quantification:

Nano Drop ND-1000 Spectrophotometer,

Peqlab. Biotechnologie GmbH.

Sodium hypochlorite solution 12 % Cl (NaClO), Roth

3.1.4 cDNA synthesis

Aqua bidestillatat sterilis „Fresenius", Fresenius

Diethylpyrocarbonate (DEPC) added ddH$_2$O for molecular biology, Roth

Dithiothreitol (DTT) 0.1 M, Invitrogen corp.

5x First Strand Buffer, Invitrogen corp.

dNTP-Mix 10 mM, Fermentas Inc.

Oligo(dt) 12-18 Primer 0,5 μg/μL, Fermentas Inc.

Random Primer 3 μg/μL, Invitrogen corp.

Recombinant Ribonuclease Inhibitor (RNaseOut^{TM}) 40 u/μL, Invitrogen corp.

Super Script II H-Reverse Transcriptase 200u/μL, Invitrogen corp.

3.1.5 qPCR

SYBR QPCR Supermix W/Rox, Invitrogen corp.

qPCR-primers: *TfIIß* murine, Invitrogen corp.

fw.   GTC ACA TGT CCG AAT CAT CCA

rev.   TCA ATA ACT CGG TCC CCT ACA A

Nat8l murine, Invitrogen corp.

fw.   CGA CGG CAT CTT GGA GCG CA

rev.   AAA CAG AGG GCG GCC AGC AG

ACSL1 murine, Invitrogen corp.

fw.   TCC TAC AAA GAG GTG GCA GAA CT

rev.   GGC TTG AAC CCC TTC TGG AT

Dgat1 murine, Invitrogen corp.

fw.   GAC GGC TAC TGG GAT CTG A

rev.   TCA CCA CAC ACC AAT TCA GG

Dgat2 murine, Invitrogen corp.

fw.   CAC AGA CTG CTG GCT GAT AGC T

rev.   CGA TCT CCT GCC ACC TTT CTT

Acss1 murine, Invitrogen corp.

fw.   GAC ACA CTA GTT TGG GAC ACT C

rev.   CCC AGA TCA AAG CTA TGG TCT C

Acss2 murine, Invitrogen corp.

fw.   CTG AGT GGA TGA AAG GAG CAA C

rev.   CAG GAG TTC ACG GTA TGT GAT C

Aspa1 murine, Invitrogen corp.

fw.   CCA TAT GAA GTG AGA AGG GCT C

rev.   CCT CAA GAA TAA GAG TGC AAC C

Atf3 murine, Invitrogen corp.

fw.   CCC CGA GCG AAG ACT GGA GCA AA

rev.   GGG ACA ATG GCG GTC GCA CT

BiP murine, Invitrogen corp.

fw.   CGG GCC GAG GAG GAG GAC AA

rev.   ACA CCG ACG CAG GAA TAG GTG GT

CHOP10 murine, Invitrogen corp.

fw.   CTG CCT TTC ACC TTG GAG AC

rev.   CGT TTC CTG GGG ATG AGA TA

Retn murine, Invitrogen corp.

fw.   AAG AAG GAG CTG TGG GAC AGG

rev.   CAG CAG TTC AGG GAC AAG GAA

ABI Prism 7000 Sequence Detection System

3.1.6 Oil red O staining

Formaldehyde, Sigma-Aldrich H. GmbH.

Isopropyl alcohol, VWR International (Merck, Margaritella)

Oil Red O, ICN

Oil red O stock: 0.25 g Oil Red O

50 mL Isopropyl alcohol

3.1.7 Triglyceride quantification

Ultrasonic homogenizer Sonopuls, Bandelin electronic GmbH. & Co. KG.

Triglycerides, Fisher Scientific Company, LLC

Glycerol 98 % Ph.Eur.,water free, Roth

EIA/RIA 96-well plate, costar

Spectra max PLUS 384, Molecular Devices

"BCA Protein Assay Kit", Pierce

3.1.8 Protein quantification

"BCA Protein Assay Kit", Pierce

3.1.9 Western blot

Antibody 1:   anti-His-Tag, Amersham Bioscience, Prod. Code: 27-4710-01

Antibody 1:   anti-β-actin, Sigma-Aldrich H. GmbH.

Antibody 1:   anti-Nat8L, Novus Biologicals LLC

Antibody 2:   anti-mouse, Dako GmbH.

Antibody 2:   anti-rabbit, Dako GmbH.

Benzonase® Nuclease, Merck

Bovine serum albumin, PAA Laboratories GmbH.

Dithioerythritol (DTE), VWR International (Merck, Margaritella)

NuPAGE® NOVEX® 10 % Bis-Tris Gel 1,0 mmX 10 well, Invitrogen corp.

Hydrochloric acid (HCl) 1 mol/L, Roth

Glycerol 98 % Ph.Eur., water free, Roth

ß-Glycerophosphate, Sigma-Aldrich H. GmbH.

KS 260 basic, IKA®-Werke GmbH. & Co. KG.

LDS Sample Buffer 4x, Invitrogen corp.

Methanol, Sigma-Aldrich H. GmbH.

Sodium fluoride (NaF), VWR International (Merck, Margaritella)

NuPAGE®, MOPS SDS Running Buffer 20x, Invitrogen corp.

NuPAGE®, Antioxidant, Invitrogen corp.

Sodium-orthovanadate, Sigma-Aldrich H. GmbH.

PBS pH 7.4, Invitrogen corp.

Phenylmethanesulfonylfluoride (PMSF), Sigma-Aldrich H. GmbH.

Protease Inhibitor Cocktail Tablets (PIC), Roche Austria GmbH.

Roto shake genie, Scientific Industries Inc.

Roentogen Liquid, Tetanal

Roentogen Superfix, Tetanal

Seeblue® Plus2 Prestained Standard, Invitrogen corp.

Sodium Dodecylsulfate (SDS), AppliChem

SuperSignal® West Pico Chemiluminescent Substrate, VWR Int. (Merck, Margaritella)

Skim Milk Powder (NFDM), Fluka analytical AG.

TGS-Buffer (10x), Bio-Rad Laboratories GmbH.

Tris ((-hydroxymethyl)-aminomethane) Ultra Quality 99,9 %, Roth

Tween 20, VWR International (Merck, Margaritella)

Blocking solution 1 (BS1):　PBST

　　　　　　　　　　　　　　5% BSA

Blocking solution 2 (BS2):　TBST

　　　　　　　　　　　　　　5% NFDM

　　　　　　　　　　　　　　1% BSA

SDS Lysis Buffer:　Aqua bidestillata sterilis "Fresenius", Fresenius

　　　　　　　　　　Glycerol 10 % v/v

　　　　　　　　　　ß-Glycerophosphate 10 mM

　　　　　　　　　　NaF 10 mM

　　　　　　　　　　Na orthovanadate 100 μM

　　　　　　　　　　SDS 2,5 % v/v

　　　　　　　　　　Tris-HCL 50 mM

PBST:　　　Tween 20 0,05 %

　　　　　　PBS

Transfer Buffer Stock:　　Tris Ultra Quality 28 g

　　　　　　　　　　　　　Glycerol 143 g

　　　　　　　　　　　　　dH$_2$O 1000 mL

Transfer Buffer:　　Transfer Buffer Stock 10 % v/v

　　　　　　　　　　Methanol 20 % v/v

　　　　　　　　　　dH$_2$O 1000 mL

3.1.10 Fluorescence microscopy

Antibody 1:   anti-Nat8L, Novus Biologicals LLC

Antibody 2:   anti-rabbit with fluorophore Cy2, kind gift of Dr. Astrid Hammer

4′,6-Diamidino-2-phenylindol (DAPI), Merck

Glutaraldehyde (GA), Sigma Aldrich H. GmbH.

KS 260 basic, IKA®-Werke GmbH. & Co. KG.

Paraformaldehyde (PFA), Sigma Aldrich H. GmbH.

SlowFade Gold mounting medium, Invitrogen corp.

Triton X 100, Roth

Tween® 20, AppliChem GmbH.

3.1.11 Electroporation

Neon transfection system, Invitrogen corp.

       with   buffer R

                   buffer E for 10 µL tips

                   buffer E2 for 100 µL tips

Neon pipette, Invitrogen corp.

Neon tips 10 µL /100 µL, Invitrogen corp.

3.2   Methods

3.2.1   Cloning of Nat8l into vectors

The Nat8l-gene was cloned in antisense direction into the vector pMSCV as well as in sense direction into the vectors pECFP-N1 and pEYFP-C1.

Data of pMSCV:

The Murine Stem Cell Virus (MSCV) vectors were derived from the Murine Embryonic Stem Cell Virus (MESV) and the LN retroviral vectors[103,104]. Upon transfection into a packaging cell line, pMSCVpuro transiently expresses, or integrates and stably expresses, a transcript containing the extended viral packaging signal Ψ^+, the puromycin resistance gene, and a gene of interest. For this purpose the gene of interest must be cloned into the multiple cloning site beforehand of the transfection. To achieve a stable integration of the gene, like mentioned as second option previously, there need to be a pre-transfection of the vector into phoenix cells, which are capable of packaging the vector derived RNA into infectious, replication-in-competent retroviral particles. These particles can infect target cells and transmit the gene of interest. During the expression, translated transcripts contain the gene of interest (GOI) as well as a puromycin- and ampicillin-resistance,

(see: Figure 5) which can be used for the selection of cells containing the plasmid.[105]

---

[103] Grez et al., "Embryonic Stem Cell Virus, a Recombinant Murine Retrovirus with Expression in Embryonic Stem Cells."
[104] Miller and Rosman, "Improved Retroviral Vectors for Gene Transfer and Expression."
[105] Clontech, "pMSCVpuro Vector Information."

Figure 5: Vector map of cloning plasmid pMSCV

Data of pECFP/YFP:

pECFP and pEYFP encode an enhanced cyan fluorescent variant or respectively a yellow green variant of the Aequorea victoria green fluorescent protein gene (GFP).The ECFP gene contains six amino acid substitutions. The Tyr-66 to Trp substitution gives ECFP fluorescence excitation (major peak at 433 nm and minor peak at 453 nm) and emission (major peak at 475 nm and a minor peak at 501 nm) similar to other cyan emission variants[106,107]. The other five substitutions enhance brightness and solubility of the protein, primarily due to improved protein folding properties and efficiency of chromophore formation[108,109,110]. The EYFP gene contains four amino acid substitutions. The fluorescent excitation maximum of EYFP is 513 nm and the emission spectrum has a peak at 527 nm (in the yellow green region). The vectors contain an SV40 origin for replication and a neomycin resistance (Neo[r]) gene for selection in eukaryotic cells. A bacterial promoter (P) upstream or Neo[r] expresses kanamycin resistance in E. coli which can be

---

[106] Heim, Prasher, and Tsien, "Wavelength Mutations and Posttranslational Autoxidation of Green Fluorescent Protein."
[107] Miyawaki et al., "Fluorescent Indicators for Ca2+ Based on Green Fluorescent Proteins and Calmodulin."
[108] Heim and Tsien, "Engineering green fluorescent protein for improved brightness, longer wavelengths and fluorescence resonance energy transfer."
[109] Cormack, Valdivia, and Falkow, "FACS-optimized Mutants of the Green Fluorescent Protein (GFP)."
[110] Yang, Cheng, and Kain, "Optimized Codon Usage and Chromophore Mutations Provide Enhanced Sensitivity with the Green Fluorescent Protein."

used for bacterial selection to ensure the incorporation of the vector inside the cells. The vector backbone also provides a pUC19 origin of replication for propagation in E. coli and a f1 origin for single-stranded DNA production recombinant vectors can be transfected into mammalian cells using any standard transfection method.

The MCS of pEYFP-C1 is located between the CDS of the fluorescence protein and the stop codon. Genes cloned into the MCS will be expressed as fusion to the C-terminus of the fluorescence protein if they are in the same reading frame (see: Frameshift correction) and there are no intervening in-frame stop codons (see: Figure 6). The fluorescence protein with a C-terminal fusion moiety retains the fluorescent properties of the native protein and thus can be used to localise fusion proteins *in vivo*.

The MCS in pECFP-N1 is between the immediate early promoter of CMV ($P_{CMV\ IE}$) and the ECFP CDS (see: Figure 7). Genes cloned into the MCS will be expressed as fusion to the N-terminus of ECFP if they are in the same reading frame (see: Frameshift correction) as ECFP and there are no intervening stop codons. The inserted gene should include an initiating ATG codon. ECFP fusion proteins retain the fluorescent properties of the native protein *in vivo*.[111,112]
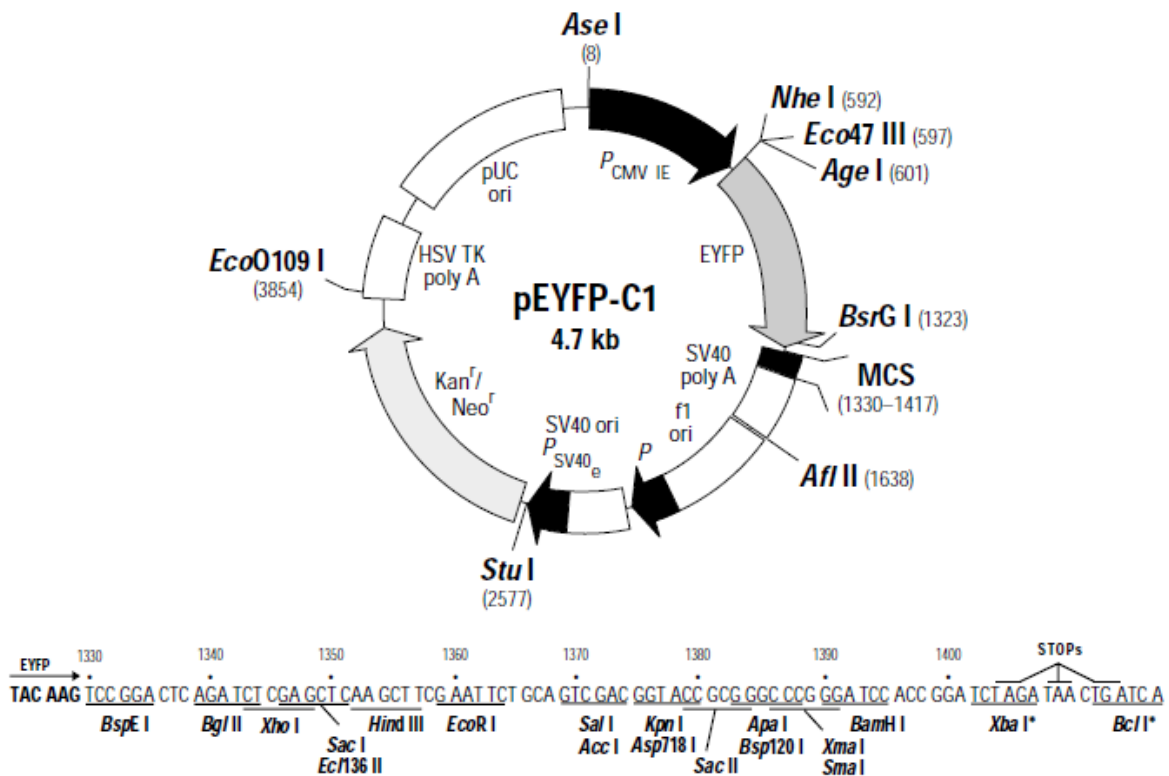
Figure 6: Vector map of cloning plasmid pEYFP-C1

---

[111] Clontech, "pEYFP-C1 Vector Information."
[112] Clontech, "pECFP-N1 Vector Information." (original reference from clontech is not available anymore)

GCTA GCG CTA CCG GAC TCA GAT CTC GAG CTC AAG CTT CGA ATT CTG CAG TCG ACG GTA CCG CGG GCC CGG GAT CCA CCG GTC GCC ACC **ATG GTG**
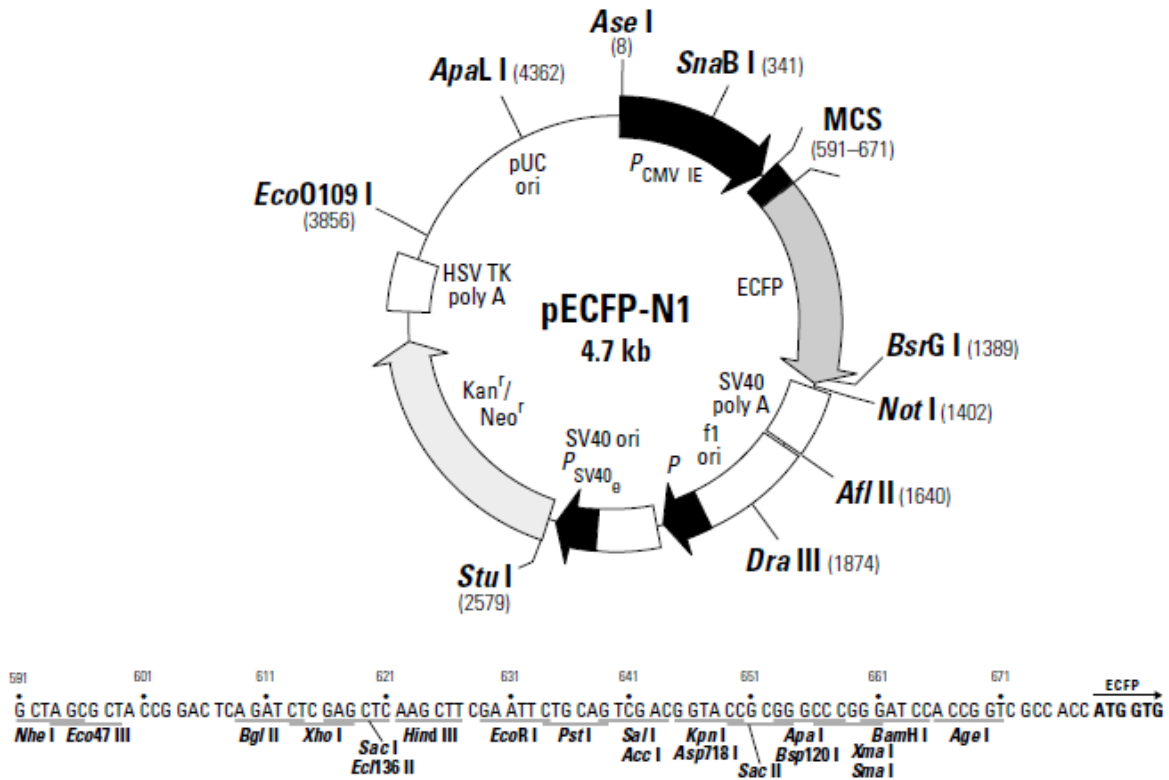
Figure 7: Vector map of cloning plasmid pECFP-N1

Primer design and cloning process:

All used vectors contain a multiple cloning site (MCS) with several restriction enzyme cutting sequences included, which do not occur any further in the rest of the plasmid. With the help of these endonucleases, it is possible to clone a GOI (on a specific position inside the MCS) to achieve the desired expression after transfection of the vector in a target cell line. Furthermore, the vector contains other cutting sites for endonucleases, which can be used for control cut-analysis, and the pUC origin of replication for propagation in bacteria. At the beginning of the cloning process, the GOI coding sequence (CDS) was amplified by the usage of the polymerase chain reaction (PCR). Prior to this step, the needed primer design was realized in consideration of the required mounting direction in such a way that the achieved primer DNA fragments had a bonding site fitting to the designated restriction enzymes on both ends. For the vector pMSCV an integration in antisense direction was requested, due to that the forward primer (fw-primer) contained the specific sequence for EcoRI and the reverse primer (rv-primer) that of BglII (5' located in the MCS in comparison to EcoRI). For the remaining vectors the CDS was integrated in sense direction, therefore the fw-primers contained a specific sequence of an endonuclease with a cutting position which is located 5' inside the MCS compared to that one of the rv-primers

restriction enzymes sequence. To determine the exact endonucleases of the primers see subsection PCR primers (see: 3.1.1).

Frameshift correction:

When searching for proper restriction sites in the MCS, it is important to control that the used endonucleases don't cut the vector in a way that produces a frameshift. Meaning that there is no shift of the DNA sequence which would lead to a wrong order of the base triplet coding, further leading to a wrong amino acid. Quite different from pMSCV, the DNA of the other vectors is cut right inside a base triplet by XhoI and EcoRI, causing a misarrangement of the amino acid coding. To prevent this error 1-2 dNTPs were added in between the cutting location and the CDS during the primer design process, leading to a frameshift correction which puts the base triplet coding back to right order thereby granting a correct translation of the CDS (see: 3.1.1).

Another important point relating to a correct primer design was the presence or the absence of start and stop codons from the cloned DNA fragments. The antisense cloning procedure never meant to generate translatable mRNA fragments but should deliver mRNA fragments which are capable of binding to the normal expressed Nat8l mRNA and build up double stranded products which cannot be translated into proteins, leading to a knock down of the normal expression of the gene. Hence to that the complete CDS of Nat8l was integrated into the pMSCV vector in antisense direction leading to a mRNA sequence complementary to the original Nat8l sequence and does not contain the start and stop codon in the regular form but a untranslatable mirror image version. For the fluorescence cloning this point appears in a completely different way because it is essential to produce translatable mRNA of fusion proteins to achieve the possibility to localise them. To assure this possibility there must not be any start or stop codon within the fusion protein otherwise the translation of the fusion protein would be disturbed. An intervening stop codon for example of the Nat8l gene which is cloned inside the vector pECFP-N1, where the MCS is prior to the fluorescence protein, would interrupt the translation right before the mRNA of ECFP and prohibit the development of a fusion protein. To prevent this error the applied primers were designed in a way which eliminates the stop codon of the Nat8l CDS during the amplification process (see: 3.1.1). Even though start codons don't seem to show such drastic effects, the ATG start codon of Nat8l was eliminated as well for the

cloning into pEYFP-C1 to exclude possible interferences during the translation process. To achieve a suitable primer, several different primer design tools were used.[113,114,115,116,117] As template for the CDS of the Nat8l gene during the amplification process served cDNA of BAT tissue as well as cDNA of differentiated 3T3-L1 cells which already stably contained a plasmid of Nat8l included into pMSCV in sense direction. The procedure itself was realized with the help of a PTC-225 Peltier Thermal Cycler. Implemented temperature programs are shown in the figures below. The first one shows the temperature curve of the amplification of the Nat8l CDS for pMSCV cloning (see: Figure 8) while the second one delivers the same information for the pECFP/pEYFP cloning (see: Figure 9). The temperature profiles show that the amplification was always realized through a 3 step PCR, which was already defined during the primer design process.
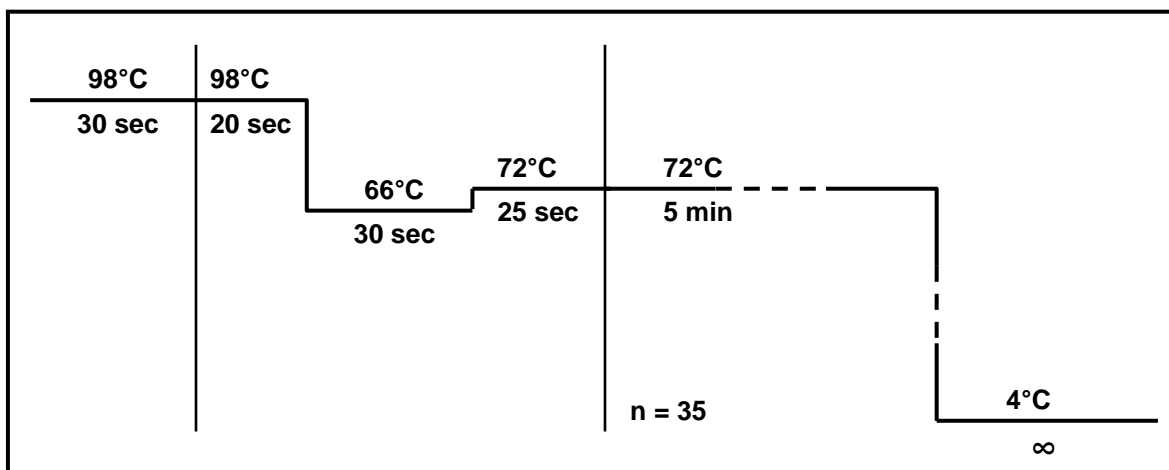
Figure 8: Temperature program for PCR of pMSCV

[113] "Tm Calculator - Finnzymes."
[114] "OligoCalc: Oligonucleotide Properties Calculator."
[115] "Primer Designing Tool."
[116] "The Mfold Web Server."
[117] Zuker, "Mfold Web Server for Nucleic Acid Folding and Hybridization Prediction."
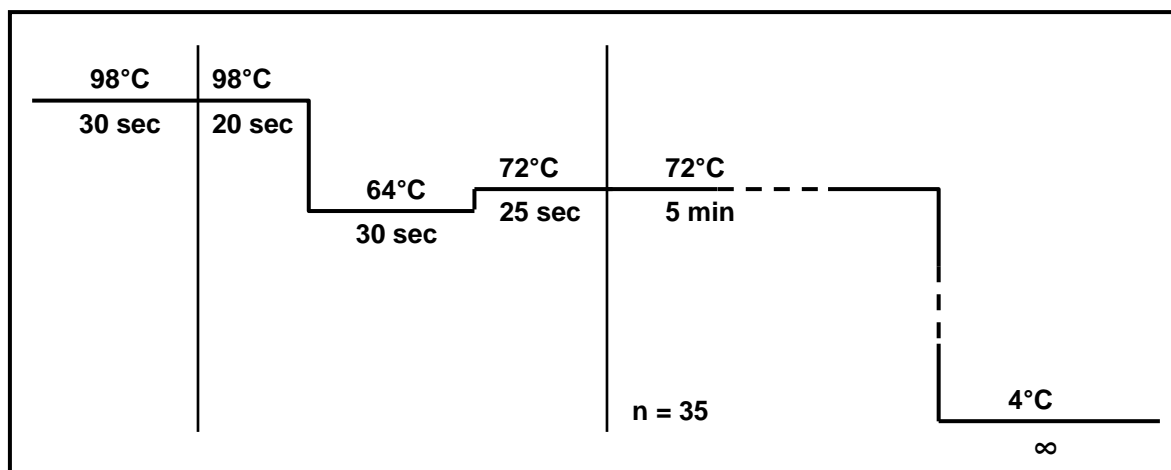
Figure 9: Temperature program for PCR of pEYFP-C1 and pECFP-N1

The amplification step is followed by the digestion of the received DNA fragments of Nat8l gene and the used vectors. For the antisense cloning into pMSCV, Nat8l as well as the vector were digested with EcoRI and BglII endonucleases and for the cloning into pECFP-N1 and pEYFP-C1 the amplified Nat8l gene DNA and the vectors were digested with EcoRI and XhoI. To determine the appropriate method conditions, the double digest tool from Fermentas[118] was consulted and the process was carried out as Fermentas suggested. The received products were purified and afterwards ligated using T4 DNA ligase (Fermentas inc.), followed by a transformation into E. coli NEB 5-alpha or Top10 cells for propagation. The amplified plasmids were recovered and purified using a miniprep kit. To ensure that the plasmids contain the requested Nat8l gene, a control restriction digesting was done. Therefore, the pMSCVpuro construct was cut by ApaI/KpnI and by a second digestion by EcoRI/BglII while the constructs of pECFP-N1 and pEYFP-C1 were cut by ApaI.

3.2.2 Cell culture

3.2.2.1 Handling

- Storage:

  For the cultivation process of cells it is necessary to have the possibility to store them over longer periods of time. For this purpose cells were kept deep frozen in liquid nitrogen tanks. The cryopreservation medium consists of StdM (standard

---

[118] "DoubleDigest™ Tool from Fermentas."

medium) which was containing 5-10% DMSO to prevent cell death during the conservation time.

The thawing of the cells had to be done very quickly, followed by a immediate dilution with 37°C warm StdM in a ratio of 1:10 to avoid cell death caused by the added DMSO. After a 24 h settling time the medium was changed with fresh standard medium to remove any residual DMSO.

- Cultivation:

3T3-L1, Cos7 and phoenix cells were cultivated in StdM which was refreshed every three days.

- Splitting:

To keep the proliferation process of a cell line going it is essential to avoid confluence especially for 3T3-L1 cells. So the cells were split at suitable intervals with 60-80% of confluence. For this purpose the present medium was removed and the cells were washed twice with PBS solution. To detach the cells from the bottom of the dish a trypsin solution (1mL for a $75cm^2$ growth plate) was added. The reaction was stopped by the addition of prewarmed StdM. The received cell suspension was used to seed the cells into various dishes.

3.2.2.2 Differentiation

The differentiation of 3T3-L1 cells was started 2 days after reaching confluence by the usage of a standard hormonal cocktail (differentiation medium 1, DM1), this point of time was defined as day 0. On day 3 the initial differentiation medium (DM1) was substituted through differentiation medium 2 (DM2) and on day 5 changed with StdM which was refreshed every two days from then on. To investigate whether the cells possess the ability to differentiate without this hormonal stimulus or with addition of only insulin to the medium, the differentiation process was also continually observed with just using StdM or DM2 until day 5.

3.2.3 Transfection

Data of Phoenix cells:

Phoenix cells are a second-generation retrovirus producer cell-line for the generation of helper free ecotropic and amphotropic retroviruses. The lines are based on a modified 293T human embryonic kidney cell line.[119]

Data of Cos7 cells:

The COS cell line was obtained by immortalizing a CV-1 cell line derived from kidney cells of the African green monkey with a version of the SV40 genome that can produce large T antigen but has a defect in genomic replication. COS stands for CV-1 origin, SV-40. When an expression construct with an SV40 promoter is introduced into COS cells, the vector can be replicated substantially by the large T antigen.

For some investigations it was necessary to transiently integrate foreign DNA into Cos7 or phoenix cells. This request was achieved by a metafectene transfection method which enables the entry of plasmids into cells. Metafectene provides the possibility to change the plasmid structure in a way which is much more compact than under normal conditions. Furthermore, it destabilises the electrostatic force of repulsion between DNA and the lipid membrane leading to better accessibility of the plasmids. Prior to transfection (~ 30 min), the StdM had to be changed to StdM without FBS. Meanwhile, 1 µg DNA per 6-well was added to 50 µL StdM without FBS and 4.5 µL metafectene per µg DNA were diluted in 50 µL StdM without FBS. Immediately after the preparation was finished, both solutions were gently mixed together and left at room temperature for 15-20 min. After the resting time, the metafectene-DNA mixture was added to the transfection medium (StdM without FBS) extremely cautious. It was made sure that the cells were not directly affected from the pipetting. After a 4 h incubation time, the transfection medium was replaced through StdM. 48-72 h later the maximum expression was reached. The transfection of a Nat8l containing plasmid into Cos7 cells was carried out to obtain an increased protein expression of Nat8l. These products served for protein assays and western blot studies. The transfection of the Nat8l_pMSCV plasmid into phoenix cells delivered a supernatant which was collected and contained amphotropic lentiviral particles. This solution was used for stable integration of the Nat8l DNA in 3T3-L1 cells through transduction. To examine the transfection success an empty vector was transfected as well as a negative control.

---

[119] "Phoenix Cell Line."

3.2.4 Transduction

The transduction of foreign DNA was realized by using lentiviral particles as carriers which were achieved from transfected phoenix cells. This method integrates the DNA stably into the 3T3-L1 cells. Before the transduction could be started, 3T3-L1 had to be seeded into 6-well plates and cultivated until the cells reached 30-40 % of confluence. At the beginning of the transduction, 1 mL of the supernatant containing the lentiviral particles was mixed with 1 mL of StdM. Polybrene was added to this solution at a final concentration of 6 μg/mL leading to higher transduction efficiency. (This is caused through the ability of polybrene as polycation to neutralize the electrostatic repulsive force between sialic acid of the cellular membrane and the pseudoviral capsid.) To obtain information about the success of the transduction a selection control (untransduced cells) was used additionally to the investigated probes. The 3T3-L1 cells were incubated over night to ensure a high transduction rate. If the cells are treated over a longer period of time with polybrene it becomes toxic to the cells and therefore the medium had to be removed after the incubation time and replaced with StdM. As selection reagent puromycin was added to the StdM at a final concentration of 3 μg/mL over a period of 7 days or at least until all cells of the selection control were dead. Successfully transduced cells survived this treatment due to the resistance abilities of the plasmid. These cells were transferred to a 75cm^2-flask and cultivated in normal StdM. The expression of the Nat8l gene during the differentiation progress, in stable integration studies, was evaluated with qPCR. Researches on the influence of transiently integrated DNA always requested fully differentiated cells prior to the transfection. The expression changes of these cells were also investigated with the help of qPCR analysis.

3.2.5 RNA isolation

For RNA isolation of cultivated cells, the StdM was removed and the cells were washed twice with PBS. Afterwards the "Gen Elute^{TM} Mammalian Total RNA Miniprep Kit" was used for the isolation steps of RNA. The procedure was realized like described in the instruction except of the elution step. The column bound RNA was resuspended through centrifugation with 30 μL of DEPC treated ddH$_2$O at a speed of 16,000 g for 1 min. This step was repeated once with the same solution to achieve a higher RNA recovery. The obtained RNA was stored at -80°C.

3.2.6 cDNA synthesis

The isolated RNA had to be transcribed to cDNA for qPCR analysis. For that purpose, up to 1 µg isolated RNA was mixed with 1 µL Oligo(dt), 1 µL Random Primers (300 ng/µL), and 1 µL dNTP mix (10 mM). The received solution was filled up to 12 µL with DEPC treated ddH$_2$O and heated to 65°C for 5 min to destroy the secondary structure and subsequently chilled on ice. Afterwards, the content of the tube was collected by brief centrifugation and gently mixed with 4 µL 5x First Strand Buffer, 2 µL 0.1 M DTT, and 1 µL RNAseOUT, followed by an incubation at 37°C for 2 min. Then 1 µL of reverse transcriptase "Super Script II" was added and mixed gently by up and down pipetting. Due to the usage of Random Primers the samples were incubated at 25°C for 10 min and then put at 37°C for 50 min. The reactions were inactivated at 70°C for 15 min and stored at -20°C.

3.2.7 qPCR

qPCR is based on the normal polymerase chain reaction (PCR) which is able to manifold exactly defined DNA sequences. The reproduction level reaches from normally 3 kbp even up to 40 kbp with special polymerases. qPCR is furthermore able to quantify the amount of these DNA sequences during the exponential production. If the reaction reaches saturation the analysis won't deliver any valuable results any more. The quantification procedure itself requires a fluorescent. During this study, SYBR-green was used to fulfil this function. The maximum absorption wavelength of SYBR-green is 498 nm which lies within the blue light spectrum. SYBR-green, as the name suggests, emits green light at a maximum wavelength of 522 nm when bound to double stranded DNA (dsDNA) after absorption. So there is a direct correlation between dsDNA amount and emitted light intensity which can be measured and delivers usable data.

To perform one qPCR run, the cDNA was solved in DEPC treated ddH$_2$O until a final concentration of 1 ng/µL. From this solution 4.5 µL were added to 4.5 µL of 800 nM primers and 9 µL SYBR-green. The temperature curve of the used qPCR program is shown in the figure below. (Figure 10)
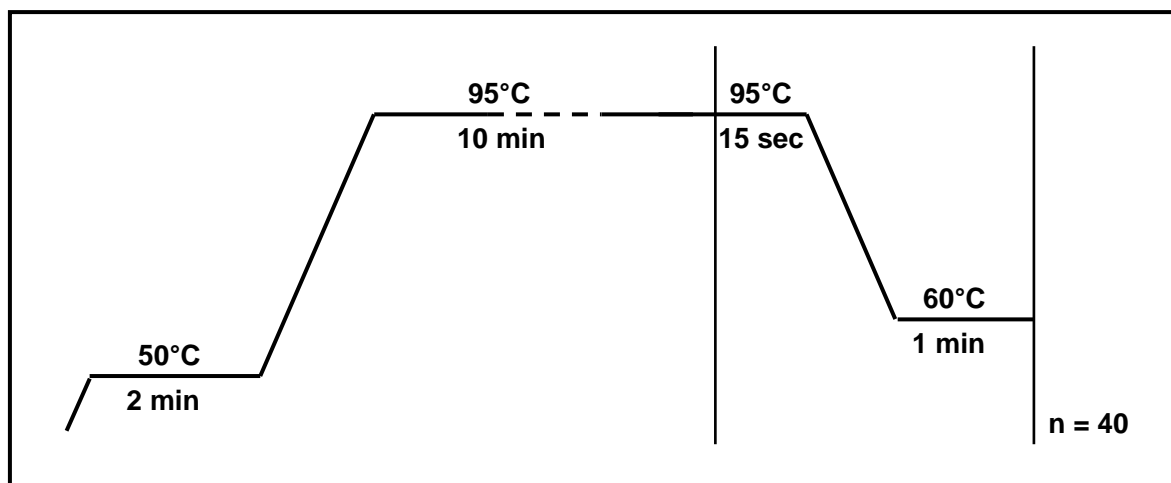
Figure 10: Temperature program for qPCR

3.2.8 Oil red O staining

Oil red O is a fat soluble colour, staining specifically fat droplets in the cytoplasm. First step of an Oil red O staining was to wash the cells twice with PBS followed by a fixation with formaldehyde (10% formalin) for 30 min. The beforehand made Oil red O stock (see: 3.1.6) was diluted with ddH$_2$O in a ratio of 6:4 and filtered through filter paper (1, Ø 110 mm). Then the formaldehyde was aspirated and the filtered Oil red O solution was cautiously pipetted onto the cells and incubated for 1 h. Afterwards the fixed and stained cells were washed twice with ddH$_2$O and instantly photographed for investigation. The stainings were stored covered in ddH$_2$O at +4°C.

3.2.9 Triglyceride quantification

The medium was removed and the cells were washed with PBS twice. Then, depending on the predicted triglyceride amount, the cells were harvested with 150 µL up to 500 µL PBS. The samples were sonicated with an ultrasonic homogenizer programmed on 40% power for 20 sec. During this process the probes were kept on ice. This step was repeated if the harvesting volume of PBS was higher than 250 µL. Through this treatment the cell membrane should be broken up and the triglycerides are dissolved in the solution. For the calibration curve a 4 mM glycerol stock was diluted with PBS rendering the following concentrations: 2 mM, 1 mM, 0.5 mM, 0.25 mM, 0.125 mM, 0.0625 mM, 0.03125 mM, and 0 mM glycerol. 6 µL of every standard series sample was pipetted into wells of a 96-well plate in duplicates. Afterwards the samples, which were previously slightly mixed with the pipette, were also analysed in duplicates. Subsequently, 200 µL of the triglyceride

solution (fisher scientific) was added to each well followed by an incubation time of 10 min at 37°C. The evaluation of the triglyceride content was done by the usage of the Spectra Max Plus384 absorbance micro-plate reader with a wavelength of 500 nm. To analyse the triglyceride content exactly, it had to be related to the protein amount in the samples. The level of proteins where determined by modified usage of the BCA protein assay kit from Pierce. In contrast to the suggested 0.9 % NaCl solution, we used PBS for dilution of the samples. Furthermore, no lysis buffer was added to the sonicated samples. The rest of the procedure was done as described in the user manual.

3.2.10 Protein quantification

The protein quantification was done with the help of the "BCA Protein Assay Kit", produced by Pierce. The method was carried out like described in the manual.

3.2.11 Western blot

3.2.11.1 Harvest

For the western blot analysis, the cell harvest started with a lysis buffer preparation which consists of 100 µL SDS lysis buffer, 1 µL PIC and 1 µL PMSF per well. The cells were washed twice with PBS after the medium was removed. Then 100 µL of the prepared lysis buffer were added per well. The cells were scraped off and stored at -20°C.

Before the samples were loaded onto the gel, they were digested with benzonase to achieve an easier handling of the probes. This process was started by heating the probes at 96°C for 5 min. The samples were chilled back to room temperature and centrifuged very shortly to collect the condensed fluids. Afterwards, 1 µL benzonase was added to the samples and incubated at room temperature for 45 min followed by a centrifugation at 13 000 rpm for 2 min. The supernatant was used for gel electrophoresis.

3.2.11.2 Gel electrophoresis

To investigate to which amount a specific protein was present in the harvested cell probes, they had to be separated according to their size and charge with the help of gel electrophoresis. Prior to this step, protein quantification was carried out to receive information about the whole protein quantity in a probe. Afterwards 20 µg (up to 40 µg if necessary) of protein were mixed with 1 µL 0.5 M DTE. The used probe volume varied between 30 µL and 40 µL. Depending on the decided volume 4x LDS was diluted to 1x concentration by filling up with ddH$_2$O. The used standard was prepared of 5 µL 4x LDS,

10 µL Seeblue® Plus2 Prestained Standard and 15 µL ddH$_2$O. Before loading the samples on the gel, they were incubated at 70°C for 10 min to denaturize the proteins. During the incubation time a 10 % NuPAGE$^{®}$ NOVEX$^{®}$ Bis-Tris Mini Gel was inserted into the Biorad western blot chamber. 10 % was chosen due to the size of the Nat8L protein. The chamber was filled with 600 mL of NuPAGE MOPS SDS running buffer which was diluted with dH$_2$O to a single concentration. After the loading of the probes and the standard, the gel was run for about 1 h at 175 V constant DC.

3.2.11.3 Transfer

For the following immunoassay investigations, the proteins were transferred to a membrane after the gel electrophoresis. Once again the charge properties of the proteins were used to move them inside a homogeneous electric field directed to the anode onto the membrane. For that purpose, the membrane was activated in dH$_2$O for 30 sec. The transfer buffer was prepared like described in subsection materials (see: 3.1.9) and the membrane, filter papers, gel, and felt were soaked with it. Then, these materials were placed on top of each other in the order which is shown in the figure below (see: Figure 11) and put into the transfer plate which was inserted into the transfer chamber afterwards. Furthermore, the transfer buffer was filled into the transfer chamber right after placing a cooling pack in it. The transfer process was realized at 120 V DC for 1.5 h in a 4°C room.
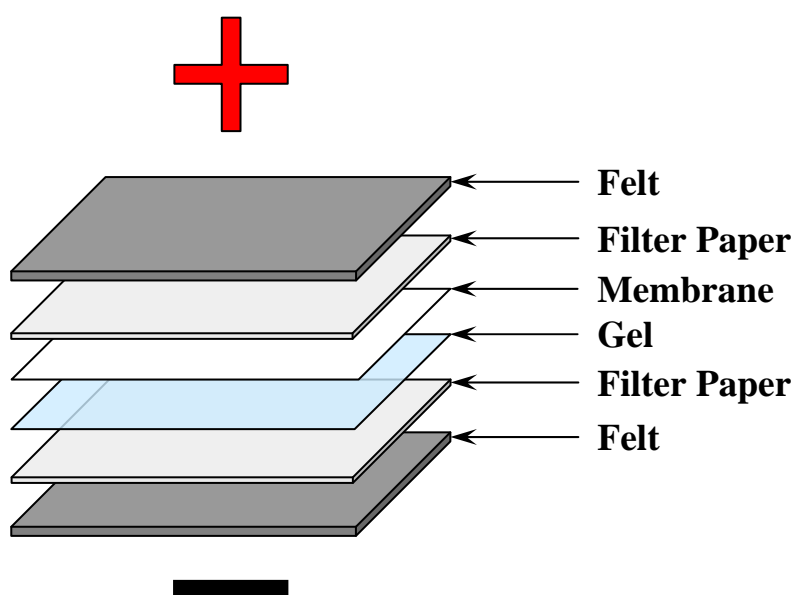
Figure 11: Structure of WB transfer stack

Due to the fact that the later used antibodies are proteins itself, the membrane was blocked for 1 h in a blocking solution to prevent unspecific binding of them right after the transfer. Subsequently, the membrane was washed three times in PBST or TBST according to the used blocking solution.

3.2.11.4 Incubation

Following the transfer, the membrane was incubated with two antibodies. The first antibody was diluted in 6 mL of the used blocking solution. The used ratios were 1:300, 1:500 and 1:1000 for Nat8L, 1:6000 for anti-His and 1:250 000 for β-actin. The Nat8L antibody binds specifically to the Nat8L protein, anti-His combines with the His-Tag of the proteins produced from the vector pHisMaxC, and β-actin is used as a loading control. The first antibody was incubated at 4°C over night on a 360° rotator. After a triple wash, each time for 10 min with PBST or TBST depending on the used blocking buffer, the diluted second antibody was added and the blot was put on a 360° rotator at room temperature for 2 h. The dilutions for the second antibodies, which bind to the first one, were 1:1000 or 1:3000 for anti-mouse and 1:5000 for anti-rabbit antibodies. Finally, the membrane was washed once again three times with PBST or TBST each time for 10 min.

3.2.11.5 Exposure

The visualisation process starts by mixing 1.5 mL of each of the "Super Signal West Pico" solutions. The received reagent was pipetted on the membrane and incubated for 5 min. Afterwards, the solution was removed and the membrane was kept in a cling film to avoid drying. The "fluorescing" light of the antibodies was detected by the usage of a photo paper (exposure time was adjusted to the varying light intensity of the antibodies) which was developed with Roentogen Liquid and Roentogen Superfix and finally washed with dH$_2$O.

3.2.12 Fluorescence microscopy

Fluorescence microscopy is a method to localise a protein of interest intracellularly. This delivers information about the place of action of the investigated protein and can furthermore give some indications of the properties of the protein. Two different variants of this technique were implemented for investigating the Nat8L protein.

3.2.12.1 Fluorescence microscopy of overexpressed Nat8L

For this type of investigation, Nat8l was cloned into the two vectors pECFP-N1 and pEYFP-C1 (see: 3.2.1). 3T3-L1 cells were grown in 75 cm^2 and 10 cm dishes to confluence and differentiated (see: 3.2.2.2) until d6. For additional analysis there were also undifferentiated 3T3-L1 cells in use which had not reached confluence. The vectors were transfected into the cells through electroporation. Prior to this step, cover slips were flamed-scarf with the help of 70 % EtOH and put into 6-well plates. All used 6-wells were filled up with StdM without Normocin and Pen/Strep. Then, the differentiated 3T3-L1 cells were electroporated with the plasmids Nat8l_pECFP-N1, Nat8l_pEYFP-C1, and the empty fluorescence vectors. The fluorescence vectors containing the Nat8l gene were also electroporated into undifferentiated 3T3-L1 cells and as a negative control differentiated 3T3-L1 cells were electroporated without the usage of a vector. For the exact procedure see subsection electroporation (see: 3.2.13). 3 μg vector DNA were used for one electroporation using 10 µL tips and 80000 cells. The trypsin reaction to loosen the cells was stopped by StdM without antibiotics and after a centrifugation step at 1200 (differentiated cells) or 1600 (undifferentiated cells) rpm for 3min and 30 sec the supernatant was removed and the cells were resuspended in PBS. The second centrifugation was done with the same speed and duration like the first one. Subsequently, the PBS was removed and the cells were resuspended with buffer R according to the counted cell number to achieve the 80000 cells per electroporation. 48 h after the transfection, the cover slips were placed on microscopy slides and analysed by a Zeiss Axiolmager Z1 epifluorescence microscope equipped with a Zeiss AxioCam MRm CCD camera.

3.2.12.2 Fluorescence microscopy of endogenous Nat8L expression

To evaluate the localisation of the endogenous expressed Nat8L, another method of fluorescence microscopy was realized. Therefore, cells were cultivated in 6-well plates each of these 6-wells contained a cover slip which was sterilised through brief inflammation with 70 % EtOH. During the growth period of the cells they were kept in StdM. After the cells reached confluence especially on the slips, they were differentiated as explained above in subsection differentiation (see: 3.2.2.2). On day four after addition of DM1, the medium was aspirated and the cells were washed once with PBS. Then, the cells were fixed with 0.2 % Glutaraldehyde and 2.0 % PFA in PBS for 15 min. During this time, it was assured that no vibrations disturbed this process. Afterwards, the cells were

quenched with 60 mM glycin in PBS at pH of 8.5 and subsequently washed with PBS three times for 5 min. The permeabilization was done by addition of 1.5 mL of 0.2 % Triton X 100 in PBS for 5 min at 4°C followed by a triple PBS washing step for 5 min. The cover slip was split with a RNAse free diamond cutter. On a microscopy slide 12.5 μL of a solution consisting of 1 μL antibody 1 (Nat8L) and 100 μL of 4 % BSA, 0.1 % Tween 20 in PBS was prepared. The slip fragments were applied to this microscopy slide and incubated in a humid chamber at 4°C over night. As an additional negative control of the immuno detection, one of the cover slip pieces was incubated without the usage of antibody 1. On the next day, the cover slip pieces were washed three times with PBS for 5 min. Then the cells were incubated with the second antibody containing a fluorophore (anit-rabbit) which was diluted 1:300 with the same Tween 20, BSA, and PBS solution like the first antibody for 1 h. After a last triple washing procedure with PBS for 5 min each time, the nuclei were counterstained for 5 min with 0.05 μg/mL DAPI in PBS. The cover slips were mounted on microscopy slides with approximately 5 μL mounting medium.

The images were taken with the same fluorescence microscope and the same equipment as mentioned in the subsection fluorescence microscopy of overexpressed Nat8L.

(see: 3.2.12.1)

3.2.13 Electroporation

Electroporation was used as transfection method to investigate the influence of Nat8l overexpression in 3T3-L1 cells after the differentiation. For this purpose, the Neon[TM] transfection system from Invitrogen was employed which offers a quite high transfection rate under right terms. Prior to the transfection, cells were grown on 75 cm^2 or 10 cm dishes to confluence and differentiated like described in subsection differentiation

(see: 3.2.2.2). After aspiration of growth medium, the cells were washed once with PBS. Then, a trypsin solution containing 0.5 mg/mL collagenase was added to the cells, and incubated at 37°C for 3 min (when cells were gathered with PBS) or 3 min and 30 sec (when cells were gathered with StdM without antibiotics). During this time, 2 mL of growth medium without normocin or pen/strep were filled in the later used 6-well plates which were given at 37°C until utilization. After the incubation, the cells were collected in a 15 mL falcon and centrifuged at 1000-1200 rpm for 3 min and 30 sec. The supernatant was removed and the cells were resuspended in up to 10 mL PBS. 30 μL of this solution was used for cell count and the rest was centrifuged a second time at the same speed and

duration as before. Afterwards, the supernatant was removed once again and the cells were resuspended in buffer R according to the requested electroporation amount of cells.

(80000 cells for 10 µL tips and 300000 cells for 100 µL tips). The plasmid DNA amount was 0.5 µg per electroporation when using 10 µL tips and 1 µg when using 100 µL tips. To achieve a higher cell rate when using 10 µL tips, three electroporations were added to each well. According to the calculated number of electroporations, the needed plasmid DNA volume was combined with the adequate quantity of cells. (To avoid problems during the electroporation procedure, 1 or 2 abundant electroporations were added to the total number. The reason for this rest is to prevent bubbles inside the pipette tip which would interfere with the electroporation process.) After filling 3 mL of buffer E (for 10 µL tips) or buffer E2 (for 100 µL tips) into the Neon tube, the cells were electroporated at 1400 V for 20 ms with one or two pulses. Prior to every electroporation, the cell suspension was mixed gently. After the electroporation, the cells were pipetted into the previously prepared 6-well plates. Thereafter, the plates were rocked gently to assure even distribution of the cells. Finally, the cells were incubated at 37°C with 5 % CO_2 and 95 % humidity.

4   **Results**

4.1 Silencing of Nat8l through overexpression of antisense RNA of the Nat8l gene CDS in 3T3-L1 cells

To investigate the possible functional influence of Nat8l on adipocyte differentiation, it was tried to silence the endogenously expressed Nat8l gene through stable overexpression of an antisense construct of the Nat8l CDS. The idea behind this attempt lies in the inhibition of the translation due to the building of dsRNA fragments consisting of the endogenously expressed Nat8l mRNA and the antisense RNA construct of the Nat8l gene CDS. For that purpose, the Nat8l CDS was cloned into the vector pMSCV in antisense direction as described in subsection 3.2.1. As already mentioned, the restriction sites added during the PCR were EcoRI in front of the Nat8l CDS and BglII at the end of the Nat8l CDS (electrophoresis gel of insert (900 bp) with added binding sites (12 bp) amplified by PCR see Figure 12).
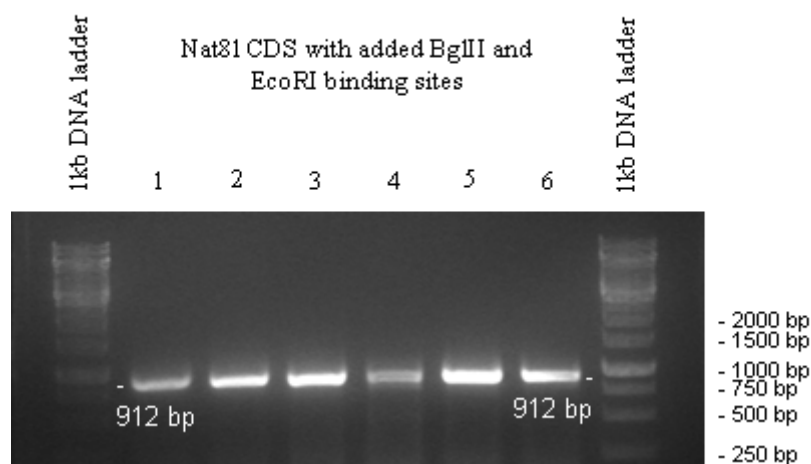
Figure 12: Electrophoresis gel: Nat8l CDS with added BglII and EcoRI binding sites amplified by PCR

According to the MCS of pMSCV in which the BglII restriction site lies prior to the one of EcoRI (see: Figure 5), Nat8l was integrated in antisense direction after ligation of the digested Nat8l construct and pMSCV vector. After the transformation of the obtained plasmid into NEB 5-alpha cells, which were seeded into 10 cm dishes containing solid agars with 100 μM of ampicillin, the cells were incubated at 37°C over night providing over 80 colonies. 18 of these colonies were picked and used as templates for a colony-PCR to prove that the Nat8l gene was integrated into the applied vector. 16 of the tested colonies possessed the Nat8l gene (900 bp plus 12 bp from the added endonucleases binding sites, see Figure 13). Two of these positive samples were used for DNA production

by miniprep. Colony 5 was chosen because the gel band showed a sharp, representative signal, and had the same length as almost all other positive colonies of the control-PCR. The other miniprep was produced from colony 7 due to the fact that the gel band seemed to have run a little bit further suggesting that the received DNA fragment was shorter. To exclude the possibility that colony 7 was correctly build up and the others were defective, it was decided to research this colony as well to assure to get one valuable construct. The received minipreps were digested with the endonucleases ApaI and KpnI as well as EcoRI and BglII to manifest that pMSCV really contained the Nat8l gene. The results of the control digest are shown in Figure 14. To evaluate these findings a virtual control cut analysis of Nat8l_pMSCV_as using Serial Cloner 2.1[120] was realized (see Figure 15).
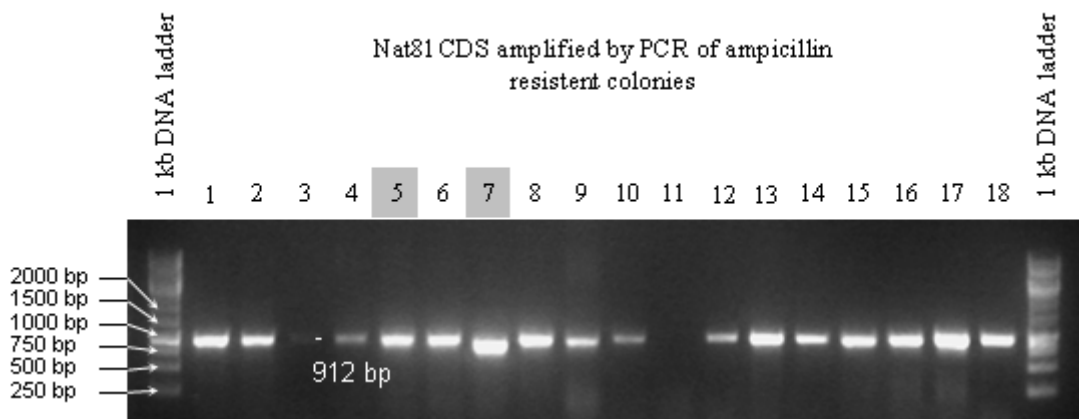
Figure 13: Electrophoresis gel: Control of Nat8l_pMSCV_as integration in ampicillin resistant colonies by PCR amplification of Nat8l CDS

---

[120] F.Perez/ SerialBasics, "Serial Cloner."
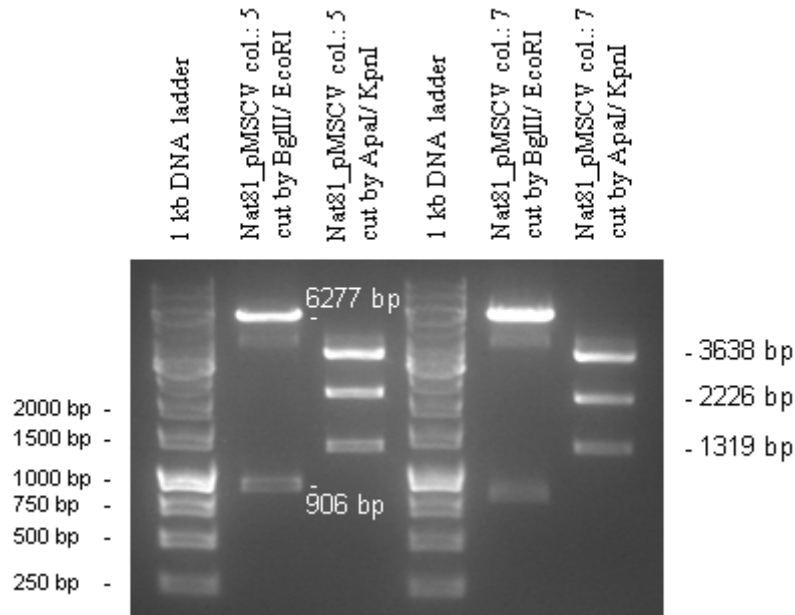
Figure 14: Electrophoresis gel: Miniprep control digests of colony 5 and 7 with BglII/ EcoRI and ApaI/ KpnI
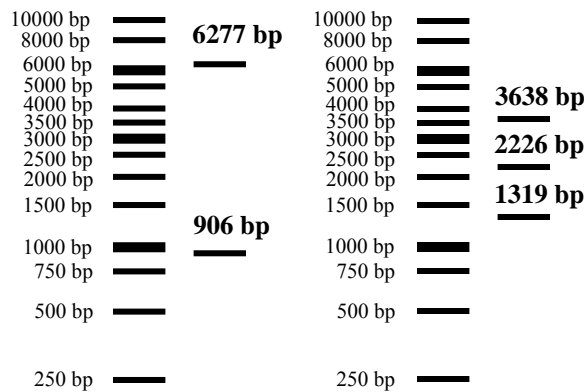
Figure 15: Virtual control digests analysis of Nat8l_pMSCV_as cut by BglII/ EcoRI and Apa1/ KpnI with the help of Serial Cloner 2.1

The control digest with EcoRI and BglII delivered DNA bands of 906 bp (900 bp of Nat8l CDS and 6 bp of the cut EcoRI and BglII restriction sites) and 6277 bp for colony 5 as predicted by the virtual analysis. Once again the DNA band of the Nat8l CDS of colony 7 had run a bit further than the insert band of colony 5. The miniprep digest with ApaI and KpnI delivered bands with 3638 bp, 2226 bp and 1319 bp for colony 5 and the result for colony 7 revealed almost the same bands except the one at 2226 bp which was localised at a shorter base pair length, proving that the sequence of colony 7 was a little bit shorter than the one of colony 5. For better understanding of the base pair lengths, a vector map of

Nat8l_pMSCV antisense construct is shown in <u>Figure 16</u> and the position of the used endonuclease binding sites were added to the graphic.
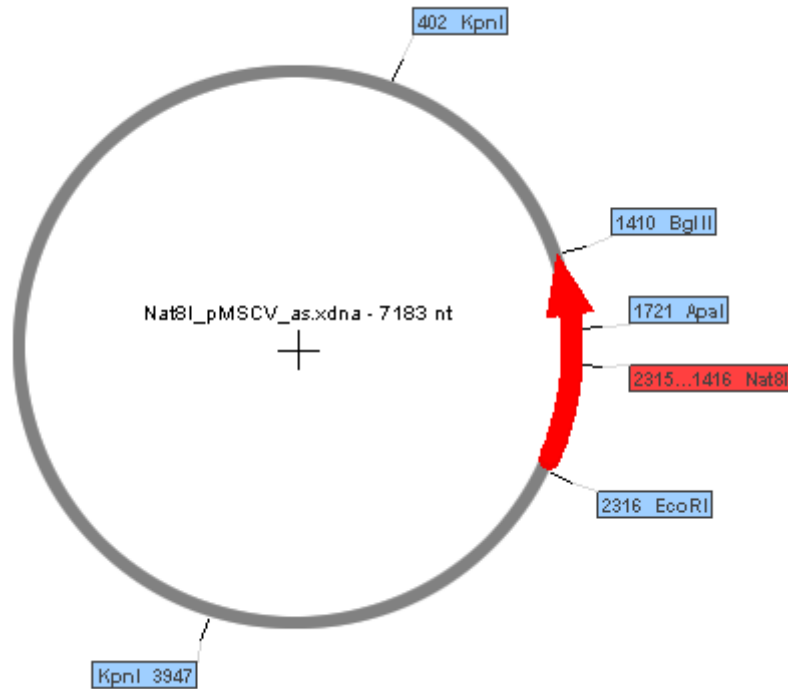
Figure 16: Vector map of Nat8l_pMSCV antisense construct with the used digestion endonucleases binding sites

Prior to the transfection of phoenix cells with the two obtained constructs, it was examined by sequencing if the entire Nat8l CDS was integrated into the pMSCV vector and if the direction of integration was according to the requested assignment. The results of the sequencing proved that the construct of colony 5 was correctly implemented and the Nat8l CDS of the colony 7 construct was lacking 92 bp as already suggested by the previously performed control digestion studies. This error should not interfere with the goal to knock-down the Nat8l gene expression in 3T3-L1 cells. Therefore, the construct of colony 7 was used in the following studies as well. After transfection of phoenix cells with the two plasmids (see: <u>3.2.3</u>), the obtained infectious particles were used to stably transduce 3T3-L1 cells (see: <u>3.2.4</u>). These cells were differentiated as described in subsection <u>3.2.2.2</u> in one 6-well plate each construct. As a reference control for the influence of these probes, 3T3-L1 cells which were containing a stably integrated empty pMSCV vector were also differentiated in one 6-well plate.

To determine if the produced 3T3-L1 cells were expressing the Nat8l antisense construct, RNA probes from cells containing one of the three plasmid forms were harvested on d0, d3 and d5 after induction (see: 3.2.5). These samples were investigated by qPCR analysis (see: 3.2.7) using a Nat8l primer to evaluate the RNA expression levels of Nat8l. Furthermore, the expression of the TFIIβ housekeeping gene was detected to normalize the obtained Nat8l data. The results of this study are shown in Figure 17. The used Nat8l primer is not able to distinguish between the endogenously expressed Nat8l mRNA and the antisense Nat8l construct. But the relative changes of Nat8l RNA levels in 3T3-L1 cells containing one of the generated antisense constructs in comparison to the empty pMSCV vector control group are mainly caused by Nat8l antisense RNA. In the control group the Nat8l expression is around one on all three points of time (d0 of the control is set to one as reference). The overexpression of Nat8l antisense RNA was increased in both examined groups and rose continuously from d0 to d5.
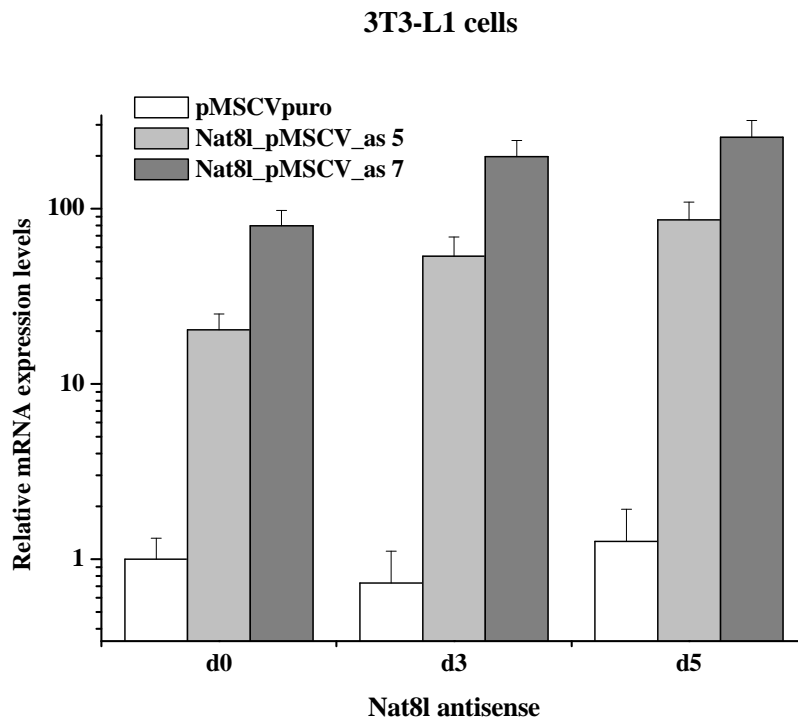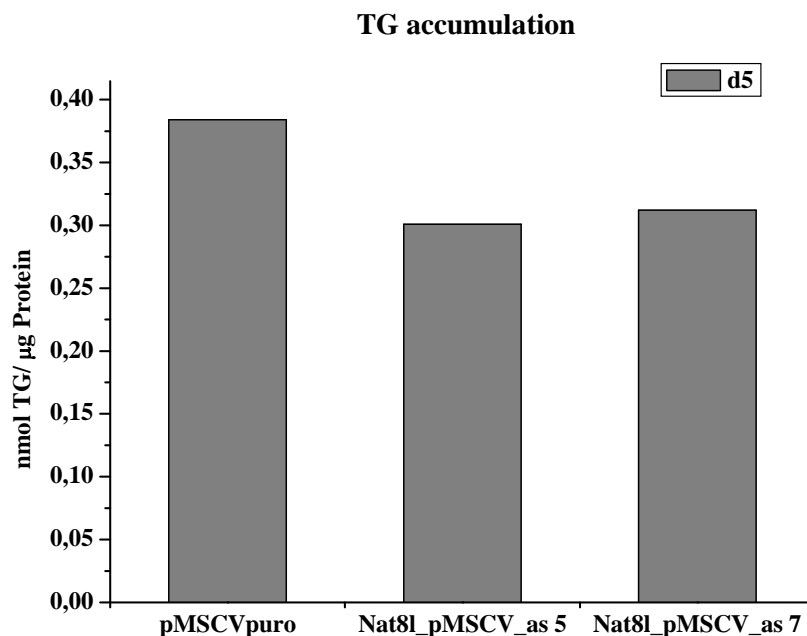
3T3-L1 cells

Figure 17: Relative expression levels of Nat8l antisense RNA in 3T3-L1 cells at d0, d3 and d5 after induction

After controlling that the cultured 3T3-L1 cells contain the Nat8l antisense construct, the next step of the investigation was to validate the TG accumulation difference between

3T3-L1 cells containing an as-construct and the empty control vector. The amount of TG is one of the commonly evaluated factors for possible changes in fat metabolism. The probes were collected at d5 after induction and examined as described in subsection 3.2.9. The following chart illustrates the received information about the TG content from this assay (see: Figure 18). This analysis was performed without technical or biological replicates but nevertheless in the harvested TG probes it has been observed that the TG content on d5 after induction was reduced about 20% in those 3T3-L1 cells which were containing the antisense plasmids. Even though this effect seemed surprising and interesting at first sight, it has not been proven with the methods used before whether these TG changes are due to the knock-down of Nat8L proteins and if the TG levels reflect the lipid droplet accumulation inside the cells. To examine these questions, the approximate amount of lipid droplets which arise throughout the differentiation process was determined by ORO staining on d5 after induction (see: 3.2.8). Pictures of these stainings are shown in Figure 19. The validity of these pictures about the real quantitative amount of lipid droplets might not be very representative but it can be stated that the possible changes are not obvious. A slight reduction might be possible but a precise statement cannot be made.

Figure 18: TG accumulation of 3T3-L1 cells containing Nat8l antisense RNA at d5 after induction

| pMSCVpuro | Nat8l_pMSCV_as 5 | Nat8l_pMSCV_as 7 |
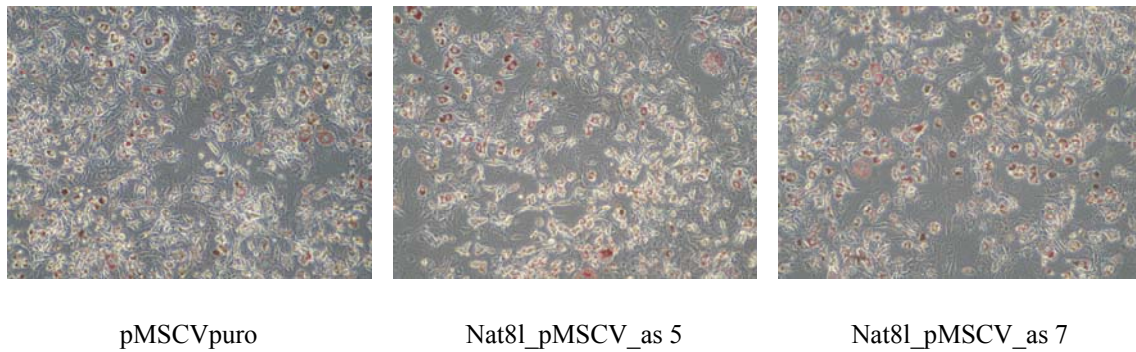
Figure 19: ORO stainings of 3T3-L1 cells containing Nat8l antisense RNA at d5 after induction

To determine if knock-down of Nat8L was successful, protein levels were detected by WB. Direct detection of Nat8L proteins was not feasible due to the fact that a specific antibody for Nat8L was not available at this time. Therefore, Cos7 cells were cultured in a 6-well plate until they reached 60% of confluence. Then, they were transfected with a pHisMaxC[121]_Nat8l plasmid (0,5 µg per well) together with one of the previously investigated plasmids (pMSCVpuro, Nat8l_pMSCV_as 5/ 7 (0,5 µg per construct and well)). The idea of this attempt was to investigate whether the as-constructs of Nat8L are able to knock-down the overexpression of a His-tagged Nat8L protein which was caused by pHisMaxC containing the Nat8l CDS in sense direction. After transfection, the cells were cultured for two days. Afterwards, they were harvested with a protein lysis buffer (see: 3.2.11.1). The His-tag of the overexpressed protein was detected through WB analysis(see: 3.2.11) by an anti-His antibody. (The received result was used to evaluate if the produced antisense constructs were capable to reduce the overexpression of the His tagged Nat8L protein inside the Cos7 cells.) Figure 20 shows the WB data and a verification of the applied protein amount through the detection of β-actin as a loading control.

---

[121] Invitrogen, "pcDNA4/ HisMax A, B, and C."
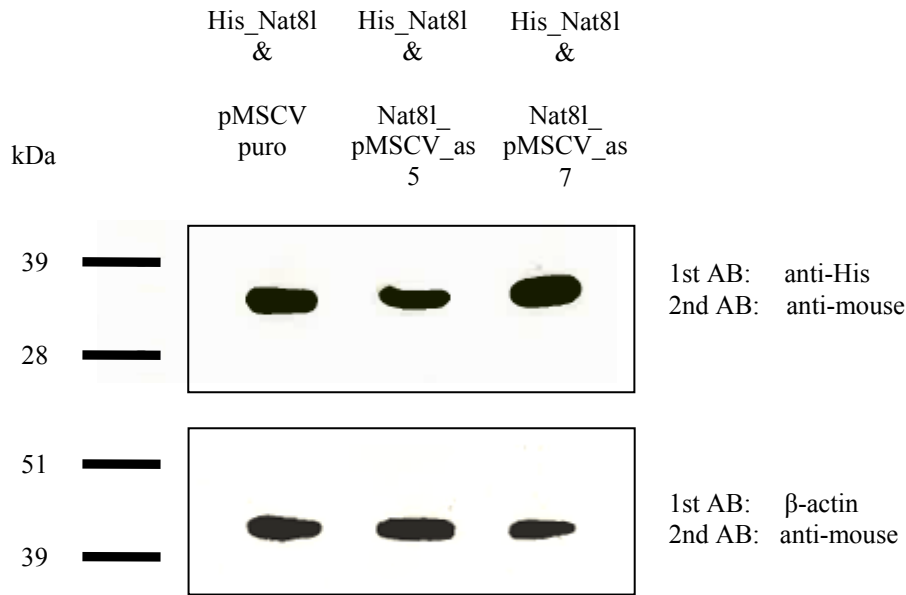
Figure 20: WB analysis of the overexpressed His-tagged Nat8L protein to evaluate the knock-down effect from Nat8l antisense RNA constructs plus added loading control examination in Cos 7 cells

The Nat8l_pMSCV_as 5 construct seemed to slightly reduce the protein amount of Nat8L, suggesting that the attempt to achieve a knock-down effect of Nat8L might be successful to some extent. But controversial to this result the protein amount of construct 7 containing Cos7 cells did not change or maybe even increased a little bit. The WB of the β-actin detection revealed that the used protein amount was almost the same for all three samples, perhaps the protein amount of construct 7 probe was slightly reduced. Due to the fact that this method did not deliver an exact objective result because of the small changes of construct 5 and the fact that construct 7 did not show the expected result, the final evidence that the knock-down of Nat8L with the help of these constructs succeeded is still debatable. So the next step of investigation was the implementation of a replicate series to determine if the previous results can be reproduced. Therefore, the same cells as before were cultured until confluence and differentiated the same way. RNA was harvested on d0, d3, and d5 after induction. ORO staining and TG harvest were implemented on d3 and d5. Furthermore, it was investigated if the used cell probes possessed the ability to differentiate when cultured just with StdM or with StdM and insulin. The result of the TG analysis is presented in Figure 21. On d3, the amount of TG is a little bit higher in the antisense constructs containing probes as in the control group. Conditioned by the differentiation process the quantity of TG rose to d5 in all three samples but it appeared once again that the TG amount of the two antisense construct cell probes were decreased about the same proportion as in the previous experiment (see: Figure 18). Even though the TG data was

not significant, a slight trend of influence of the produced antisense constructs was detectable. Whether this trend is significant for the used antisense constructs and was really caused through the desired Nat8L knock-down or other cellular changes must be investigated in further studies. Figure 22 shows the ORO stainings of the investigated probes and once again changes of lipid droplet amounts were not obvious. A slight decrease may be observable but this is not sure.
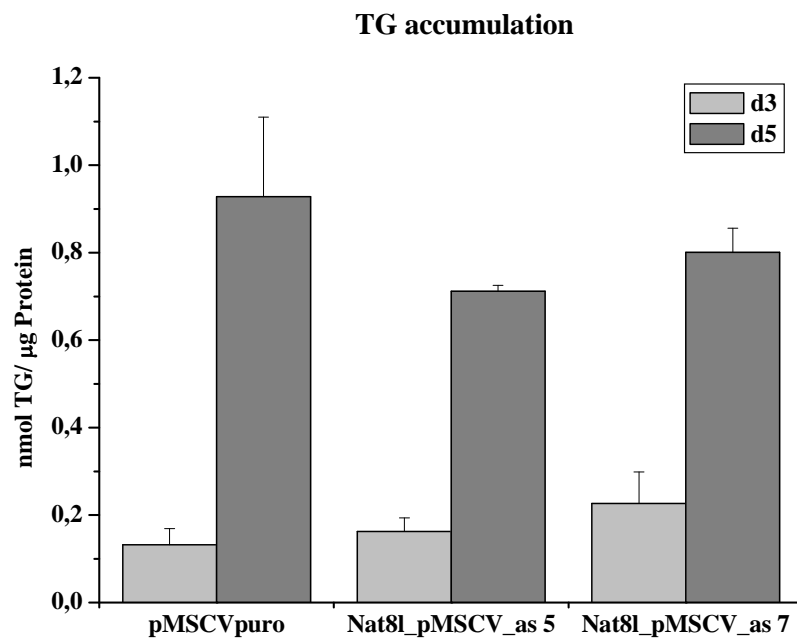
Figure 21: TG accumulation of 3T3-L1 cells containing Nat8l antisense RNA at d3, d5 after induction (replica)

| | pMSCVpuro | Nat8l_pMSCV_as 5 | Nat8l_pMSCV_as 7 |
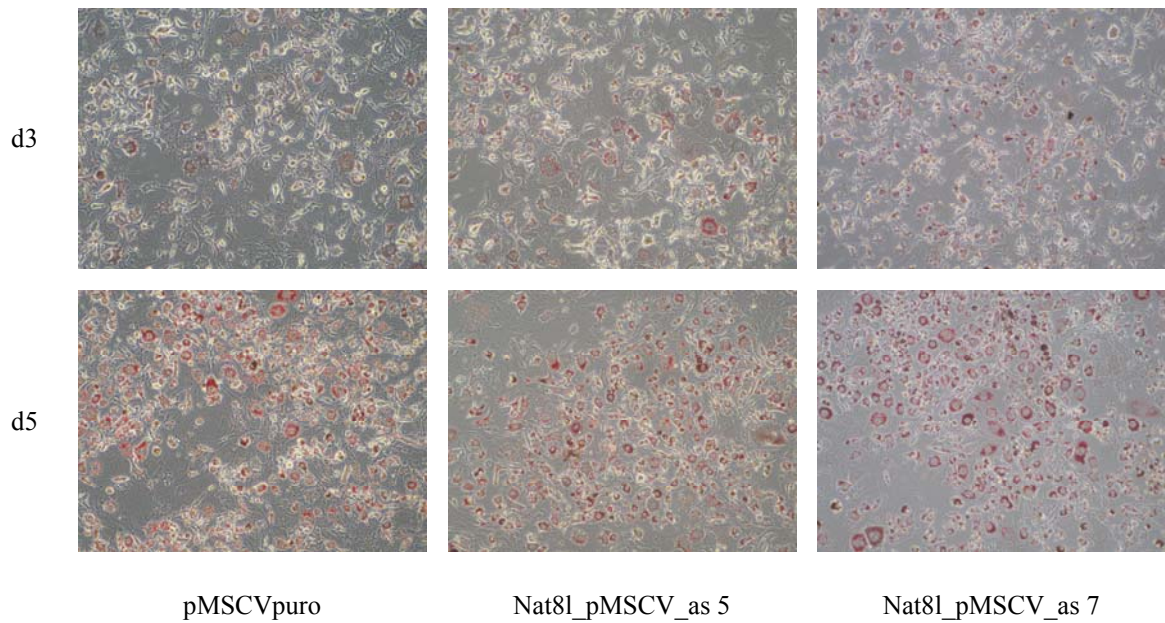
Figure 22: ORO stainings of 3T3-L1 cells containing Nat8l antisense RNA at d3, d5 after induction (replica)

The differentiation capacity of the control and the 2 antisense probes in the absence of IBMX and DEX was evaluated with the help of an ORO staining on d5 after induction. The obtained results are shown in Figure 23 and imply that 3T3-L1 cells were not able to accumulate lipid droplets without the right hormonal stimulus and that the produced Nat8l antisense constructs could not compensate this effect.
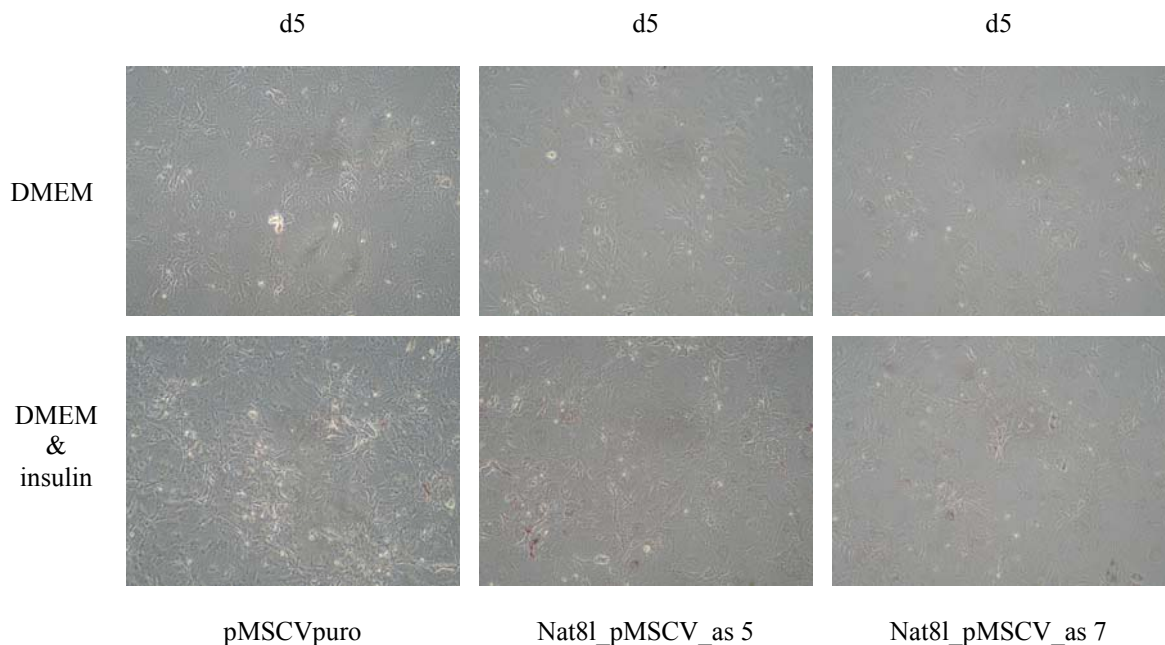
Figure 23: ORO stainings of 3T3-L1 cells containing Nat8l antisense RNA at d5 without induction and with an insulin stimulus

4.2 Stable overexpression of Nat8l through transduction of 3T3-L1 cells with a Nat8l CDS containing pMSCVpuro vector

Even though the evidence is lacking that the changed TG content during the Nat8l knock-down attempt was really caused through a reduced Nat8L expression, the influence of Nat8l on the differentiation of 3T3-L1 cells was investigated in further detail. Therefore, it was evaluated if the stable overexpression of Nat8l leads to changes in the differentiation process. For that purpose, 3T3-L1 cells transduced with a pMSCV vector containing the Nat8l CDS in sense direction or an empty pMSCV vector were seeded in 6-well plates and cultured until confluence. Subsequently, the cells were differentiated as described in subsection 3.2.2.2. RNA was harvested on d0, d2, d4, and d6 after induction and analysed through qPCR to verify if the overexpression was successful (see: Figure 24). The increase of Nat8l in overexpressing cells compared to the control group was about 45-fold (d0, d2) at the beginning of the differentiation and rose on d4 up to 87-fold before it decreased to a 35-fold overexpression on d6. The influence of these expression changes was investigated once again through determination of the TG content of Nat8l overexpressing cells in comparison to the control cells. The TG harvest for this study was implemented at the same time points as the RNA harvest for the qPCR analysis and is presented in Figure 25. This experiment condition granted the possibility to interpret the TG values depending on the Nat8l mRNA changes. The presented mRNA and TG findings were representative examples confirmed by two biological replicas which were implemented during this study. The obtained data showed an interesting result proving that the TG amount in Nat8l overexpressing 3T3-L1 cells was significantly reduced on d4 and d6 after induction. The reduction of TG on d0 was not as obvious as the one at later points of differentiation because i) the standard deviation bars interfere with an exact interpretation and ii) there is hardly any lipid droplet accumulation at this time point. Even though the TG values of d2 contradict the possibility of a reduced TG amount in Nat8l overexpressing cells during the whole time series at first sight, this circumstance is again questionable i) due to the error bars and ii) still there is hardly any TG accumulation at day 2. Additionally, the implemented replicas of this analysis, although the harvest points were not exactly the same(d3, d5, d8), never showed an increase of the TG content for Nat8l overexpressing 3T3-L1 cells compared to the appropriate pMSCV vector control group.
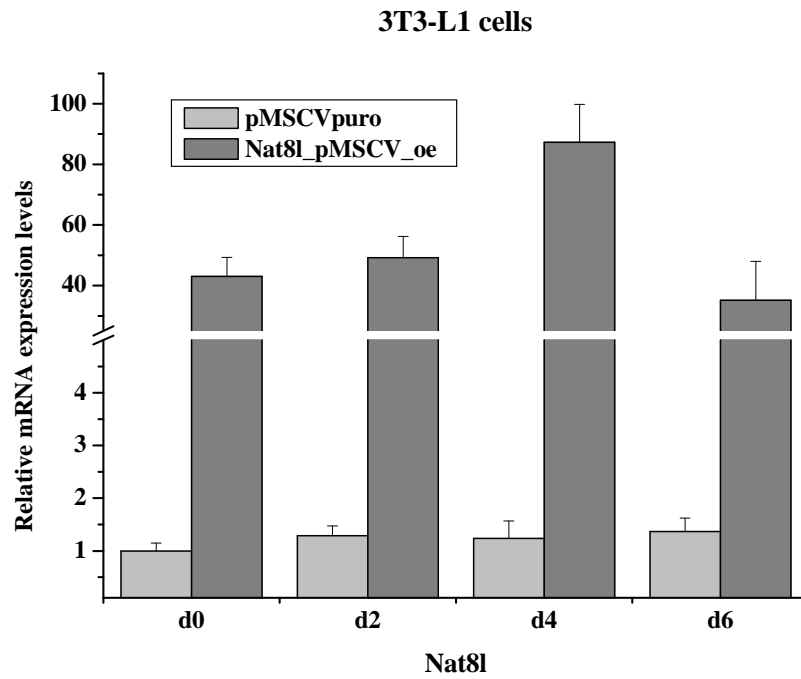
3T3-L1 cells

Figure 24: Relative mRNA expression levels of Nat8l overexpressing 3T3-L1 cells at d0, d2, d4, and d6 after induction
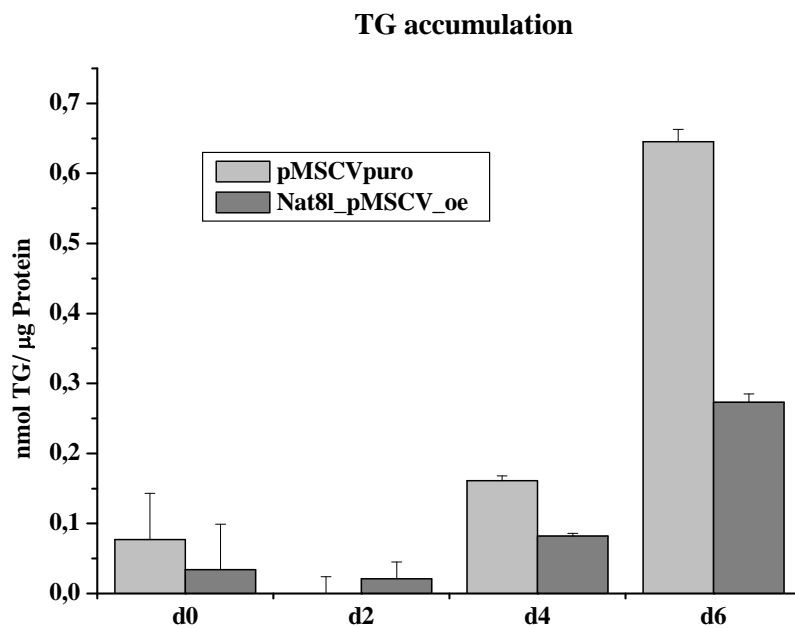
TG accumulation

Figure 25: TG accumulation of 3T3-L1 cells containing a Nat8l overexpressing plasmid at d0, d2, d4, and d6 after induction

Identical to the knock-down attempt, the next step of research was the examination if these TG changes affect the lipid droplet accumulation. To determine this possible influence, ORO stainings were realized from 3T3-L1 cells containing the Nat8l_pMSCV_oe construct or the empty pMSCV vector on d2 and d6. The obtained photographs are presented in Figure 26.

| | pMSCVpuro | Nat8l_pMSCV_oe |
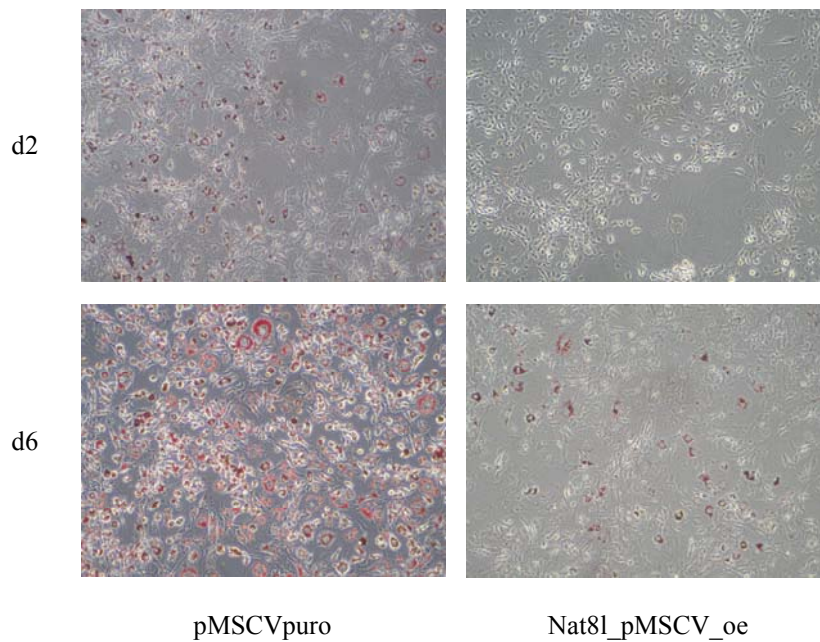
Figure 26: ORO stainings of 3T3-L1 cells overexpressing the Nat8l gene at d2 and d6 after induction

The red regions represent the lipid droplets inside the 3T3-L1 cells. On day 2, the lipid droplet accumulation in the control group had been commenced to a common extent for this early phase of differentiation. In contrast to this result, there were no lipid droplets detectable in Nat8l overexpressing 3T3-L1 cells. This difference in lipid droplet content became even more obvious on d6. Compared to the fully differentiated 3T3-L1 cells of the control group, the lipid droplet accumulation in Nat8l overexpressing cells was severely decreased. The ORO changes on d2 made the previously already mentioned dubious TG values on d2 after induction even more unreliable. Also the ORO results were confirmed with the help of two biological replicas. These interesting and drastic changes in phenotype detected by ORO stainings of differentiated 3T3-L1 cells overexpressing Nat8l led to further investigations of the influence of Nat8l on common known lipid markers. Therefore, the expression of Dgat1 an enzyme which catalyzes the terminal and only committed step for the creation of triglycerides and Acsl1 which is known to play a key role in lipid biosynthesis and therefore also in the differentiation process were determined.

The results of the qPCR analysis from Nat8l overexpressing 3T3-L1 cells and the control group on d0 and d6 are presented in <u>Figure 27</u>. Both lipid markers were reduced on d0 about 60% in those cells which contained the overexpressing Nat8l construct and the proportion of the reduction between control and investigated probe was at the same level on d6 which cannot be seen directly due to the logarithmic scale. These results were confirmed with two biological replicas which detected these reductions on d0, d3, d5, and d7 after induction. These findings corroborate the theory that Nat8l might have an influence on the triglyceride synthesis.
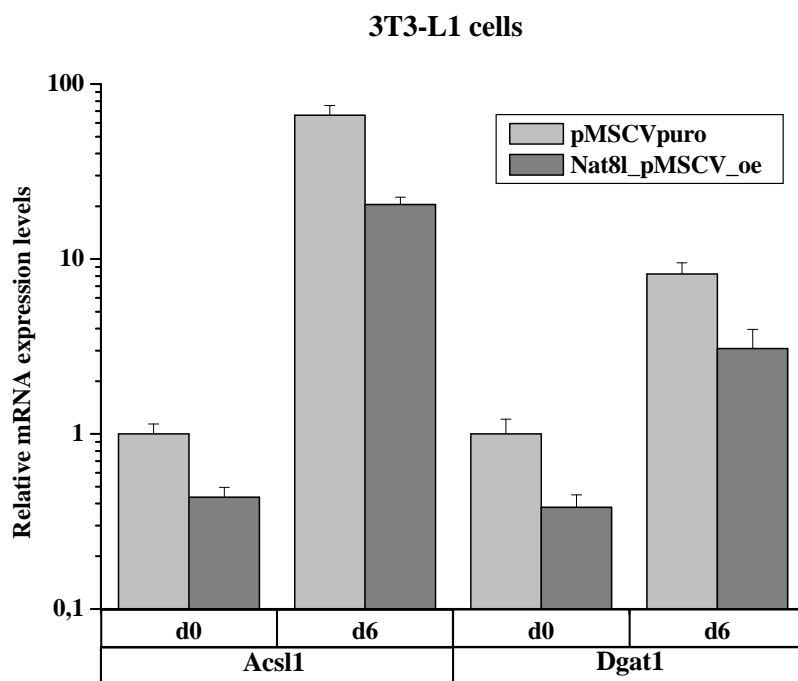
Figure 27: Relative mRNA expression levels of Acsl1 and Dgat1 in Nat8l overexpressing 3T3-L1 cells at d0 and d6 after induction

To get a better idea about the influence of Nat8l on fat metabolism, the stated function of Nat8l to catalyze the reaction of acetyl-CoA and L-asp to NAA should be investigated particularly. Especially the amount of acetyl-CoA, one of the most essential substrates of energy metabolism which can be created out of acetate through enzymes like Acss1 and Acss2, should deliver some hints about the impact of Nat8l. Furthermore, the enzyme Aspa1 which catalyzes the reaction to L-asp and acetate out of NAA was examined as well. The influence of Nat8l overexpression in 3T3-L1 cells on the expression of Acss1,

Acss2, and Aspa1 is presented in Figure 28. Acss2 was significantly reduced at all points of time which could be confirmed through two biological replicas. The extent of this reduction was continuously increased during the differentiation process. Even though Aspa1 was significantly reduced, the replicas rather suggested that the reduction of Aspa1 is more distinct at later points of differentiation (d5, d7), because on d0 and d3 there were no severe changes of expression. Also d4, as seen in Figure 28, shows just a slight reduction of Aspa1. The only expression change which could not be confirmed with replicas was the one of Acss1. As seen in Figure 28 the detection of Acss1 on d0 and d4 failed as well, probably due to the low expression of Acss1 in 3T3-L1 cells. Nevertheless, the changes of Acss1 were so severe on d6 in Nat8l overexpressing cells, so it should be taken in consideration that Nat8l might have an influence on this enzyme as well. But this term needs to be investigated in more detail in future studies.
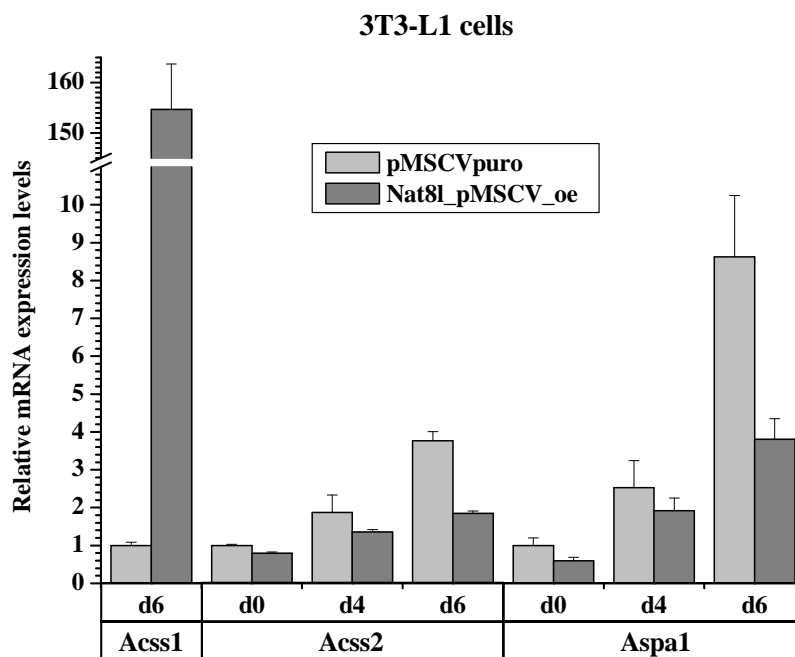

Figure 28: Relative mRNA expression levels of Acss1, Acss2, and Aspa1 in Nat8l overexpressing 3T3-L1 cells at d0, d4, and d6 after induction

Finally, Nat8l stably overexpressing 3T3-L1 cells were evaluated for their differentiation abilities in the absence of DEX and IBMX. For that purpose, 3T3-L1 cells containing the overexpressing construct and a pMSCV control group were cultured with StdM or with insulin containing StdM until d5 after treatment initiation, which was d7 after reaching

confluence. The possible differentiation progress was examined once again by an ORO staining which is shown in Figure 29. In both cases, no lipid droplets were detectable leading to the conclusion that the overexpression of Nat8l cannot initiate the differentiation if DEX and IBMX are missing.
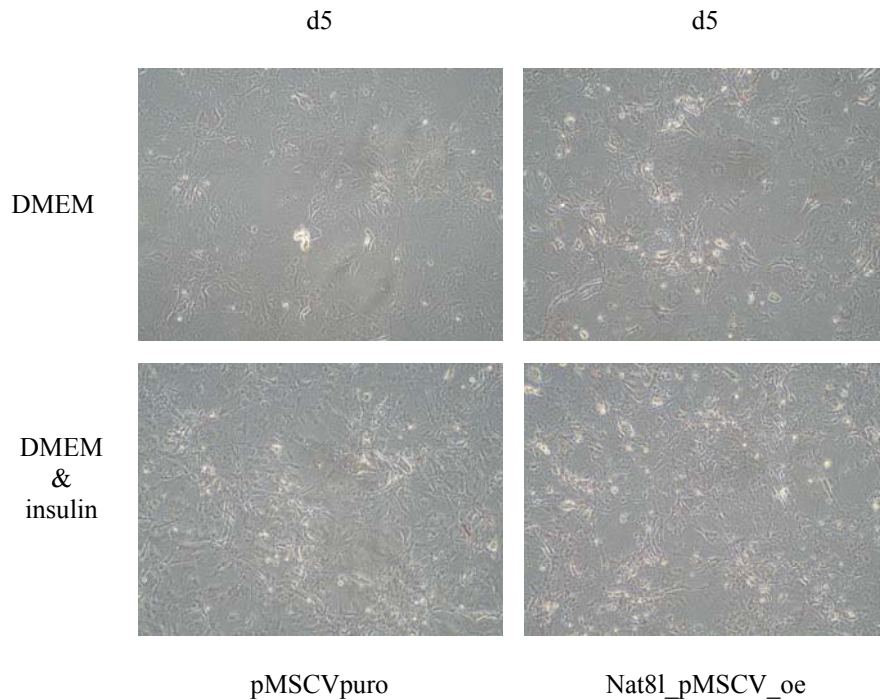
Figure 29: ORO stainings of Nat8l overexpressing 3T3-L1 cells at d5 without induction and with an insulin stimulus

4.3 Transient overexpression of Nat8l through electroporation of 3T3-L1 cells with a Nat8l CDS containing pMSCVpuro vector

After investigation of the stable overexpression of Nat8l in 3T3-L1 cells and the evaluation of the influence on differentiation, it was determined if an overexpression of Nat8l affects the fat metabolism of differentiated 3T3-L1 cells as well. Therefore, 3T3-L1 cells were cultured in 75 cm^2 flasks and 10 cm dishes until confluence and differentiated as described in subsection 3.2.2.2. Depending on the rate of progress of the differentiation, the cells were electroporated when the lipid droplet amount was at a level that permitted the conclusion that the differentiation process was nearly finished. This normally happened from d4 to d6 after induction. The differentiated cells were electroporated with the same constructs as used for the stable overexpression (Nat8l_pMSCV_oe, pMSCVpuro). The electroporation process was implemented as described in subsection 3.2.13. Thereafter,

cells were culture in StdM without antibiotics for one day to reduce cellular stress. Then the media was replaced with StdM. To examine if the electroporation was successful, RNA was harvested on d2 and d6 after electroporation. These probes were investigated by qPCR on their Nat8l mRNA expression levels. The obtained result is presented in Figure 30. On d2 a 72-fold overexpression of Nat8l was achieved which decreased to a 5-fold overexpression referred to d2 of the pMSCV control group (value set to 1 on purpose) in which the Nat8l expression on d6 was 1.5-fold higher than on d2. These results represent quite accurate the expression profile of a transient overexpression of a gene which is high in the early phase after electroporation and decreases over time.
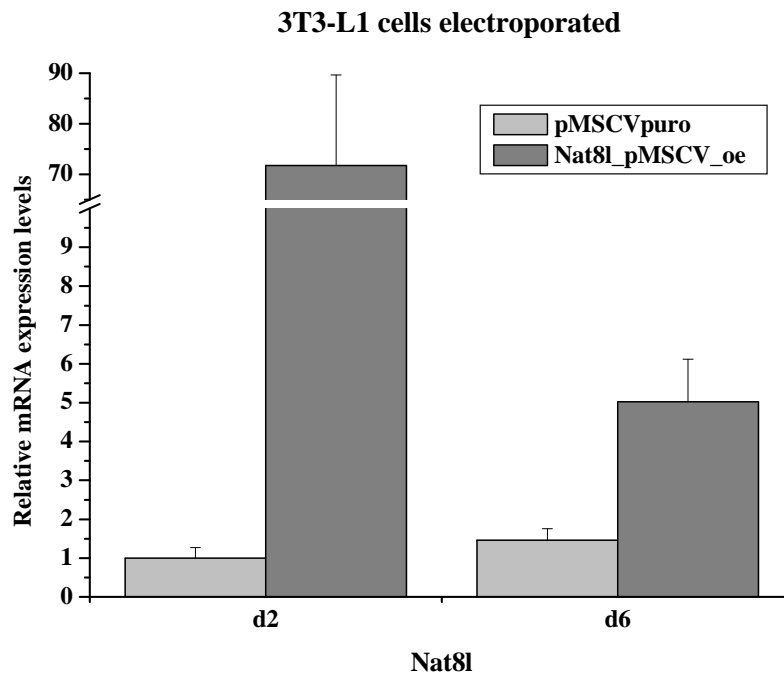
Figure 30: Relative mRNA expression levels of differentiated, Nat8l overexpressing 3T3-L1 cells at d2 and d6 after electroporation

To determine the influence of these changes on differentiated 3T3-L1 cells the TG levels were examined at the same points of time. This analysis was carried out like described in subsection 3.2.9 and the obtained results are shown in Figure 31. The amount of TG in 3T3-L1 cells transiently overexpressing Nat8L was 27% reduced on d2 and about 18% on d6, respectively (the error bar on d6 of Nat8l_pMSCV_oe is to small to visualize it). However, this result was not consistent in three replicas. The first and second attempt had and overexpression about 20- and 45-fold on d2 and no TG changes were detectable. But

the last one with an overexpression of Nat8l at an even higher level than the original examination showed a decrease of TG about 17% (The exact value of the overexpression could not be determined due to the high standard deviation caused through a small reference value). Because the results were not distinct, it should be taken into debate that there might be a correlation between the amount of Nat8l overexpression and changes of TG levels in differentiated 3T3-L1 cells. Nevertheless, for investigation purposes of the intra-cellular function of Nat8l the samples of the original examination, where TG changes were detected, seemed more promising than the low expressing replicas. Therefore, these samples were tested through qPCR analysis for the same lipid markers as probes of the stable overexpression. Furthermore, Dgat2 was added to this study to examine another possibly influenced enzyme. Dgat2, even though it has no sequence homology, is able to catalyze a similar reaction as Dgat1. The results of this analysis are presented in Figure 32. Acsl1, which is known to have an influence especially during the differentiation, did not show changes between the two tested constructs and there was no expression variation between d2 and d6 after electroporation. Dgat1 was not effected either. Furthermore, there were no differences of Dgat2 between Nat8l overexpressing 3T3-L1 cells and the control group at both time points. However, the overall amount of Dgat2 increased about 60% on d6 compared to d2 in both samples and at least this result shows that the cells differentiated properly.
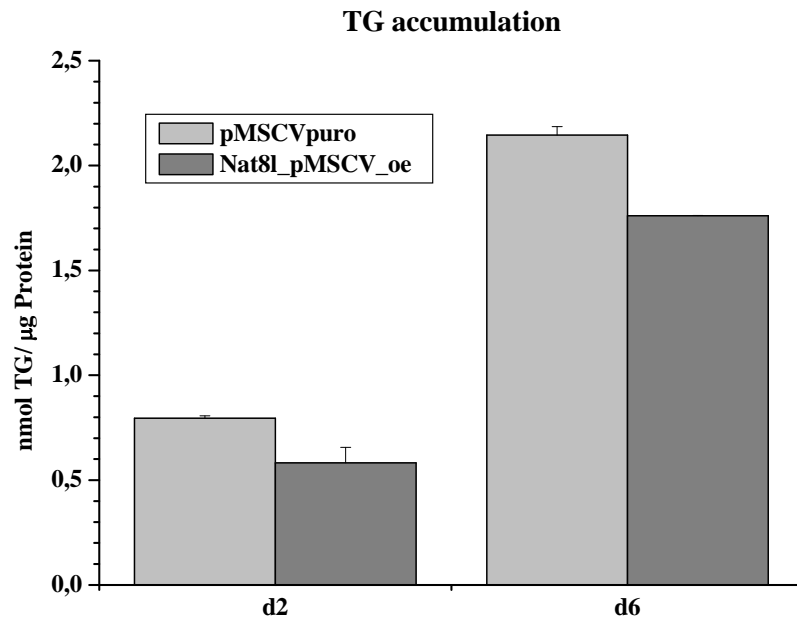
Figure 31: TG accumulation of differentiated 3T3-L1 cells containing a Nat8l overexpressing plasmid at d2 and d6 after electroporation
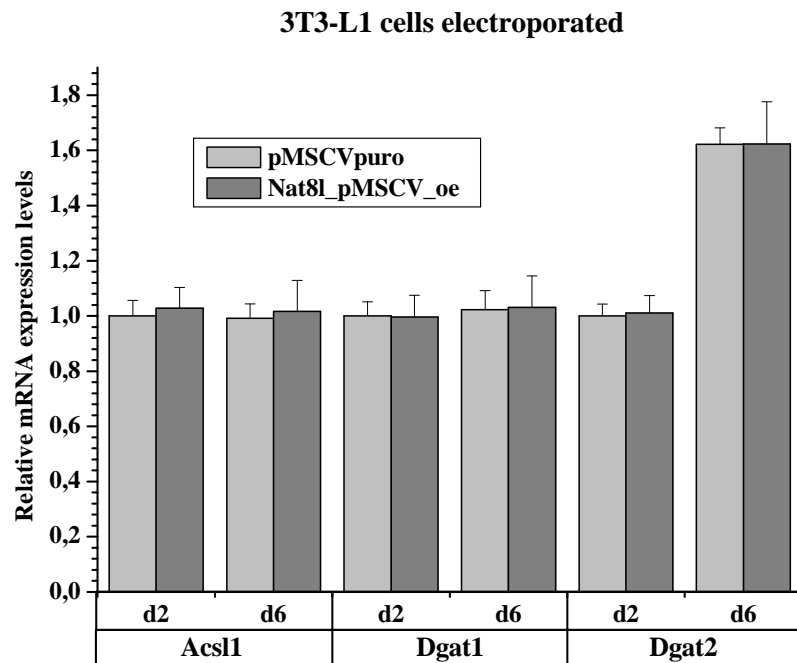
Figure 32: Relative mRNA expression levels of Acsl1, Dgat1, and Dgat2 in differentiated, Nat8l overexpressing 3T3-L1 cells at d2 and d6 after electroporation

Due to the fact, that lipid markers did not show any changes between the differentiated 3T3-L1 cells transiently overexpressing Nat8l and 3T3-L1 cells containing the empty pMSCVpuro vector it should be determined whether Aspa1, Acss1, or Acss2 were effected to evaluate possible influences on acetyl-CoA metabolism. The obtained qPCR results are presented in <u>Figure 33</u>. There were no changes of the expression of Acss2 and Aspa1 between Nat8l_pMSCV_oe and pMSCVpuro containing cells but in both cell models the quantity of Acss2 and Aspa1 rose from d2 to d6. Acss1 showed a slight decrease in Nat8l overexpressing cells on d2. Remarkably, on d6 the expression of Acss1 was hardly detectable in Nat8l overexpressing cells in comparison to the control cells and thus significantly reduced. However, the expression in the control group showed a 1.6-fold increase of Acss1 until d6.
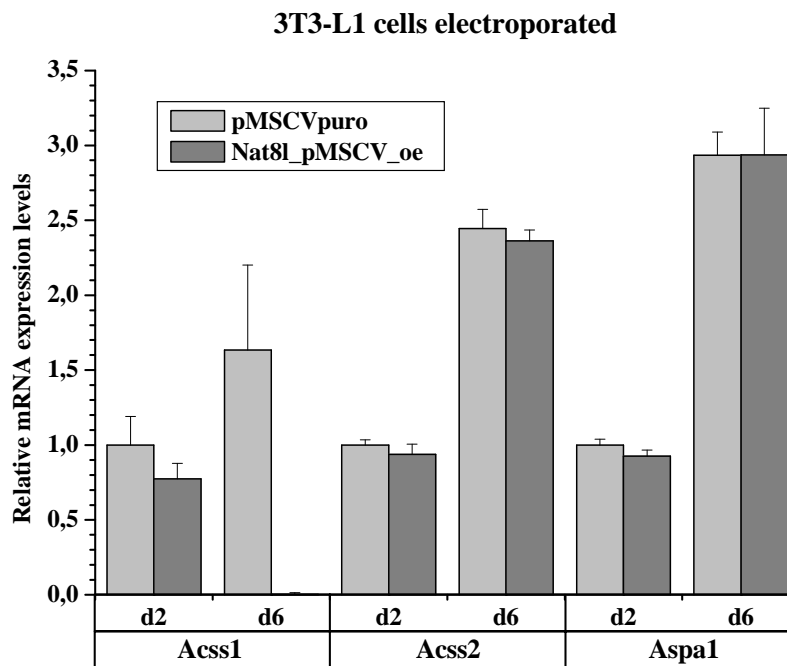
Figure 33: Relative mRNA expression levels of Acss1, Acss2 and Aspa1 in differentiated, Nat8l overexpressing 3T3-L1 cells at d2 and d6 after electroporation

Considering the until now achieved results, the decrease of TG accumulation in Nat8l transiently overexpressing 3T3-L1 cells compared to the control probes is unaccountable. So it might be of interest whether the electroporation process leads to cellular stress which could influence the TG accumulation in the ascertained way. Therefore, the expression of stress marker genes was determined and compared with the samples of the stable

overexpression. Atf3, BiP, and CHOP10 are stress markers which are known to be up-regulated under stress conditions and are detectable in stably and transiently transfected cells. Retn, which only reacts in transiently transfected cells, decreases when ER stress arises. As expected, the electroporation process induced some stress to the 3T3-L1 cells which could allusively be seen with Atf3, BiP, and CHOP10, but significantly with Retn RNA levels. However, comparing electroporated control and Nat8l overexpressing cells, the stress levels are at same dimensions (see: Figure 34). Thus the transient overexpression of Nat8l in comparison to control cells has no influence on stress marker expression and TG accumulation. Nevertheless, with the until now obtained findings, the influence of Nat8l in differentiated 3T3-L1 cells is questionable and needs further studies to evaluate the received results precisely.
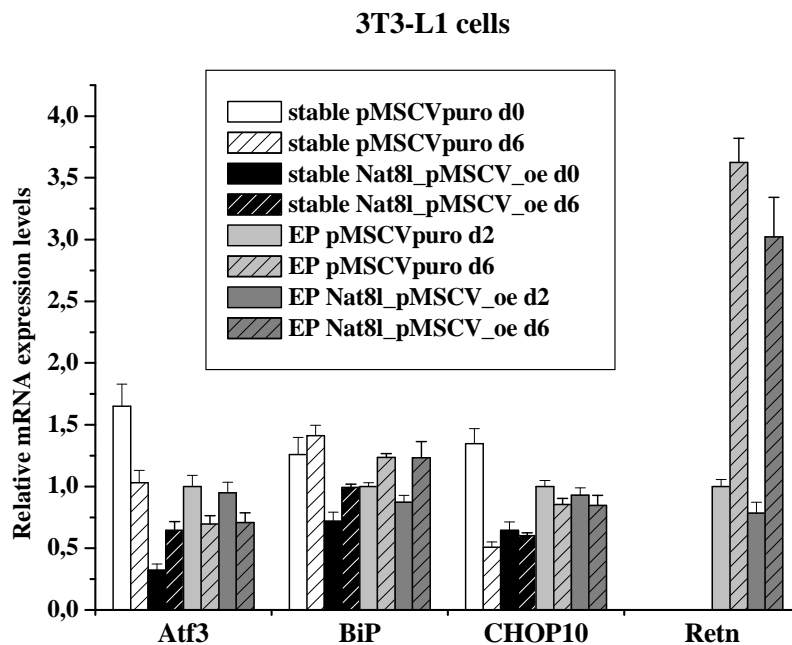

Figure 34: Relative mRNA expression levels of Atf3, BiP, CHOP10, and Retn in Nat8l stably or transiently overexpressing 3T3-L1 cells at d0 and d6 after induction or d2 and d6 after electroporation

4.4   Localisation of Nat8L in 3T3-L1 cells through overexpression of a protein complex consisting of Nat8L and a fluorescent co-protein

Until now implemented studies (4.1, 4.2, and 4.3) had the aim to detect metabolic changes in 3T3-L1 cells during and after differentiation through modification of Nat8l expression. These experiments evaluated the functional effect of Nat8L on cell metabolism. The next important step of investigation was to determine where Nat8L is localised in the cell to execute its function. This issue gives further insight into the direct interaction partners of Nat8L and the impact of Nat8L on specific metabolic pathways. For that purpose, Nat8l CDS was cloned into the MCS of pEYFP-C1 and pECFP-N1 as described in subsection 3.2.1. These vectors possess a nucleotide sequence encoding a fluorescent protein which is located prior or after the MCS. This feature enables to build fusion proteins of a POI (protein of interest) and the fluorescent protein. Due to the fact that the POI is still able to translocate to its point of action, it can be localised through fluorescence detection of the co-protein. First step of the cloning process was the amplification of Nat8l CDS by PCR, using primers which attach the specific sequences of endonucleases (XhoI, EcoRI) to the CDS. Furthermore, those primers corrected the frameshifts and eliminated the start codon of the insert for integration in pEYFP-C1 and the stop codon for integration in pECFP-N1. The electrophoresis gel with the obtained DNA bands is presented in Figure 35. The two constructs were digested with XhoI and EcoRI and subsequently ligated into pECFP-N1 or pEYFP-C1. The obtained plasmids were transformed into E. coli NEB 5-alpha and TOP10 cells and afterwards seeded into 10 cm dishes containing a solid agar mixed with 30 µM of kanamycin. The dishes were incubated at 37°C over night providing about 20 to 30 colonies of each construct. 16 colonies of both constructs were picked and used as a template for a colony-PCR to verify the integration of Nat8l. Furthermore, two positive controls were added to this procedure to assure the localisation of Nat8l on the electrophoresis gel. The results of these two PCRs are presented in Figure 36 and Figure 37 (897 bp of the Nat8l gene, either without TGA or ATG, plus 12 bp for the endonuclease extensions and 1 or 2 bp for the frameshift correction).
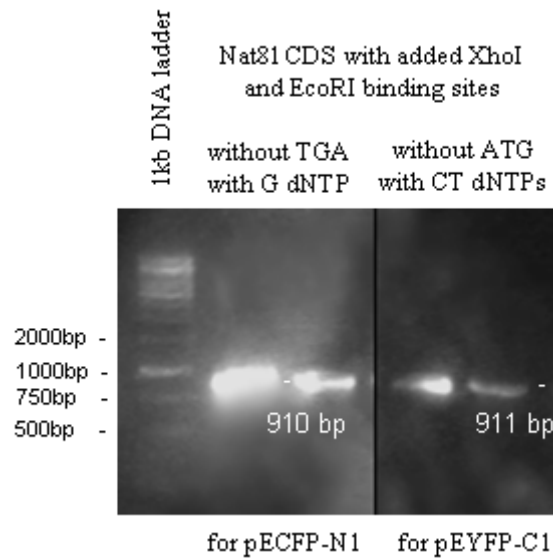
Figure 35: Electrophoresis gel: Nat8l CDS with added XhoI and EcoRI extensions without start codon (ATG) or stop codon (TGA) and a frameshift correction (G or CT) amplified by PCR
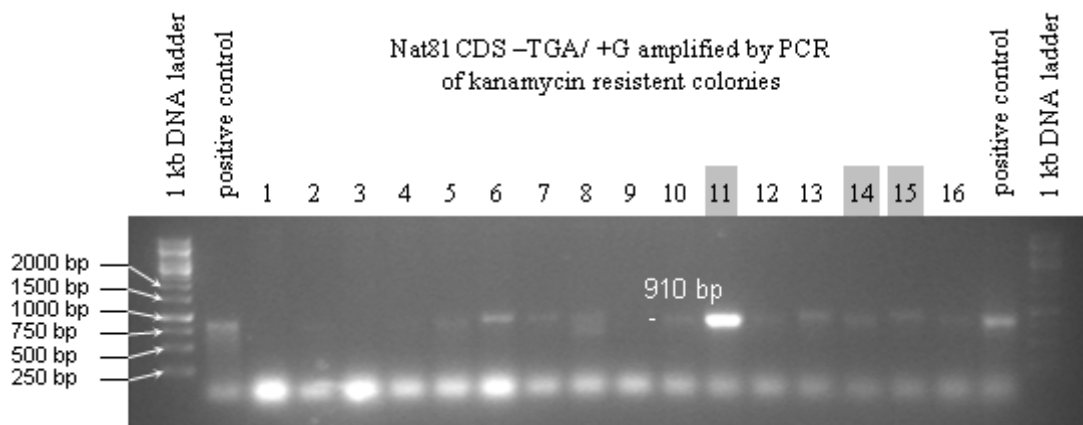
Figure 36: Electrophoresis gel: Control of Nat8l_pECFP-N1 integration in kanamycin resistant colonies by PCR amplification of Nat8l CDS
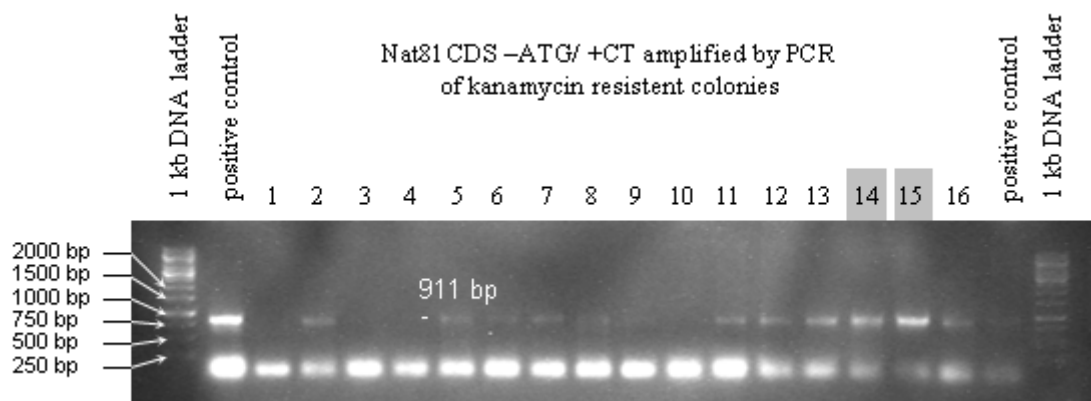
Figure 37: Electrophoresis gel: Control of Nat8l_pEYFP-C1 integration in kanamycin resistant colonies by PCR amplification of Nat8l CDS

The control-PCR of Nat8l_pECFP-N1 showed 11 positive colonies and the one of Nat8l_pEYFP-C1 showed 10 positive samples which contained Nat8l. 3 colonies (11, 14, 15) of Nat8l_pECFP-N1 and 2 (14, 15) of Nat8l_pEYFP-C1 were chosen for miniprep production. Afterwards, these minipreps were digested with the restriction enzyme ApaI to validate the integration of Nat8l. The electrophoresis gels of the control digests are shown in Figure 38. To assure that the received results correspond to the expected predictions a virtual control cut analysis of the two plasmids was performed with Serial Cloner 2.1 (see Figure 39).
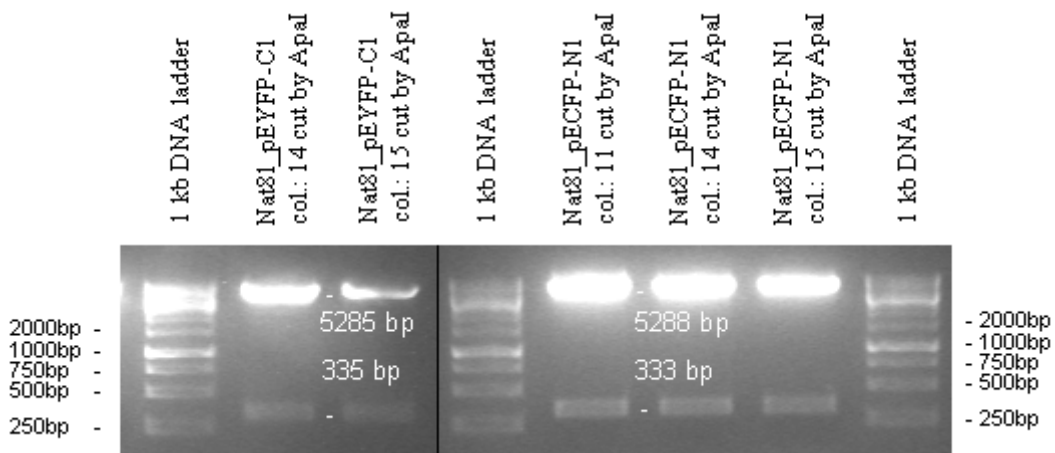
Figure 38: Electrophoresis gel: Miniprep control digest of colonies 14, 15 of Nat8l_pEYFP-C1 and colonies 11, 14, 15 of Nat8l_pECFP-N1 with ApaI
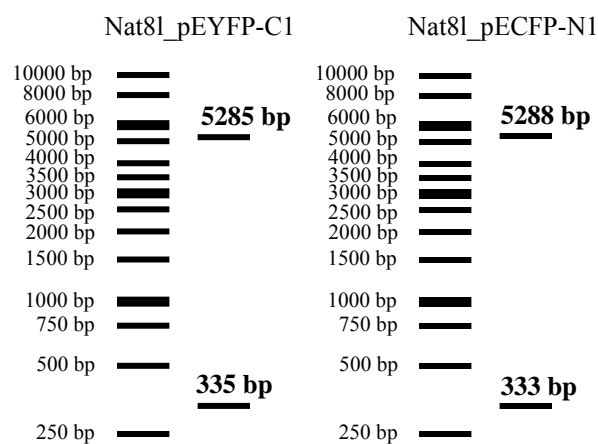
Figure 39: Virtual control digest analysis of Nat8l_pEYFP-C1 and Nat8l_pECFP-N1 cut by Apa1 with the help of Serial Cloner 2.1

According to the virtual control digest, the electrophoresis gel of the two with ApaI cut plasmids revealed DNA bands of 335 bp and 5285 bp for Nat8l_pEYFP-C1 and 333 bp and 5288 bp for Nat8l_pECFP-N1. To improve the comprehensibility of these results, the two vector maps of the used plasmids are presented in Figure 40 and Figure 41. Those graphics contain the used endonucleases, the location of the CDS of Nat8l, the frameshift correction, and the fluorescent protein. The evaluation of these findings proved that the Nat8l gene was integrated into the tested colonies of the fluorescent vectors. Nevertheless, to assure that the two plasmids were correctly produced and the frameshift was corrected in the requested way, colony 14 of Nat8l_pEYFP-C1 and colony 15 of Nat8l_pECFP-N1 were sent to sequencing. The company LGC Genomics which implemented this step could confirm that the two plasmids were appropriate to the required assignments.
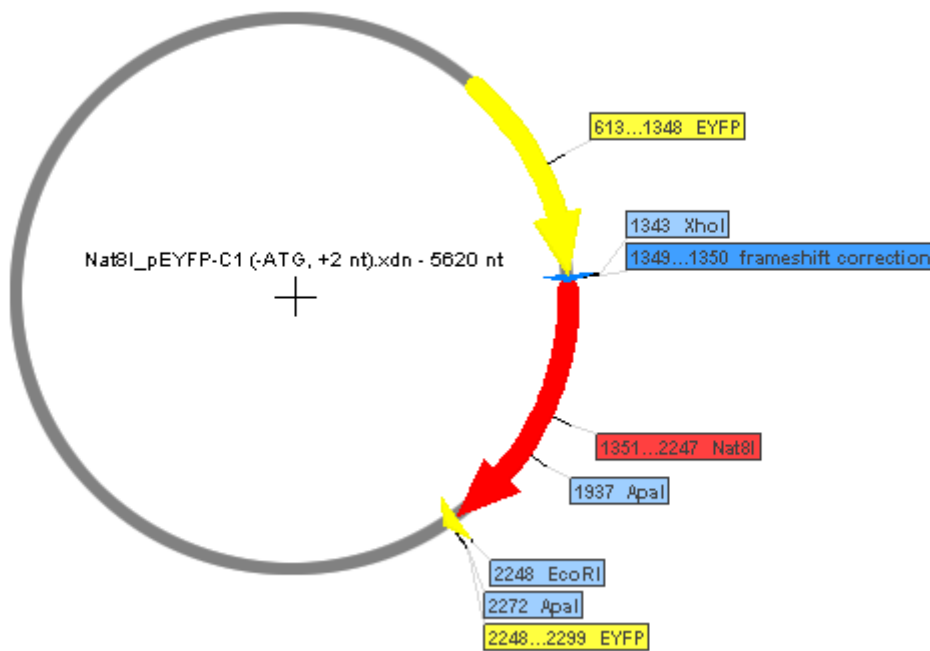
Figure 40: Vector map of Nat8l_pEYFP-C1 construct with the used digestion endonucleases binding sites and the frameshift correction
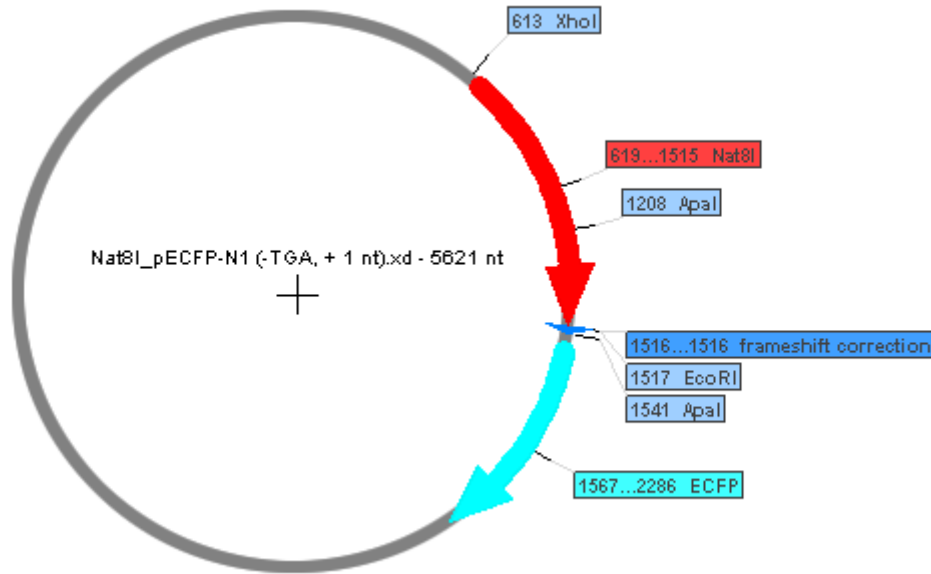
Figure 41: Vector map of Nat8l_pECFP-N1 construct with the used digestion endonucleases binding sites and the frameshift correction

After this verification the two constructs were transfected into differentiated and undifferentiated 3T3-L1 cells through electroporation as described in subsection 3.2.12.1. The electroporated cells were cultured for 2 days on cover slips followed by the microscope analysis. The obtained fluorescence photographs of undifferentiated and differentiated 3T3-L1 cells containing one of the produced constructs are presented in Figure 42.

undifferentiated
3T3-L1 cells

differentiated
3T3-L1 cells

Nat8l_pECFP-N1   Nat8l_pEYFP-C1
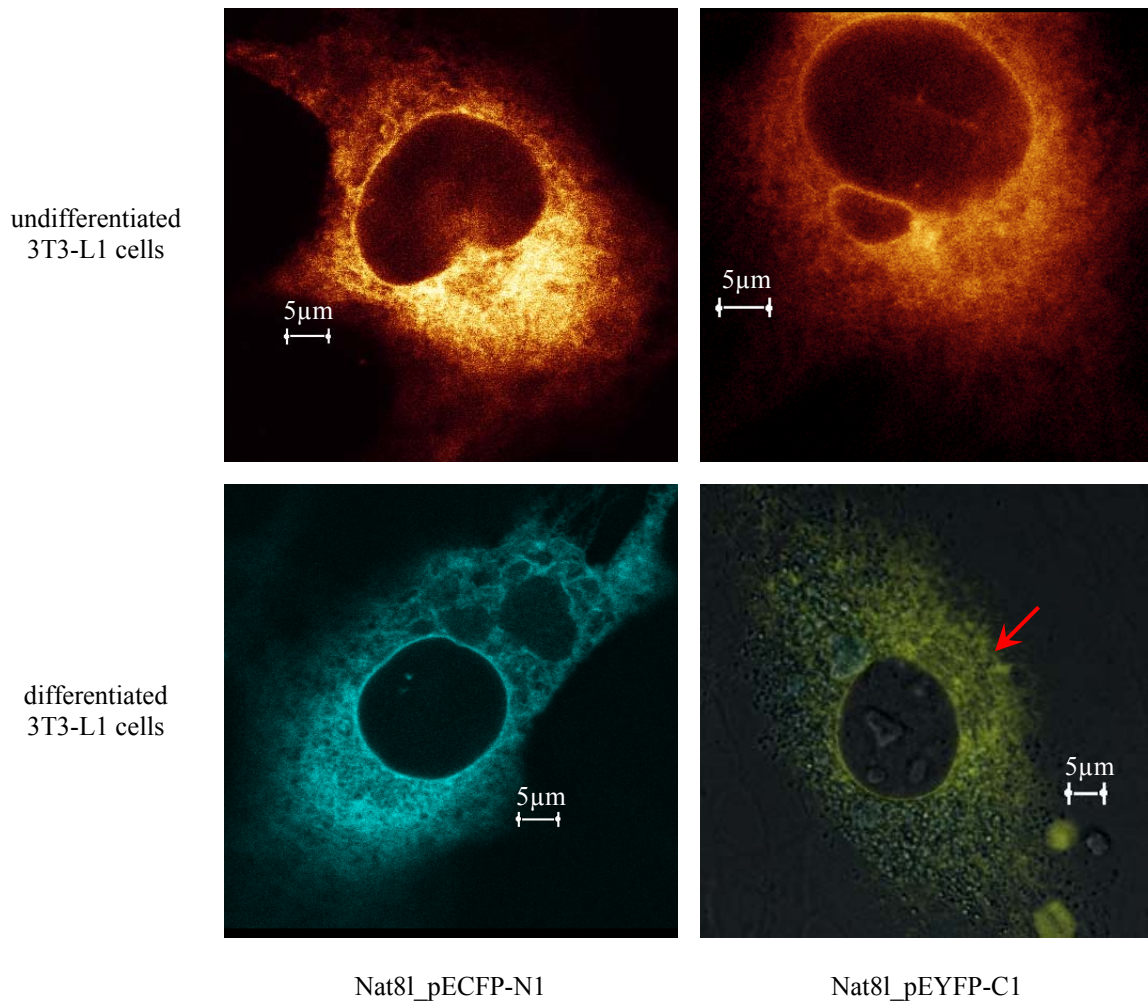
Figure 42: Fluorescence microscopy photographs of the localisation of Nat8l through ECFP and EYFP
in undifferentiated and differentiated 3T3-L1 cells

In all four pictures the main locus of light emission was at a confined region near the nucleus of 3T3-L1 cells. This position and kind of shape is commonly known from ER (endoplasmic reticulum) markers. Therefore, the obtained data from this experiment suggested that the ER might be the point of action of Nat8L. Especially, the photograph of Nat8l_pEYFP-C1 in differentiated 3T3-L1 cells supported this assumption due to the fact that an ER shaped structure was detectable in the luminous region (marked with a red arrow). Even though, these results predict that Nat8L localises at the ER, this method is only able to detect the overexpressed co-protein constructs. Thus, further studies will be necessary to determine if the endogenously expressed Nat8L localises according to the overexpressed constructs.

4.5 Localisation of endogenously expressed Nat8L in 3T3-L1 cells through immunofluorescence staining

The fluorescence microscopy of the overexpression of a protein complex of Nat8L and a fluorescent co-protein delivered promising results that Nat8L localises at the ER. However, to determine the endogenous Nat8L localisation, immunofluorescence staining is used. 3T3-L1 cells were cultured on cover slips in 6-well plates until confluence and differentiated as described in subsection 3.2.2.2. On day 4 after induction, the cells were fixed on the cover slips, followed by a permeabilization step and subsequently incubated with a Nat8L specific antibody as described in subsection 3.2.12.2. A fluorescent anti-rabbit antibody was used for detection of this complex, which was performed with a Zeiss fluorescence microscope. Unfortunately, the detection of the endogenously expressed Nat8L was not successful, even though every step of the protocol was precisely executed. There were no fluorescence differences between the cells treated with the Nat8L antibody and the negative controls. Due to failure of the detection of the endogenously expressed Nat8L, the efficiency of the specific Nat8L antibody was evaluated by WB analysis. For this purpose, Cos7 cells were stably transfected with His_Nat8l (pHisMaxC containing the Nat8l CDS), Nat8l_pMSCV and an empty pHisMaxC plasmid. The cells were cultured for two days in StdM and subsequently RNA and protein probes were harvested as described in subsection 3.2.5 and 3.2.11.1. The extent of the Nat8l overexpression was examined by qPCR analysis (see: Figure 43).
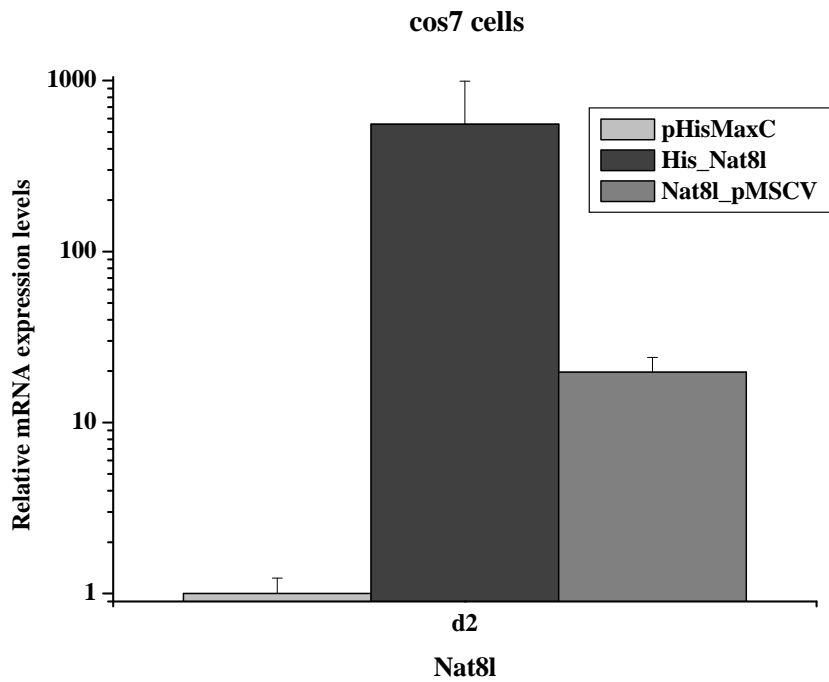
Figure 43: Relative mRNA expression levels of Nat8l overexpressing Cos7 cells at d2 after transfection

The Nat8l expression of control cells transfected with pHisMaxC was set to one as reference. Related to this expression, the overexpression of Nat8l in the Nat8l_pMSCV containing Cos7 cell probes was about 20-fold. The expression of Nat8l in the His_Nat8l samples was at a level of ~ 550-fold compared to the control group. Even though, the precision of this value is questionable regarding to the high standard deviation which cannot be seen directly due to the logarithmic scale, the overexpression of these samples should be sufficient for the WB analysis with the Nat8L antibody. After the protein quantification (see: 3.2.10) of these samples, the WB analysis was performed as described in subsection 3.2.11. The result of this investigation is shown in Figure 44.

pHisMaxC : 1, 4, 7

His_Nat8l : 2, 5, 8

Nat8l_pMSCV: 3, 6, 9

	1	2	3	4	5	6	7	8	9

39 ▬

kDa

28 ▬

Blocking Buffer: PBST + 5% NFDM +1% PBST + 5%
1st AB: Nat8L 1:1000 1:500 1:1000
2nd AB: anti-rabbit 1:5000

	4	5	6

51 ▬

kDa

39 ▬

1st AB: β-actin 1:250 000
2nd AB: anti-mouse 1:3000
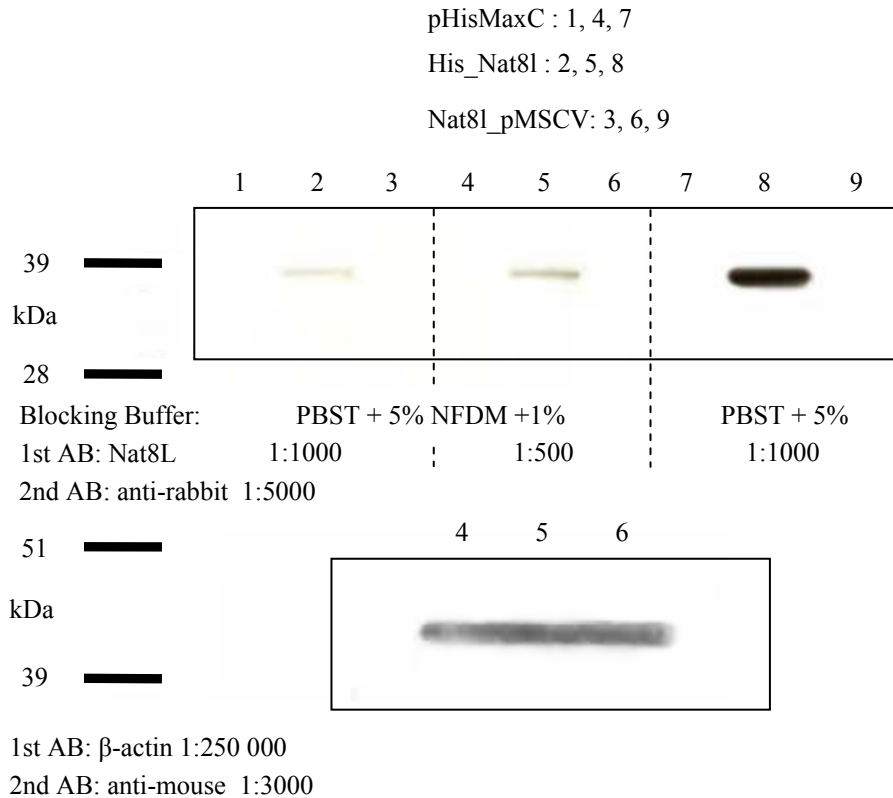
Figure 44: WB analysis of the overexpressed Nat8L protein to evaluate the effectiveness of the Nat8L specific antibody plus added loading control examination in Cos 7 cells

Two different blocking buffers and also different concentrations of the Nat8L antibody were used to assure that the result was independent of handling variations. Nevertheless, the detection of Nat8L succeeded only in the high overexpressing His_Nat8l samples. The 20-fold mRNA overexpression of Nat8l_pMSCV could not be shown on protein level. This result confirmed that the specific antibody was able to detect Nat8L but the required Nat8L protein amount must be at a quite high level. In 3T3-L1 cells, the endogenous expression of Nat8L is rather moderate, so this might be an explanation why the immunofluorescent labelling of Nat8L was not successful. The loading control with β-actin which was only performed with gel slots 4, 5, and 6 proved that the applied protein amount was almost equal for the three tested constructs. Further studies with more effective antibodies or in other cell lines must be performed to determine the intracellular location of the endogenously expressed Nat8L protein.

5   Discussion

5 Discussion

Until today, an evaluation of the functional influences of Nat8L on adipocytes has not been reported. A common way to investigate this issue is to analyse metabolic expression changes which result from a knock-down or an overexpression of the Nat8l gene.

To give a little bit of an insight in previous investigations related to the biosynthetic activity of Nat8L, the following paragraph will summarise the published facts about Nat8L to support the understanding of the subsequent discussion of the outcome of my work. Regarding to existing contradictions on the functionality of Nat8L due to highly controversial endogenous localisation, the following conclusion should anyway be considered with caution. One of the first investigations on the intracellular Nat8L activity was performed by Patel and Clark in 1979. They recognised an increase of the aspartate efflux across the mitochondrial membrane of rat brain tissue by offering malate and glucose with the medium. This increase was severely reduced by addition of pyruvate or hydroxybutyrate accompanied by a drastic increase of NAA efflux from inner mitochondria to cytosol. Suggesting that the added substrates produce intra-mitochondrial acetyl-CoA for the synthesis of NAA and thereby reducing the amount of aspartate. Thereafter, the obtained NAA is most likely transported to cytosol by the dicarboxylic acid translocase (DIC). These results were only observed by addition of adenosine diphosphate (ADP) which might correspond to the electrogenic dependence of the glutamate-aspartate translocase.[122] A study of Madhavarao based on the usage of a TLC assay to detect Nat8L activity in comparison to the citrate synthase activity in mitochondria and furthermore in the presence of different concentrations of L-Asp, acetyl-CoA, NAA, and CoA, led to a first possible model of a metabolic pathway where Nat8L might be involved. In this model pyruvate is transformed to acetyl-CoA by pyruvate dehydrogenase thereafter the produced acetyl-CoA can either enter the TCA (tricarboxylic acid) cycle or be used by Nat8L for the acetylation of aspartate leading to the synthesis of NAA. The intra-mitochondrial aspartate is thereby derived from oxaloacetate through the enzyme aspartate-aminotransferase which coincidently catalyses the reaction of L-glutamate to α-ketoglutarate. This reaction seems to be promoted by the depletion of aspartate via Nat8L. The produced NAA is translocated to the cytosol and later on used as a supply for acetate which contributes to myelinogenesis.[123] Another research which supports the idea of Madhavarao in terms of NAA being a provider of acetyl groups for myelin synthesis was performed by Lu. He

---

[122] Patel and Clark, "Synthesis of N-acetyl-l-aspartate by Rat Brain Mitochondria and Its Involvement in Mitochondrial/cytosolic Carbon Transport."
[123] Madhavarao et al., "Characterization of the N-acetylaspartate Biosynthetic Enzyme from Rat Brain."

reported that NAA might be a transport metabolite for the transfer of acetyl groups from neurons along the axon to oligodendrocytes, even though he conceded that NAA might be involved in a variety of other functions. Controversial to Madhavarao, he suggested a bimodal distribution of Nat8L with the main locus in the ER and to a lesser extent in mitochondria.[124] This finding is supported by results of Ariyannur but with a reversed distribution profile, where Nat8L localises rather in mitochondria than the ER.[125] Seizing the previously obtained results and extending the knowledge through experiments with an aspartate aminotransferase inhibitor, Arun adapted the model of Madhavarao. He proposed that cytosolic aspartate can be metabolised by Nat8L (ER) to NAA or be converted to oxaloacetate followed by a transformation to malate which can enter the intra mitochondrial compartment by the malate-aspartate-shuttle (MAS), followed by an opposite reaction back to aspartate which can be metabolised by Nat8L (mitochondrial) to NAA. In this process, the malate-aspartate-shuttle transports malate and glutamate into mitochondria while aspartate and α–ketoglutarate are transported from mitochondria to cytosol with the help of carrier aralar1 and the oxoglutarate carrier.[126] This model comprises most of until now obtained data related to the functionality of Nat8L. Nevertheless, the circumstance that it is explicitly dependent on an intra-mitochondrial localisation of Nat8L, which is uncertain until now, leads to a contentious assessment about the validity of this model. However, the conclusions of the previously published studies on Nat8L might provide some indications for the evaluation of the obtained results in this study.

The first functional analysis was aimed to achieve a knock-down of the endogenously expressed Nat8l gene through hybridisation with a homologous antisense RNA construct. The applied method is based on the knowledge that different natural endogenous regulatory mechanisms utilize antisense RNA to control gene expression. Thereby, cells initiate a high sophisticated process leading to a binding of the two complementary RNAs, followed by the degradation of the obtained construct through specific nucleases. This process is affected by different factors as physiological ionic strength, temperature, concentration of complementary RNAs, compartmentalisation, and accessibility for hybridisation. In addition, physiological mechanisms influence this step by proteins

---

[124] Lu et al., "N-Acetylaspartate Synthase Is Bimodally Expressed in Microsomes and Mitochondria of Brain."

[125] Ariyannur, Madhavarao, and Namboodiri, "N-acetylaspartate Synthesis in the Brain."

[126] Arun, Moffett, and Namboodiri, "Evidence for Mitochondrial and Cytoplasmic N-acetylaspartate Synthesis in SH-SY5Y Neuroblastoma Cells."

capable of mediating RNA-RNA interactions and structural changes.[127] So, there is a high variety of almost uncontrollable factors which contribute to the efficiency of the formation of dsRNA strands. Nevertheless, in the past scientists attained great success by the usage of procedures very similar to the one used during this study. Unfortunately, we were unable to demonstrate that the knock-down of Nat8L was really successful. The attempt used to verify the knock-down was the WB analysis which did not reveal the anticipated result. The slight changes which were detected for antisense construct 5 (as can be seen in Figure 20) are not distinctive enough to permit the conclusion that the obtained results are undoubtedly correlated with a decrease of Nat8L expression. One possible reason for the outcome of the WB analysis might be the high difference in expression of the two used plasmids. It is known that pHisMaxC expresses the integrated gene to a much higher extend than the vector pMSCV. So, even if the Nat8l antisense RNA (expressed through the pMSCV vector) would have prevented the production of His-tagged Nat8L, the changes would not be sufficient enough to produce discernible results. At this time point, the usage of pHisMaxC was essential for this examination because the WB detection was based on the binding of an antibody to the His-tag of the synthesised protein. Meanwhile, an antibody against Nat8L is available. Even though the evidence of the Nat8L knock-down is lacking, the generated results revealed some alterations between the 3T3-L1 cells containing the antisense constructs and the control cells. Though, we could not proof if this impact is related to an actual knock-down or other cellular interferences. However, the TG analysis revealed that the TG accumulation on day 5 after induction was slightly decreased. This trend was observed twice. Anyway, the accumulation of TG on day 3, an early phase of differentiation, was rather unaffected (see: Figure 18, Figure 21). This finding was quite surprising due to the fact that Nat8L is rather suggested to deplete the present acetyl-CoA pool and therefore an inhibition of its activity would lead to an increase in TG accumulation, especially when assuming that Nat8L localises in the ER. But supposing that the Nat8L knock-down was successful and that Nat8L is localised inside the mitochondria, at least to some extent, a possible explanation for the decrease might be an interference with the translocation of acetyl-CoA (which is mainly synthesised intra-mitochondrially and essential for the accumulation of TG) from mitochondria to cytosol. The idea behind this hypothesis is that NAA might serve as an acetyl-CoA shuttle through the mitochondrial membrane parallel to the tricarboxylic anion carrier (TAC). This conclusion

---

[127] Nellen and Lichtenstein, "What Makes an mRNA Anti-sense-itive?".

is drawn from the proposed function of NAA to be a transport metabolite for acetyl-CoA from neurons to oligodendrocytes[128]. So, intra-mitochondrial Nat8L possibly transforms acetyl-CoA to NAA, which is subsequently translocated via the dicarboxylic acid translocase (DIC) to cytosol. There, the N-acetyl-L-aspartate amidohydrolase (ASPA) catalyses the reaction from NAA to L-aspartate and acetate. Followed by the synthesis of acetyl-CoA from acetate by the cytosolic acetyl-CoA synthetase short chain family member 2 (Acss2). Therefore, the prevention of NAA synthesis through inhibition of Nat8L expression might lead to a reduction of the amount of NAA passing the mitochondrial membrane as a "facilitated" acetyl-CoA carrier. This hypothesis might also explain the observed 2-fold increase of Nat8L during the differentiation of 3T3-L1 cells (see section 2) which could promote the translocation of acetyl-CoA from mitochondria to cytosol where it is required for lipid synthesis. The examination of the differentiation ability of 3T3-L1 cells containing the knock-down plasmid in comparison to control cells without an induction cocktail or only treated with insulin revealed that the differentiation capacity was not changed. Therefore, the obvious conclusion might be that Nat8L does not directly interact with the transcriptional cascade of the differentiation process if assuming that the knock-down was successful. More precise, a reduction of the Nat8L expression is not able to initiate the differentiation. This seems to be comprehensible in the light of until now acquired information of the Nat8L functionality as an enzyme which catalyses the reaction from acetyl-CoA and aspartate to NAA and not as an influencing factor of gene expression (like PPARγ). Summarising the obtained results, even if it is uncertain that the knock-down succeeded, there are indications that the Nat8L function might have been reduced which could be explained through the above mentioned hypothesis about a possible metabolic interaction of Nat8L.

For further investigations it was analysed if a stable overexpression of Nat8L has an influence on adipogenesis in 3T3-L1 cells. In comparison to the knock-down attempt, this approach is far less questionable because the most insecure but essential factor for a successful knock-down, the building of double stranded RNAs, is not required for overexpression. Even though, it was not possible to assure the overexpression on protein level, due to a missing Nat8L antibody at that time, it is feasible to assume that the overexpression could be achieved on account of previous results related to this method. Once again, it was from interest if Nat8L has an influence on TG accumulation during the

---

[128] Madhavarao et al., "Characterization of the N-acetylaspartate Biosynthetic Enzyme from Rat Brain."

5 Discussion

differentiation of 3T3-L1 cells. The analysis which was performed for that reason could demonstrate that overexpression of Nat8L severely reduces the intracellular TG content. The next investigation derived from this result was concerned with the effect of this, from increased Nat8L levels evoked, reduced TG amount on lipid synthesis. The performed ORO staining exposed that the lipid droplet accumulation was drastically decreased. This reduction of lipid droplet accumulation was further examined by the analysis of the expression of common known lipid synthesis markers. Acyl-CoA synthetase long-chain family member 1 (Acsl1), a key regulator of lipid synthesis during the differentiation, and diacylglycerol O-acyltransferase 1 (Dgat1), an essential factor for the development of lipid droplets, were both reduced in 3T3-L1 cells overexpressing Nat8L. The reduced expression levels of Acsl1 and Dgat1 might contribute to the decreased lipid droplet content but this poses the question how Nat8L contributes to these changes and, additionally, how these findings could be incorporated in the previously proposed hypothesis about Nat8L functionality. Supposing that Nat8L promotes the translocation of acetyl-CoA from mitochondria to cytosol, an increase of Nat8L activity would rather increase the cytosolic acetyl-CoA content and therefore support the production of lipid droplets which would strengthen the idea that Nat8L expression increases during the differentiation of 3T3-L1 cells. A plausible explanation might be that the overexpressed Nat8L proteins do not translocate into mitochondria and possibly rather persist in cytosol, probably in the ER. This suggestion is supported by our findings during the investigations related to the localisation of Nat8L which will be discussed later on. This Nat8L increase would lead to a reduction of the cytosolic acetyl-CoA quantity accompanied by an increase of NAA. Thereafter, NAA would normally be used to produce acetate which is transformed to acetyl-CoA again. So, this assumption might explain the TG changes to some extent but the dimension of this reduction seems still surprising. However, the next step was to improve the knowledge about the possibility of the hypothesis and therefore the expression changes of potential metabolic interaction factors was determined. First, it should be evaluated if the production of intra-mitochondrial acetyl-CoA from acetate which is catalysed by acyl-CoA synthetase short-chain family member 1 (Acss1) is affected. The q-PCR analysis exhibited a drastic increase of Acss1 on d6 after induction in the overexpressing cells. There are two possible explanations for this effect which might contribute to this result synergistically. The first one is that Nat8L is translocated to some extent to mitochondria where it depletes the acetyl-CoA amount and therefore promotes the production of this substrate. The second suggestion is that the acetyl-CoA content

inside of mitochondria is reduced passively through the severe decrease of acetyl-CoA in cytosol. So, the increase of Acss1 might be a reaction on a decrease of intra-mitochondrial acetyl-CoA. The hypothesis also includes the enzymes Aspa1 and Acss2 and the expression of both were significantly reduced on all investigated time points. Even though, the reason of this alteration is at the moment unexplainable this result provides an explanation for the question why the reduction of the TG content is so drastically. Due to the increase of Nat8L, the NAA levels might be elevated and as a consequence of the inhibition of the reconversion via Aspa1 and Acss2 to acetyl-CoA, this metabolite gets trapped in cytosol in the form of NAA and therefore is not available for the production of TG and the subsequent synthesis of lipids. To complete the perception of Nat8L in terms of stable overexpression, it was evaluated as already during the antisense cloning research if Nat8L is able to initiate the differentiation process in the absence of DEX and IBMX. Once again, it appeared that the 3T3-L1 cells were not able to accumulate lipid droplets through modification of the Nat8L expression. This circumstance confirmed the conclusion related to this issue which was obtained from the results of the knock-down of Nat8L. All in all, the achieved findings could be brought into accordance with the above proposed hypothesis and even though a lot of aspects on this matter are still not resolved nothing refuted the hypothesised metabolic model absolutely.

Prompted by the results of the stable Nat8l modification which should give insight into the interferences with the differentiation process, it was also from interest to determine the influence of Nat8L on the maintenance of mature adipocytes. Therefore, transient overexpression of Nat8l which was accomplished by electroporation of differentiated 3T3-L1 cells should deliver this information. The performed TG analysis revealed a decrease on both time points suggesting that the effect already detected during the stable overexpression might be applicable on the transient overexpression of Nat8L, even though the alterations were less profound. But as already mentioned in subsection 4.3 of the results chapter this effect could not be demonstrated in all the replicas and this outcome might possibly correlate with the degree of overexpression. After this finding, it was investigated whether this reduction has also an influence on lipid synthesis. Due to technical reasons it was not possible to perform ORO stainings because the attachment of the electroporated cells to the surface of the dishes was not strong enough to withstand the washing steps. So, it was examined if the lipid markers were affected in the same way as during the stable overexpression. This time the expression of diacylglycerol O-acyltransferase 2 (Dgat2), which catalyses the same reaction as Dgat1, was evaluated as well. Surprisingly, there

were no changes detectable between overexpressing and control cells. Apparently, the lipid synthesis of already differentiated cells might not be affected through transient Nat8L overexpression. But since the cells already accumulated lipid droplets during the differentiation this occurrence might be derived from a reduced need to synthesise lipid droplets. The next step was the screening of the expression of possible interaction partners on the proposed metabolic pathway. Acss1 showed a decrease which is very surprising and until now inexplicable when assuming that the cytosolic as well as the mitochondrial acetyl-CoA pool is depleted through the overexpression of Nat8L like during the stable attempt. Nevertheless, the expression profiles of Aspa1 and Acss2 did not seem to be affected and showed almost the same expression levels in Nat8L overexpressing and control cells. Hence, the question arose which factor is responsible for the decrease in TG. Once again, the conclusion of the previous investigations might deliver a possible explanation. When assuming that the major extent of overexpressed proteins probably localises in the ER, then, despite the circumstance that Aspa1 and Acss2 were unaffected, the acetyl-CoA amount would still be reduced through overexpressed Nat8L and transformed to NAA. In this experiment, NAA might not represent a storage form for acetyl-CoA because it seemed to be retransformed to acetyl-CoA by Aspa1 and Acss2 (as their expression levels were not changed) but nevertheless a certain quantity might pass this reaction cycle and therefore be lost for TG synthesis. This could be the reason why the TG content is reduced but much less in comparison to the stable overexpressing cells. Furthermore, this might also be the reason why the low expressing replicas did not show this kind of TG changes because the depletion of acetyl-CoA might not be distinctive enough especially when the produced NAA is subsequently metabolised to acetyl-CoA again. Just to exclude the possibility that the loss of TG is caused by cellular stress which arose during the electroporation, some stress marker genes were investigated in the electroporated cells in comparison to stable transfected cells. It became apparent that the stress produced through electroporation was in the same range as that of stable transfected control cells. So, cellular stress might not be a comprehensible explanation for the decreased TG content. All the findings during this research are explainable through the proposed model. But the investigations were not extensive enough to be certain that the observed effects are really caused by the suggested explanations. Together, the work about the functional analysis of Nat8L delivered some good and promising findings of the impact of Nat8L on adipocytes. Since this was just the beginning of investigations of Nat8L in

adipose tissue the proposed hypothesis might hopefully stimulate other researches to work on this topic.

The localisation of the endogenous Nat8L protein is as already mentioned during the introduction as a rather difficult issue and therefore still a matter of debate. One of the reasons for these complications is the fact that Nat8L is a membrane bound protein. Nevertheless, especially the solution of the still pending question where Nat8L is located would narrow down the quantity of the possible metabolic interaction pathways. This could strongly promote the clarification of the functional properties of Nat8L. Previous work related to the functional analysis of Nat8L, as can be read above, rather suggested a mitochondrial localisation but as already stated this consumption is considered very controversial[129,130,131,132]. Therefore, experiments for a precise determination of the Nat8L localisation were performed. The first attempt executed during this study was the detection with the help of an overexpressed fluorescent co-protein complex which resembles considerably the localisation method of Wiame and colleagues from 2009[133]. In contrast to our method, they tried to verify their results through co-transfection of a tagged Nat8L construct with an ER tracker as well as an mitochondrial tracker, in regard to an increased likelihood of these two possible localisation suggested by previous work[134,135]. Their results revealed that even though the accordance of the ER tracker and the overexpressed tagged Nat8L construct were not exactly accurate, it seemed sufficient enough for Wiame et al. to interpret this circumstance as an ER localisation of Nat8L. Their finding was further promoted by the fact that the used mitochondrial tracker did not show any co-localisation with the Nat8L signal. Additionally, the Nat8l sequence is lacking a mitochondrial propeptide which seems also to be indicative for the relation of Nat8L to the ER.[136] Comparing the microscopy photographs of Wiame with Figure 42 the striking resemblance of a confined detection region near the nucleus suggests the assumption that at least the overexpressed Nat8L protein localises in the ER. This conclusion is promoted

---

[129] Patel and Clark, "Synthesis of N-acetyl-l-aspartate by Rat Brain Mitochondria and Its Involvement in Mitochondrial/cytosolic Carbon Transport."

[130] Madhavarao et al., "Characterization of the N-acetylaspartate Biosynthetic Enzyme from Rat Brain."

[131] Ariyannur, Madhavarao, and Namboodiri, "N-acetylaspartate Synthesis in the Brain."

[132] Arun, Moffett, and Namboodiri, "Evidence for Mitochondrial and Cytoplasmic N-acetylaspartate Synthesis in SH-SY5Y Neuroblastoma Cells."

[133] Wiame et al., "Molecular Identification of Aspartate N-acetyltransferase and Its Mutation in Hypoacetylaspartia."

[134] Lu et al., "N-Acetylaspartate Synthase Is Bimodally Expressed in Microsomes and Mitochondria of Brain."

[135] Ariyannur, Madhavarao, and Namboodiri, "N-acetylaspartate Synthesis in the Brain."

[136] Wiame et al., "Molecular Identification of Aspartate N-acetyltransferase and Its Mutation in Hypoacetylaspartia."

by the severe differences between the detection pattern of a mitochondrial tracker and the fluorescent signals of <u>Figure 42</u> (For comparison of a mitochondrial tracker use microscopy photographs of Wiame[137] or Ariyannur[138]). Taking these findings together it is statable that the high accordance between Wiame's results and the results presented in this study which were performed through almost the same procedure yield the same conclusions about the overexpressed Nat8L localisation. Even though, their investigations were performed with CHO cells or primary neurons and not with the 3T3-L1 cell line which is commonly used for investigations related to fat tissue. A refutation of the subcellular localisation discoveries of Wiame and therefore being also very crucial for this investigation was brought up by Namboodiri and colleagues in 2010. He queried the technique that the detection of an artificial overexpression cannot automatically lead to the conclusion that this localisation would correspond to the native subcellular localisation of the endogenously expressed protein.[139] Especially, the reticular structure of the ER where proteins are probably rather proned to remain than to translocate and vanquish the mitochondrial membrane contributes to the suggestion of Namboodiri and colleagues. Therefore, the detection of the endogenously expressed Nat8L protein with the help of immunofluorescence staining seems to be a promising method to validate the results of the localisation of the overexpression and probable providing a more biologically relevant expression pattern. The used method is based on the procedure of Namboodiri, who was able to localise the endogenously expressed Nat8L protein in mitochondria and to a decreased extent in cytoplasmic regions of SH-SY5Y cells, applying anti-Nat8L polyclonal antibodies.[140] Unfortunately, this approach did not produce any evaluable results in our lab and therefore can neither contribute to an assessment of the previous results nor to the solution of the actual Nat8L localisation debate. Hence, an error analysis of this investigation was performed to expose possible interference factors and come up with improvement suggestions for later studies on this issue. For that purpose, the determination of the specificity and effectiveness of the anti-Nat8L antibody represents a good approach to limit the reasons for the negative results. The implemented investigations revealed that even though a detection of highly overexpressed Nat8L is possible, the detection of minor quantities of the protein was unfeasible, leading to the conclusion that the effectiveness of

---

[137] Ibid.
[138] Ariyannur et al., "Methamphetamine-induced Neuronal Protein NAT8L Is the NAA Biosynthetic Enzyme."
[139] Ibid.
[140] Ibid.

the antibody might not be high enough for the endogenous localisation of Nat8L in 3T3-L1 cells. As stated in the introduction, those cells indeed express Nat8L but not to an extent which would enable the cellular localisation with the present antibody. Therefore, it would be of interest if a more effective antibody is able to produce results in 3T3-L1 cells which resemble those of Namboodiri or possibly detect Nat8L in other locations. The argument of Wiame et al. that Nat8l does not possess an N-terminal mitochondrial targeting sequence was contradicted by Namboodiri et al. through the possibility of a hard to identify internal targeting sequence which is known from other mitochondrial membrane-associated proteins[141]. Summarising all these results and statements, the solution to the question about the intracellular Nat8L location seems to be very intricate. A further option for the analysis of the endogenously expressed protein would be the detection of it in a different cell line. Especially, for fat tissue related investigations, BAT cells would provide a suitable cell model, due to the fact that BAT expresses Nat8L to a much higher extent than WAT (our unpublished data). Other methods which could lead to further insight into this query for adipocytes would be the techniques used by Lu and also by Ariyannur by investigating subcellular fractions of fat cells. Both reports could demonstrate a dual compartment localisation in mitochondria and microsomes of brain tissue. However, Lu's results rather suggested a microsomal location and Ariyannur's results favoured the mitochondria.[142,143]

The problem of the localisation of Nat8L was also investigated by Tahay and he ascertained that Nat8L possesses a C-terminal hydrophobic tail which is necessary and sufficient to bind to membranes. The results he obtained also suggested an ER localisation. Nevertheless, he acknowledged that this tail may also cause an association with the mitochondrial outer membrane and therefore lead to the detection complications.[144] To summarise the findings, even though the results of Wiame et al. could be confirmed in 3T3-L1 cells, there are too many contradictions to assure that Nat8L localises exclusively in the ER region.

So, all in all this study is the first that showed the importance of Nat8L for the development of white adipocytes. These investigations might therefore lead to a better understanding of the possible metabolic interactions causing obesity and they render Nat8L as a possible target in the combat against this epidemic disease.

---

[141] Ibid.

[142] Lu et al., "N-Acetylaspartate Synthase Is Bimodally Expressed in Microsomes and Mitochondria of Brain."

[143] Ariyannur, Madhavarao, and Namboodiri, "N-acetylaspartate Synthesis in the Brain."

[144] Tahay et al., "Determinants of the Enzymatic Activity and the Subcellular Localization of Aspartate N-acetyltransferase."

6   References

6 References

Ahima, R S. "Digging Deeper into Obesity." *J Clin Invest* 121 (2011): 2076–2079.

Ariyannur, Prasanth S, Chikkathur N Madhavarao, and Aryan M A Namboodiri. "N-acetylaspartate Synthesis in the Brain: Mitochondria Vs. Microsomes." *Brain Research* 1227 (August 28, 2008): 34–41.

Ariyannur, Prasanth S, John R Moffett, Pachiappan Manickam, Nagarajan Pattabiraman, Peethambaran Arun, Atsumi Nitta, Toshitaka Nabeshima, Chikkathur N Madhavarao, and Aryan M A Namboodiri. "Methamphetamine-induced Neuronal Protein NAT8L Is the NAA Biosynthetic Enzyme: Implications for Specialized Acetyl Coenzyme A Metabolism in the CNS." *Brain Research* 1335 (June 4, 2010): 1–13.

Armani, A, C Mammi, V Marzolla, M Calanchini, A Antelmi, G M Rosano, A Fabbri, and M Caprio. "Cellular Models for Understanding Adipogenesis, Adipose Dysfunction, and Obesity." *J Cell Biochem* 110 (2010): 564–572.

Aronne, L J. "Classification of Obesity and Assessment of Obesity-related Health Risks." *Obes Res* 10 Suppl 2 (2002): 105S–115S.

Arun, Peethambaran, John R Moffett, and Aryan M A Namboodiri. "Evidence for Mitochondrial and Cytoplasmic N-acetylaspartate Synthesis in SH-SY5Y Neuroblastoma Cells." *Neurochemistry International* 55, no. 4 (September 2009): 219–225.

Billon, N, M C Monteiro, and C Dani. "Developmental Origin of Adipocytes: New Insights into a Pending Question." *Biol Cell* 100 (2008): 563–575.

Birsoy, Kivanç, Zhu Chen, and Jeffrey Friedman. "Transcriptional Regulation of Adipogenesis by KLF4." *Cell Metabolism* 7, no. 4 (April 2008): 339–347.

Bray, G A, and T Bellanger. "Epidemiology, Trends, and Morbidities of Obesity and the Metabolic Syndrome." *Endocrine* 29 (2006): 109–117.

Bray, George A. "Medical Consequences of Obesity." *Journal of Clinical Endocrinology & Metabolism* 89, no. 6 (June 1, 2004): 2583–2589.

Bray, George, and Donna Ryan. "Clinical Evaluation of the Overweight Patient." *Endocrine* 13, no. 2 (October 1, 2000): 167–186.

Butterwith, S C. "Molecular Events in Adipocyte Development." *Pharmacology & Therapeutics* 61, no. 3 (1994): 399–411.

Cao, Z, R M Umek, and S L McKnight. "Regulated Expression of Three C/EBP Isoforms During Adipose Conversion of 3T3-L1 Cells." *Genes & Development* 5, no. 9 (September 1991): 1538–1552.

6 References

Cawthorn, W P, and J K Sethi. "TNF-alpha and Adipocyte Biology." *FEBS Lett* 582 (2008): 117–131.

Chakraborty, Goutam, Praveen Mekala, Daniel Yahya, Gusheng Wu, and Robert W Ledeen. "Intraneuronal N‐acetylaspartate Supplies Acetyl Groups for Myelin Lipid Synthesis: Evidence for Myelin‐associated Aspartoacylase." *Journal of Neurochemistry* 78, no. 4 (August 15, 2001): 736–745.

Chawla, A, J J Repa, R M Evans, and D J Mangelsdorf. "Nuclear Receptors and Lipid Physiology: Opening the X-files." *Science (New York, N.Y.)* 294, no. 5548 (November 30, 2001): 1866–1870.

Chen, Zhu, Javier I Torrens, Ashim Anand, Bruce M Spiegelman, and Jeffrey M Friedman. "Krox20 Stimulates Adipogenesis via C/EBPbeta-dependent and -independent Mechanisms." *Cell Metabolism* 1, no. 2 (February 2005): 93–106.

Clontech. "pECFP-N1 Vector Information", n.d. http://www.liv.ac.uk/physiology/ncs/catalogue/Cloning/pECFP-N1-Map.htm.

———. "pEYFP-C1 Vector Information." Pdf. *pEYFP-C1*, October 3, 2002. http://www.google.at/url?sa=t&rct=j&q=peyfp-c1%20pdf%20-pegfp&source=web&cd=1&ved=0CCAQFjAA&url=http%3A%2F%2Fmicrob205.med.upenn.edu%2FLinks%2Fdownloads%2FMaps%2FpEYFP-C1.pdf&ei=7b4FT8ShO_Tb4QSy5eGNCA&usg=AFQjCNFWeG2h0lIwNpYYNZC89NANpwL0pA&cad=rja.

———. "pMSCVpuro Vector Information." *pMSCVpuro Retroviral Clontech*, July 23, 2003. http://www.google.at/url?sa=t&rct=j&q=pmscv%20puro%20clontech&source=web&cd=2&sqi=2&ved=0CCoQFjAB&url=http%3A%2F%2Fwww.clontech.com%2Fxxclt_ibcGetAttachment.jsp%3FcItemId%3D17671&ei=lmuqTvOSKNGj-ga2uMnADw&usg=AFQjCNEC-uVlY9TYtkF4SAc9kbPGS5eHkQ&cad=rja.

Cormack, B P, R H Valdivia, and S Falkow. "FACS-optimized Mutants of the Green Fluorescent Protein (GFP)." *Gene* 173, no. 1 Spec No (1996): 33–38.

Cypess, Aaron M, Sanaz Lehman, Gethin Williams, Ilan Tal, Dean Rodman, Allison B Goldfine, Frank C Kuo, et al. "Identification and Importance of Brown Adipose Tissue in Adult Humans." *The New England Journal of Medicine* 360, no. 15 (April 9, 2009): 1509–1517.

6 References

Darlington, G J, S E Ross, and O A MacDougald. "The Role of C/EBP Genes in Adipocyte Differentiation." *The Journal of Biological Chemistry* 273, no. 46 (November 13, 1998): 30057–30060.

Dietz, W. H. "Critical Periods in Childhood for the Development of Obesity." *The American Journal of Clinical Nutrition* 59, no. 5 (May 1, 1994): 955–959.

"DoubleDigest™ Tool from Fermentas", n.d. http://www.fermentas.com/en/tools/doubledigest/?country_code=AT.

F.Perez/ SerialBasics. "Serial Cloner", n.d. http://serialbasics.free.fr/Serial_Cloner.html.

Farmer, Stephen R. "Transcriptional Control of Adipocyte Formation." *Cell Metabolism* 4, no. 4 (October 2006): 263–273.

Friedman, J M. "A War on Obesity, Not the Obese." *Science* 299 (2003): 856–858.

———. "Obesity: Causes and Control of Excess Body Fat." *Nature* 459 (2009): 340–342.

Friedman, Jeffrey M., and Jeffrey L. Halaas. "Leptin and the Regulation of Body Weight in Mammals." *Nature* 395, no. 6704 (October 22, 1998): 763–770.

Gesta, S, Y H Tseng, and C R Kahn. "Developmental Origin of Fat: Tracking Obesity to Its Source." *Cell* 131 (2007): 242–256.

Green, H, and O Kehinde. "An Established Preadipose Cell Line and Its Differentiation in Culture. II. Factors Affecting the Adipose Conversion." *Cell* 5, no. 1 (May 1975): 19–27.

Green, H, and M Meuth. "An Established Pre-adipose Cell Line and Its Differentiation in Culture." *Cell* 3, no. 2 (October 1974): 127–133.

Green, Howard, and Olaniyi Kehinde. "Sublines of Mouse 3T3 Cells That Accumulate Lipid." *Cell* 1, no. 3 (March 1974): 113–116.

Gregoire, F M, C M Smas, and H S Sul. "Understanding Adipocyte Differentiation." *Physiol Rev* 78 (1998): 783–809.

Grez, M, E Akgün, F Hilberg, and W Ostertag. "Embryonic Stem Cell Virus, a Recombinant Murine Retrovirus with Expression in Embryonic Stem Cells." *Proceedings of the National Academy of Sciences of the United States of America* 87, no. 23 (December 1990): 9202–9206.

Haslam, D. "Obesity: a Medical History." *Obes Rev* 8 Suppl 1 (2007): 31–36.

Hauner, H. "The New Concept of Adipose Tissue Function." *Physiol Behav* 83 (2004): 653–658.

Hausman, D B, M DiGirolamo, T J Bartness, G J Hausman, and R J Martin. "The Biology of White Adipocyte Proliferation." *Obesity Reviews: An Official Journal of the*

6 References

International Association for the Study of Obesity 2, no. 4 (November 2001): 239–254.

Heim, R, D C Prasher, and R Y Tsien. "Wavelength Mutations and Posttranslational Autoxidation of Green Fluorescent Protein." *Proceedings of the National Academy of Sciences of the United States of America* 91, no. 26 (December 20, 1994): 12501–12504.

Heim, R, and R Y Tsien. "Engineering Green Fluorescent Protein for Improved Brightness, Longer Wavelengths and Fluorescence Resonance Energy Transfer." *Current Biology: CB* 6, no. 2 (February 1, 1996): 178–182.

Hyde, R. "Europe Battles with Obesity." *Lancet* 371 (2008): 2160–2161.

Invitrogen. "pcDNA4/ HisMax A, B, and C." Pdf, October 31, 2010. http://www.google.at/url?sa=t&rct=j&q=hismax%20vector&source=web&cd=1&sqi=2&ved=0CB0QFjAA&url=http%3A%2F%2Ftools.invitrogen.com%2Fcontent%2Fsfs%2Fmanuals%2Fpcdna4hismax_man.pdf&ei=-bIFT_2qH8bS4QSNmJSSCA&usg=AFQjCNGvLpdWX1A_SQGTrenFUIet55JXAg&cad=rja.

Kahn, C R. "Medicine Can We Nip Obesity in Its Vascular Bud?" *Science* 322 (2008): 542–543.

Kimm, Sue Y. S, Nancy W Glynn, Andrea M Kriska, Bruce A Barton, Shari S Kronsberg, Stephen R Daniels, Patricia B Crawford, Zak I Sabry, and Kiang Liu. "Decline in Physical Activity in Black Girls and White Girls During Adolescence." *New England Journal of Medicine* 347, no. 10 (2002): 709–715.

Kopelman, P G. "Obesity as a Medical Problem." *Nature* 404, no. 6778 (April 6, 2000): 635–643.

Kotani, K, M Nishida, S Yamashita, T Funahashi, S Fujioka, K Tokunaga, K Ishikawa, S Tarui, and Y Matsuzawa. "Two Decades of Annual Medical Examinations in Japanese Obese Children: Do Obese Children Grow into Obese Adults?" *, Published Online: 25 September 1997; | Doi:10.1038/sj.ijo.0800492* 21, no. 10 (September 25, 1997): 912–921.

Lau, David C W, Bikramjit Dhillon, Hongyun Yan, Paul E Szmitko, and Subodh Verma. "Adipokines: Molecular Links Between Obesity and Atheroslcerosis." *American Journal of Physiology. Heart and Circulatory Physiology* 288, no. 5 (May 2005): H2031–2041.

6 References

Lefterova, Martina I, and Mitchell A Lazar. "New Developments in Adipogenesis." *Trends in Endocrinology and Metabolism: TEM* 20, no. 3 (April 2009): 107–114.

Lehrke, Michael, and Mitchell A Lazar. "The Many Faces of PPARgamma." *Cell* 123, no. 6 (December 16, 2005): 993–999.

Lu, Zi-Hua, Goutam Chakraborty, Robert W Ledeen, Daniel Yahya, and Gusheng Wu. "N-Acetylaspartate Synthase Is Bimodally Expressed in Microsomes and Mitochondria of Brain." *Brain Research. Molecular Brain Research* 122, no. 1 (March 17, 2004): 71–78.

Madhavarao, C N, C Chinopoulos, K Chandrasekaran, and M A A Namboodiri. "Characterization of the N-acetylaspartate Biosynthetic Enzyme from Rat Brain." *Journal of Neurochemistry* 86, no. 4 (August 2003): 824–835.

Miller, A D, and G J Rosman. "Improved Retroviral Vectors for Gene Transfer and Expression." *BioTechniques* 7, no. 9 (October 1989): 980–982, 984–986, 989–990.

Miyawaki, A, J Llopis, R Heim, J M McCaffery, J A Adams, M Ikura, and R Y Tsien. "Fluorescent Indicators for Ca2+ Based on Green Fluorescent Proteins and Calmodulin." *Nature* 388, no. 6645 (August 28, 1997): 882–887.

Nammi, Srinivas, Saisudha Koka, Krishna M Chinnala, and Krishna M Boini. "Obesity: An Overview on Its Current Perspectives and Treatment Options." *Nutrition Journal* 3 (April 14, 2004): 3.

National Institutes of Health (NIH), National Heart, Lung, and Blood Institute (NHLBI). "Clinical Guidelines on the Identification, Evaluation, and Treatment of Overweight and Obesity in Adults--The Evidence Report. Obes. Res." 6 Suppl 2, no. April (1998): 51S–209S.

Nedergaard, Jan, Tore Bengtsson, and Barbara Cannon. "Unexpected Evidence for Active Brown Adipose Tissue in Adult Humans." *American Journal of Physiology. Endocrinology and Metabolism* 293, no. 2 (August 2007): E444–452.

Nellen, W, and C Lichtenstein. "What Makes an mRNA Anti-sense-itive?" *Trends in Biochemical Sciences* 18, no. 11 (November 1993): 419–423.

Niwa, Minae, Atsumi Nitta, Hiroyuki Mizoguchi, Yasutomo Ito, Yukihiro Noda, Taku Nagai, and Toshitaka Nabeshima. "A Novel Molecule 'Shati' Is Involved in Methamphetamine-Induced Hyperlocomotion, Sensitization, and Conditioned Place Preference." *The Journal of Neuroscience* 27, no. 28 (July 11, 2007): 7604–7615.

Ogden, Cynthia L, Margaret D Carroll, Lester R Curtin, Margaret A McDowell, Carolyn J Tabak, and Katherine M Flegal. "Prevalence of Overweight and Obesity in the

United States, 1999-2004." *JAMA: The Journal of the American Medical Association* 295, no. 13 (April 5, 2006): 1549–1555.

"OligoCalc: Oligonucleotide Properties Calculator", n.d. http://www.basic.northwestern.edu/biotools/oligocalc.html.

Otto, Tamara C, and M Daniel Lane. "Adipose Development: From Stem Cell to Adipocyte." *Critical Reviews in Biochemistry and Molecular Biology* 40, no. 4 (August 2005): 229–242.

Patel, Tarun B., and John B. Clark. "Synthesis of N-acetyl-l-aspartate by Rat Brain Mitochondria and Its Involvement in Mitochondrial/cytosolic Carbon Transport." *Biochemical Journal* 184, no. 3 (December 15, 1979): 539–546.

"Phoenix Cell Line", n.d. http://www.stanford.edu/group/nolan/retroviral_systems/phx.html.

Pi-Sunyer, F X. "The Obesity Epidemic: Pathophysiology and Consequences of Obesity." *Obes Res* 10 Suppl 2 (2002): 97S–104S.

Pinent, M, H Hackl, T R Burkard, A Prokesch, C Papak, M Scheideler, G Hammerle, R Zechner, Z Trajanoski, and J G Strauss. "Differential Transcriptional Modulation of Biological Processes in Adipocyte Triglyceride Lipase and Hormone-sensitive Lipase-deficient Mice." *Genomics* 92 (2008): 26–32.

Pinent, M, A Prokesch, H Hackl, P J Voshol, A Klatzer, E Walenta, U Panzenboeck, et al. "Adipose Triglyceride Lipase and Hormone-Sensitive Lipase Are Involved in Fat Loss in JunB-Deficient Mice." *Endocrinology* 152 (2011): 2678–2689.

Prentice, A. M., and S. A. Jebb. "Obesity in Britain: Gluttony or Sloth?" *BMJ : British Medical Journal* 311, no. 7002 (August 12, 1995): 437–439.

"Primer Designing Tool", n.d. http://www.ncbi.nlm.nih.gov/tools/primer-blast/.

Rosen, E D, and O A Macdougald. "Adipocyte Differentiation from the Inside Out." *Nat Rev Mol Cell Biol* 7 (2006): 885–896.

Rosen, E D, and B M Spiegelman. "Adipocytes as Regulators of Energy Balance and Glucose Homeostasis." *Nature* 444 (2006): 847–853.

Rosen, Evan D, Chung-Hsin Hsu, Xinzhong Wang, Shuichi Sakai, Mason W Freeman, Frank J Gonzalez, and Bruce M Spiegelman. "C/EBPalpha Induces Adipogenesis Through PPARgamma: a Unified Pathway." *Genes & Development* 16, no. 1 (January 1, 2002): 22–26.

6 References

Russell, T R, and R Ho. "Conversion of 3T3 Fibroblasts into Adipose Cells: Triggering of Differentiation by Prostaglandin F2alpha and 1-methyl-3-isobutyl Xanthine." *Proc Natl Acad Sci U S A* 73 (1976): 4516–4520.

Stommel, Manfred, and Charlotte A. Schoenborn. "Variations in BMI and Prevalence of Health Risks in Diverse Racial and Ethnic Populations." *Obesity* 18, no. 9 (2010): 1821–1826.

T OD, AR O G J, and EN H G RE. "Quantitative Studies of the Growth of Mouse Embryo Cells in Culture and Their Development into Established Lines." *J Cell Biol* 17 (1963): 299–313.

TALLAN, H H, S MOORE, and W H STEIN. "N-Acetyl-L-aspartic Acid in Brain." *The Journal of Biological Chemistry* 219, no. 1 (March 1956): 257–264.

Tahay, Gaëlle, Elsa Wiame, Donatienne Tyteca, Pierre J Courtoy, and Emile Van Schaftingen. "Determinants of the Enzymatic Activity and the Subcellular Localization of Aspartate N-acetyltransferase." *The Biochemical Journal* 441, no. 1 (January 1, 2012): 105–112.

"The Mfold Web Server", n.d. http://mfold.rna.albany.edu/?q=mfold.

"Tm Calculator - Finnzymes", n.d. https://www.finnzymes.fi/tm_determination.html.

"WHO | Obesity and Overweight." *WHO*, March 2011. http://www.who.int/mediacentre/factsheets/fs311/en/.

White, Ursula A, and Jacqueline M Stephens. "Transcriptional Factors That Promote Formation of White Adipose Tissue." *Molecular and Cellular Endocrinology* 318, no. 1–2 (April 29, 2010): 10–14.

Wiame, Elsa, Donatienne Tyteca, Nathalie Pierrot, François Collard, Mustapha Amyere, Gaëtane Noel, Jonathan Desmedt, et al. "Molecular Identification of Aspartate N-acetyltransferase and Its Mutation in Hypoacetylaspartia." *The Biochemical Journal* 425, no. 1 (January 1, 2010): 127–136.

Yang, T T, L Cheng, and S R Kain. "Optimized Codon Usage and Chromophore Mutations Provide Enhanced Sensitivity with the Green Fluorescent Protein." *Nucleic Acids Research* 24, no. 22 (November 15, 1996): 4592–4593.

Yeh, W C, Z Cao, M Classon, and S L McKnight. "Cascade Regulation of Terminal Adipocyte Differentiation by Three Members of the C/EBP Family of Leucine Zipper Proteins." *Genes & Development* 9, no. 2 (January 15, 1995): 168–181.

Zhang, Jiang-Wen, Dwight J Klemm, Charles Vinson, and M Daniel Lane. "Role of CREB in Transcriptional Regulation of CCAAT/enhancer-binding Protein Beta Gene

6 References

During Adipogenesis." *The Journal of Biological Chemistry* 279, no. 6 (February 6, 2004): 4471–4478.

Zhang, Y, R Proenca, M Maffei, M Barone, L Leopold, and J M Friedman. "Positional Cloning of the Mouse Obese Gene and Its Human Homologue." *Nature* 372, no. 6505 (December 1, 1994): 425–432.

Zuker, Michael. "Mfold Web Server for Nucleic Acid Folding and Hybridization Prediction." *Nucleic Acids Research* 31, no. 13 (July 1, 2003): 3406 –3415.